NUMERICAL SIMULATIONS OF TWO DIMENSIONAL QUANTUM ELECTRODYNAMICS

Thesis

submitted by

SIMON ROLAND CARSON

for the degree of

DOCTOR OF PHILOSOPHY

Department of Physics

University of Edinburgh

September 1984

To my Mother and my Father,
and to Elaine.

´Aw thowt some idiot might ax me,
sooa Aw measured it to mek sure.´

Bill o´ Jack´s Lancashire Monthly (vol. 2).

ACKNOWLEDGEMENTS

I should like to thank my supervisor, Richard Kenway, for his help and encouragement, and for his patience and good humour, during the course of my research. I am also grateful to Tony Burkitt for his advice and help in the early stages. I should like to thank all the staff and students in the theory group for helpful discussions, the Edinburgh Regional Computing Centre for their support in the computing aspects of this work, and the SERC for financial support.

I am particularly indebted to those who kept me sane and made me laugh - especially my office mate, Bruno Meyer, and all on the third floor: Tim Killingback, Beate Schmittmann, John Sim, and Peter Swift.

I should like too to thank my family and friends for their continual interest and encouragement in my work.

Finally, I am indebted to all the teachers who have helped me on the way, especially Chris Shilladay:

'And hū maeg se gelēafa bēon forþgenge
gif sēo lār and þā lārēowas ātēoriaþ?'

Aelfric, Preface to his Latin Grammar.

DECLARATION

Some of the work presented in chapters two and three was done in collabaration with R.D. Kenway. All other work is entirely my own, except where otherwise indicated.

ABSTRACT

A review of lattice gauge theory calculations is presented, and the advantages of two dimensional models as a testing ground for numerical techniques are summarised. A review of analytical continuum results for the Schwinger model and its generalisations is followed by a new analysis of the massive quenched model in the continuum.

The models are formulated on a two dimensional hypercubic lattice, according to a Euclidean discretisation, using Kogut-Susskind fermions. The continuum flavours hidden in the lattice action are identified according to the Kahler-Dirac formulation. The flavour degeneracy of the lattice formulation is broken by a one-link mass term. This is used to decouple one of the flavours by giving it a mass of order the cut-off. Mesonic operators for both the two flavour and one flavour models are identified.

Numerical techniques are reviewed, and tested with free fermions.

Calculations of the fermion condensate and of particle masses are presented for the two flavour and one flavour models, and for both the quenched and the unquenched cases.

CONTENTS

CHAPTER ONE

LATTICE GAUGE THEORY

Present day particle physics is dominated by gauge theories, the most successful of which to date is quantum electrodynamics. The detection of the W and Z bosons in 1982 at CERN justified belief in the electroweak theory of Glashow, Salam and Weinberg. The prime candidate for a fundamental theory of the strong interactions is quantum chromodynamics, a generalisation of QED in which the Abelian U(1) gauge group of QED is replaced by a non-Abelian SU(3) colour group. In QCD, the fundamental charges, quarks, interact through an octet of gauge bosons, the gluons, via the minimal Yang-Mills interaction. The gluon fields are able to interact with themselves due to the non-Abelian nature of the gauge group. Within this picture, hadrons are bound states of quark and gluon fields.

Our belief in the existence of quarks is supported by deep inelastic lepton-hadron scattering experiments, which suggest the existence of point-like objects within the hadrons, and by the eightfold way of Gell-Mann and Ne'eman (1964), so successful in predicting the low energy hadron spectrum, in terms of different 'flavours' of quarks. These phenomenological ideas are put on a firmer theoretical footing in QCD.

Whilst QCD may be an aesthetically pleasing model, it does not form as simple a calculation model as QED. Calculations in QED have centred on perturbation theory, where the expansion parameter is the fermion-gauge coupling, g, and whilst the short distance behaviour of QCD can be calculated within the framework of standard

perturbation theory, as the coupling is small at high energies (asymptotic freedom), the large distance behaviour of QCD remains an unsolved problem, due to infra-red singularities. At short distances perturbative calculations successfully predict the scaling properties observed in deep inelastic scattering experiments, but at large distances, where the QCD coupling moves out of the perturbative regime, it becomes difficult to disentangle non-perturbative effects from those that are genuinely perturbative. As an isolated quark has never been observed (no coloured state has ever been seen), one is led to speculate on the existence of an exact confining mechanism for the quarks and gluons. The confinement phenomenon makes QCD qualitatively different from gauge theories of weak and electromagnetic forces - the fundamental fields of the Lagrangian do not appear in the physical spectrum, and it becomes necessary to study the theory outside the framework of perturbation theory.

The introduction of a space or space-time lattice is one way in which the limits of perturbation theory can be overcome. This prescription seems a little strange, as it clearly destroys the continuous symmetries of the Lorentz group, but as a mathematical trick it provides a gauge invariant cut-off that removes ultra-violet divergences by the simple expedient of eliminating all wavelengths less than twice the lattice spacing. As with any regulator, the lattice must be removed after renormalisation, and one hopes that in the limit of zero lattice spacing one recovers Lorentz invariance and is able to extract real physics.

On a lattice, a field theory becomes mathematically well-defined, and may be studied in various ways. Ordinary perturbation theory, though awkward, may be performed, and yields results in agreement with other regularisation schemes. The lattice formulation of field theory emphasises

the deep connection with statistical mechanics: in Euclidean space, the Feynman path integral formulation of a quantum field theory is identical to the partition function of an analagous statistical system, the square of the field theoretic coupling corresponding directly with the temperature of the statistical system. Thus the particle physicist is able to use the techniques of the statistical physicist.

The lattice formulation is particularly well suited to strong coupling (high temperature) expansions, and in this limit confinement occurs naturally, the theory reducing to one of quarks on the ends of strings with a finite energy per unit length, as is shown below. However, the coupling constant on the lattice represents a bare coupling at a length scale of the lattice spacing. We have already noted that QCD displays asymptotic freedom, and the consequence of this for the lattice theory is that the bare coupling must go to zero as the lattice spacing goes to zero. Thus, in the language of statistical physics, we are led from a high temperature region to one of low temperature in approaching the continuum limit. In a statistical system, one might then expect to encounter phase transitions and if this were to occur in the lattice gauge theory, it would be difficult to extract continuum results. Investigations of the phase structure of lattice gauge theories are therefore important, and studies have been performed. The most important results of these studies are summarised below.

We now discuss the formulation of a gauge theory on a lattice in more detail.

The lattice may be introduced in a number of ways, the most obvious and widely used of which is the hypercubic Euclidean lattice. The connection with ordinary Minkowski space is made through a Wick rotation, enabling an

interpretation of one's results in the usual physical space at the end of a calculation, with no loss of information. The hypercubic lattice is clearly the simplest choice, but any lattice is in principle possible, provided that in the limit of zero lattice spacing, the correct continuum limit is recovered. Christ, Friedberg and Lee (1982) have examined a formulation in which the lattice sites are themselves randomly distributed. The choice of lattice is closely connected to renormalisation group and fixed point considerations.

An alternative formulation of lattice gauge theory is the Hamiltonian approach of Kogut and Susskind (1975). One remains in Minkowski space, discretising only the spatial directions. The fields are quantised according to the usual canonical prescription. This method will not be pursued further here, and from hereon we work on a Euclidean lattice.

The field theory is quantised using the path integral formalism. We define an action, $S[\varphi]$, depending on some set of classical fields, $\varphi(x)$. Then some physical quantity, the expectation value of some operator, $\hat{O}(\varphi)$, is given by:

$$\langle \hat{o} \rangle = \frac{1}{Z} \int \mathcal{D}\varphi \, \hat{O}(\varphi) \exp[-S(\varphi)]$$

$$Z = \int \mathcal{D}\varphi \exp[-S(\varphi)] \qquad (1.1)$$

On the lattice, there is no problem with the definition of the measure, as there is in the continuum: the functional integral is defined as the product (finite on a finite lattice, denumerable on an infinite lattice) of the integrals over the fields at every site of the lattice.

In constructing a lattice gauge theory, one would like to display the gauge symmetry of the continuum theory explicitly in the lattice formulation, and in the continuum limit recover the Yang-Mills action. The first theory to have a local gauge symmetry on a lattice was a generalisation of the Ising model introduced by Wegner (1971). His interest in introducing a local invariance group arose from the fact that spontaneous magnetisation is forbidden in such a theory. Despite the absence of a local order parameter, Wegner showed that the model has a phase transition, and suggested ways in which the phases could be labelled and distinguished. Wilson (1974) generalised the Ising lattice gauge theory from the discrete group Z_2 to continuous groups, of more interest to the particle physicist. We now consider Wilson's formulation in some detail.

Taking a general gauge group G, we associate an independent element of G with each link of the lattice, joining two nearest neighbour sites:

$$U_\mu(\underline{n}) \in G \tag{1.2}$$

μ labels the direction of the link, and n labels a lattice site. On traversing the link in the opposite direction, one should obtain the inverse element:

$$U_{-\mu}(\underline{n}+a\underline{e}_\mu) = U_\mu^{-1}(\underline{n}) \tag{1.3}$$

where $\underline{e}_\mu$ is a unit vector in the μ direction. We now consider G to be the group SU(N). Define a vector potential by writing :

$$\begin{aligned} U_\mu(\underline{n}) &= \exp\{\tfrac{1}{2} i a g \tau_i A_\mu^i(\underline{n})\} \\ &= \exp\{\tfrac{1}{2} i a g A_\mu(\underline{n})\} \end{aligned} \tag{1.4}$$

where g is the field theoretic coupling, and τ_i are the generators of SU(N). The group volumes are finite, so that the group integrals necessary to the path integral formulation of the quantum field theory are well-defined. Local gauge symmetry corresponds to an arbitrary group rotation, G(n), at every lattice site. Link variables then transform as:

$$U_\mu(\underline{n}) \rightarrow U'_\mu(\underline{n}) = G(\underline{n})\, U_\mu(\underline{n})\, G^{-1}(\underline{n}+a\underline{e}_\mu) \qquad (1.5)$$

G(n) defines the orientation of a local colour frame of reference at each site, and $U_\mu(n)$ transports us from one reference frame to another. It should be noted that faithfulness to an exact gauge symmetry is not a prerequisite of a regularisation scheme: the physics of a renormalisable theory should be independent of the details of the regularisation scheme. Nevertheless, Wilson's formulation is particularly elegant, and almost universally employed.

To determine the dynamics of the field variables, we need to construct an action. In the continuum limit, we require that the lattice action reduce to the classical Yang-Mills action. The field strength is a generalised curl of the vector potential, and this suggests using integrals of the vector potential A_μ around small closed contours. On the lattice, this means constructing products of U matrices around closed paths. Such an action is clearly gauge invariant, because all SU(N) indices are locally contracted. The simplest such action is composed of the sum of products of U matrices around elementary squares of the lattice, called plaquettes:

$$S(U) = \beta \sum_{\underline{n},\mu,\nu} \left\{ 1 - \frac{1}{N} Re\, Tr\, U_\mu(\underline{n}) U_\nu(\underline{n}+a\underline{e}_\mu) U_\mu^\dagger(\underline{n}+a\underline{e}_\nu) U_\nu^\dagger(\underline{n}) \right\} \quad (1.6)$$

The additive constant here ensures that the action vanishes when the group elements approach the identity. N is a normalisation, equal to the dimensionality of the group matrices. The trace may be performed in any representation of the group. We consider only the fundamental representation here, and show now that this action indeed reduces to the ordinary Yang-Mills action in the continuum limit, $a \to 0$. Consider a vector potential smooth enough to enable us to Taylor expand the slowly varying field:

$$A_\nu(\underline{n}+a\underline{e}_\mu) = A_\nu(\underline{n}) + a\partial_\mu A_\nu(\underline{n}) + O(a^2) \quad (1.7)$$

Using the Baker-Campbell-Hausdorff identity, we can write :

$$U_\mu(\underline{n})\, U_\nu(\underline{n}+a\underline{e}_\mu)\, U^\dagger(\underline{n}+a\underline{e}_\nu)\, U_\nu^\dagger(\underline{n}) = \exp\left\{ ia^2 g \left(\partial_\mu A_\nu(\underline{n}) - \partial_\nu A_\mu(\underline{n}) \right) + ig\left[A_\mu(\underline{n}), A_\nu(\underline{n}) \right] + O(a^3) \right\} \quad (1.8)$$

The leading term here is clearly the Yang-Mills field strength, $F_{\mu\nu}$, with corrections of higher order in a^2 which do not contribute in the naive continuum limit. For slowly varying smooth fields, we have $a^2 g F_{\mu\nu} << 1$, and hence, expanding the exponential:

$$Tr\left[UUU^\dagger U^\dagger \right] \simeq Tr \exp\left(ia^2 g F_{\mu\nu} \right) \simeq Tr\, 1 - \frac{1}{2} a^4 g^2 Tr\, F_{\mu\nu} F^{\mu\nu} + O(a^6) \quad (1.9)$$

The $O(a^2)$ term disappears as we are dealing with hermitian matrices (for unitary groups) and Tr1 contains no dynamics, and can be dropped. Finally, we make the replacement:

$$\sum_{\underline{n},\mu,\nu} \longrightarrow \int \frac{d^4x}{a^4} \sum_{\mu,\nu} \quad (1.10)$$

and thus obtain the Euclidean Yang-Mills action:

$$S = \frac{1}{4} \int d^4x \, F_{\mu\nu} F^{\mu\nu} \tag{1.11}$$

where we have idntified the coupling β as:

$$\beta = \frac{2N}{g^2} \tag{1.12}$$

for an SU(N) gauge group in 4 dimensions. The terms of higher order in a^2 vanish in the continuum limit, although they can give rise to a finite renormalisation of the coupling constant. The local invariance of the lattice action ensures that we recover the standard field strength tensor. The resulting continuum action is clearly Euclidean O(4) invariant - the discrete hypercubical symmetry of the lattice disappears into the higher order terms. Actions that differ from that we have considered only in higher order terms clearly have the same continuum limit, and thus are equally acceptable lattice actions. Such actions need investigation, as it may be possible to write a lattice action that is in some sense closer to the continuum (Symanzik, 1982; Martinelli, Parisi, Petronzio, 1982; Weisz, 1982; Berg, Meyer, Montvay, Symanzik, 1983).

Having defined our action, we quantise the theory by writing down the path integral:

$$Z = \int \mathcal{D}U \, e^{-S(U)} \tag{1.13}$$

(For a discussion of the meaning of the group measure see for example 'Quarks, Gluons and Lattices' ,Creutz, 1983). As noted earlier, the expectation value of some operator $\hat{O}(U)$

is given by :

$$\langle \hat{O} \rangle = \frac{1}{Z} \int \mathcal{D}U \, \hat{O}(U) \, e^{-S(U)} \qquad (1.14)$$

In the quantum mechanical Hilbert space, this is the vacuum expectation value of the corresponding time ordered operators. Note that no gauge fixing term has been included in the path integral, a procedure which is necessary in the continuum to control divergences resulting from integration over all gauges. Here, the gauge variables are elements of a compact group, and as a result, the gauge orbits are themselves compact. For gauge invariant quantities, it is harmless to include an integral over all gauges, although in order to formulate perturbation theory, such gauge fixing is necessary. No such gauge fixing is required in numerical simulations of lattice gauge theory, and hence we do not pursue the subject any further here.

The Wilson form of the pure gauge theory emphasises the analogy with statistical mechanics, particularly with models of magnetism. The gauge variables $U_\mu(n)$ are much like spins located on crystal bonds, interacting through the four spin coupling of the Wilson action. This leads us to ask whether the lattice gauge theory can ever develop a spontaneous magnetisation. Thus, we might look for phases of the lattice gauge theory where:

$$\langle U^\mu(\underline{n}) \rangle \neq 0 \qquad (1.15)$$

However, in lattice gauge theory, such an expectation value breaks the local symmetry of gauge invariance. Hence the magnetisation vanishes in a pure gauge theory (Elitzur, 1975) and so cannot be used as an order parameter to

distinguish phases. To get around this problem, we need to look for a gauge invariant parameter. For the pure gauge theory, the simplest gauge invariant operator is the trace of the product of four link variables around a plaquette. Its expectation value is the internal energy of the corresponding thermodynamic system, and is given by a derivative of the partition function:

$$P = \langle 1 - \frac{1}{N} \mathrm{Tr}\, U_\square \rangle = \frac{1}{6} \frac{\partial}{\partial \beta} \ln Z \qquad (1.16)$$

The factor of 1/6 is the ratio of the number of sites to the number of plaquettes in four dimensions.

It should be noted that this order parameter lacks the useful property of a magnetisation in that it never vanishes identically, except exactly at zero temperature. Wilson has generalised this simple local order parameter to a non-local order parameter, the Wilson loop. This is the trace of a product of link variables around any closed path, and is clearly gauge invariant. The expectation value of such an operator is the Wilson loop :

$$W(C) = \langle \mathrm{Tr} \prod_{\mu, \underline{n} \in C} U_\mu(\underline{n}) \rangle \qquad (1.17)$$

C is any closed contour, and the group elements are path ordered. To understand the significance of such a quantity, consider its continuum analogue (Kogut, 1983). This is intimately related to the heavy quark potential.

Suppose one adiabatically separates a $\bar{q}q$ pair to a distance R, holds this configuration for a time T and then allows the quark-antiquark pair to annihilate. The Euclidean amplitude for this process is:

$$\langle i | e^{-HT} | f \rangle \tag{1.18}$$

where H is the Hamiltonian of the theory, and i and f label initial and final states respectively, that is a $\bar{q}q$ pair a distance R apart. Then:

$$\langle i | e^{-HT} | f \rangle = \frac{\int \mathcal{D}A^a_\mu \mathcal{D}c_a \mathcal{D}c^*_a \exp\{-S + ig\int A_\mu J_\mu d^4x\}}{\int \mathcal{D}A^a_\mu \mathcal{D}c_a \mathcal{D}c^*_a \exp\{-S\}} \tag{1.19}$$

J_μ is an external current, c_a the Fadeev-Popov ghost fields. For the path we are discussing, J_μ is equal to unity along the contour C tracing out the closed path of the quarks, and equal to zero elsewhere. Hence:

$$\langle i | e^{-HT} | f \rangle = \frac{\int \mathcal{D}A^a_\mu \mathcal{D}c_a \mathcal{D}c^* \exp\{-S + ig\oint_c A_\mu dx_\mu\}}{\int \mathcal{D}A^a_\mu \mathcal{D}c_a \mathcal{D}c^*_a \exp\{-S\}} \tag{1.20}$$

As the process is static, and $|i\rangle$ and $|f\rangle$ are identical,

$$\langle i | e^{-HT} | f \rangle = e^{-V(R)T} \langle i | f \rangle \tag{1.21}$$

that is, the energy difference between the ground state of the Hamiltonian with the charges included and with charges omitted is purely potential. V(R) is the heavy quark potential if we define:

$$V(R) = -\lim_{T\to\infty} \frac{1}{T} \ln \langle \mathrm{Tr}\, P \exp ig\oint_c A_\mu dx_\mu \rangle \tag{1.22}$$

P reminds us that operator order is important. The quantity

$$\langle \mathrm{Tr}\, P \exp ig \oint_c A_\mu dx_\mu \rangle \tag{1.23}$$

is the continuum analogue of the Wilson loop defined above. Hence, on the lattice, the heavy quark potential is given by:

$$V(R) = -\lim_{T\to\infty} \frac{1}{T} \ln \langle \mathrm{Tr} \prod_{\mu,n \in C} U_\mu(n) \rangle$$
$$= -\lim_{T\to\infty} \frac{1}{T} \ln W(C) \qquad (1.24)$$

If the heavy quark potential grows linearly at large separation:

$$V(R) \xrightarrow[R\to\infty]{} KR \qquad (1.25)$$

then, for large loops, we expect:

$$W(R,T) \underset{T\to\infty}{\sim} \exp(-KRT) \qquad (1.26)$$

and so the loop expectation value grows with the exponential of the area of the loop, and the coefficient of this area law is the coefficient of the linear potential (the string tension). In this case, an infinite amount of energy would be required to separate the quarks, and consequently they are confined.

In a theory without confinement, the energy of a quark-antiquark pair should not grow indefinitely with separation, but rather approach twice the self energy of an isolated quark, so that a new pair may be created from the vacuum. The Wilson loop then decreases more slowly with loop size. In fact,

$$W(C) \sim \exp\{-K'(R+T)\} \qquad (1.27)$$

and we have perimeter law behaviour.

To examine the strong coupling behaviour of a lattice pure gauge theory, we need to know how to perform functional integrals over the link variables, $U_\mu(n)$. In fact, we need only the following properties of group integrals:

$$\int \mathcal{D}U_\mu(\underline{n}) = 1 \qquad \int \mathcal{D}U_\mu(\underline{n})\, U_\mu(\underline{n}) = 0$$

$$\int \mathcal{D}U_\mu(\underline{n})\, U_\mu(\underline{n})\, U_\nu^\dagger(\underline{n}') = c\,\delta_{\underline{n},\underline{n}'}\,\delta_{\mu\nu} \tag{1.28}$$

for some normalisation, c. The behaviour of W(C) is now obtained by expanding the exponential of the action in the functional integral. The lowest order behaviour is obtained by diagrammatically covering the interior of the contour C with plaquettes. Each plaquette is associated with a factor $1/g^2$, and hence this minimal tiling procedure gives a leading order term:

$$\left\langle \prod_C U_\mu(\underline{n}) \right\rangle = \left(\frac{1}{g^2}\right)^{N_C} = \exp\left\{-(\ln g^2)(\text{Area}/a^2)\right\} \tag{1.29}$$

N_C is the minimal number of plaquettes contained in C, and is a measure of the area. This area law leads to a confining potential for heavy quarks, as we have seen, and we can identify the string tension at strong coupling as:

$$\sigma a^2 = \ln g^2 + \cdots \tag{1.30}$$

Higher orders in strong coupling may be obtained by considering tiling the surface in a way that is not minimal, but contains surface fluctuations. The first order term, then, consists of moving a single plaquette out of the plane of the contour C by one lattice spacing, and inserting an additional four plaquettes to connect the displaced plaquette with the rest of the minimally tiled surface. This process can be extended to higher orders.

So we have seen that confinement arises naturally in the strong coupling limit of a lattice pure gauge theory. Note that the string tension provides another order parameter for lattice gauge theory, one which does vanish in non-confining phases, remaining finite whenever the quark sources experience a linear long-range potential.

We note, without further comment here, that the area law criterion for confinement loses its value when quarks are introduced as dynamical variables. In this case, widely seperated sources may reduce their energy by pair production from the vacuum, and the Wilson loop then measures the potential between two mesons rather than simple bare quarks.

The lattice, considered as an ultraviolet cut-off, must finally be removed - the lattice spacing must be allowed to go to zero, and we approach the continuum limit. As when removing any cut-off, physical variables should approach their measureable, observable values. Consider a physical quantity q, with dimensions d in a theory with a dimensionless coupling. Then we may write:

$$q = a^d f(g) \tag{1.31}$$

The dependence of q on the lattice spacing is trivial, and the non-trivial aspects of the theory are embodied in the dimensionless function f, of the coupling. One may define a non-trivial continuum limit only if as $a \to 0$, g can be renormalised so that q remains finite. There must exist a critical value g^* such that:

$$\lim_{g \to g^*} f(g) = \infty \tag{1.32}$$

If q is to remain finite, g must be a function of the lattice spacing:

$$q = a^d f(g(a)) \tag{1.33}$$

Also the critical point, $g=g^*$, must have scaling properties, that is, once the functional relationship between g and a is established by demanding constancy of a definite observable, the same relation must make all other observables tend to well-defined values as $a \to 0$. To establish the existence of such a scaling critical point is a non-trivial problem, but for non-Abelian gauge theories, perturbative arguments show that g=0 is such a point: the infra-red unstable fixed point in the neighbourhood of which one can use perturbation theory.

In the continuum limit, all physical quantities should become independent of the lattice cut-off, that is:

$$a \frac{dq}{da} = 0 = a \frac{\partial q}{\partial a} - \beta(g) \frac{\partial q}{\partial g} \tag{1.34}$$

where

$$\beta(g) = - a \frac{\partial g}{\partial a} \tag{1.35}$$

The Callan-Symanzik β function has been calculated in perturbation theory by Politzer (1973) and by Gross and Wilczek (1973):

$$-\beta(g) = \beta_0 g^3 + \beta_1 g^5 + \cdots \tag{1.36}$$

where for an SU(N) theory:

$$\beta_0 = \frac{11}{3}\left(\frac{N}{16\pi^2}\right) \qquad \beta_1 = \frac{34}{3}\left(\frac{N^2}{16\pi^2}\right) \tag{1.37}$$

Consider a physical mass m in the theory. One may write:

$$m = \frac{1}{a} f(g) \tag{1.38}$$

Then writing:

$$a \frac{dm}{da} = 0 \tag{1.39}$$

we have:

$$f(g) + \beta(g) \frac{df(g)}{dg} = 0 \tag{1.40}$$

whence:

$$f(g) = \exp\left\{-\int^g \frac{dg'}{\beta(g')}\right\} \tag{1.41}$$

One can then write down the functional relationship between a and g in the general form:

$$a = \frac{1}{\Lambda} f(g) \tag{1.42}$$

and so:

$$\Lambda^{latt} = \frac{1}{a} \exp\left\{-\int^g \frac{dg'}{\beta(g')}\right\} \tag{1.43}$$

where Λ^{latt} is a physical mass which sets the scale for all masses in the theory. One can write Λ^{latt} in terms of β_1 and β_0 (Gross and Wilczek, 1973; Politzer, 1973; Caswell, 1974; Jones, 1974):

$$\Lambda^{latt} = \frac{1}{a} \exp\left(-\tfrac{1}{2}\beta_0 g^2\right)\left(\beta_0 g^2\right)^{-\beta_1/2\beta_0^2}\left(1+O(g^2)\right) \quad (1.44)$$

and hence we find that ratios of dynamically generated masses are pure numbers depending only on the gauge group - once the scale is set, all the masses of the theory are determined with no free parameters. Thus, one concludes that for pure gauge theories, the strong interaction has no free parameters. The cut-off is absorbed into g(a), and this is in turn absorbed into the renormalisation group dependence of physical masses. The only remaining dimensionful parameter is Λ. Coleman and Weinberg (1973) have given this process the name dimensional transmutation.

One is now able to relate lattice calculations to ones based on continuum regularisation schemes by relating their Λ parameters. This is done by calculating both the divergent and finite parts of the one-loop coupling constant renormalisation. Hasenfratz and Hasenfratz (1980) found, in the Feynman gauge:

$$\begin{aligned} \Lambda^{mom} &= 57.5\ \Lambda^{latt} \qquad SU(2) \\ &= 83.5\ \Lambda^{latt} \qquad SU(3) \end{aligned} \quad (1.45)$$

So far, we have shown that the pure gauge theory is confining in the strong coupling limit, and that the continuum limit is reached when g=0. If the phenomenon of confinement is to remain in the continuum limit, it is necessary that there be no phase transition for intermediate values of the coupling separating the two

regimes. It is known that such a transition occurs in the U(1) gauge theory: there is a critical point separating the charge confining phase from the free charge phase. This is of course as it should be: continuum QED in four dimensions is not a confining theory. Much work has been done on the investigation of phase diagrams for various gauge theories using a variety of techniques: high and low temperature expansions, duality transformations, mean field theory, and numerical simulations based on a search for hysteresis loops in the behaviour of some quantity as the coupling β is varied, which occur due to a critical slowing down of numerical algorithms as a critical point is approached.

Having constructed our pure gauge theory and shown that it has some potentially useful properties, we wish to formulate a theory of interacting fermionic and gauge fields on a lattice, but before going on to do so, we first mention some of the quantities that have been calculated in pure gauge theories., with particular attention to Monte Carlo results. For more details, see the various reviews in the literature (Kogut, 1979; Kogut, 1983; Creutz, Jacobs and Rebbi, 1983; Creutz, 1983).

Above, we discussed the importance of the critical points of the lattice theory. Monte Carlo results are particularly well suited to a study of the non-perturbative effects responsible for the critical behaviour of a statistical system. The U(1) phase transition mentioned above has been studied by Lautrup and Nauenberg (1980), and by Bhanot (1981) and Hamber (1981). The results of these analyses provide strong evidence for a second order phase transition. DeGrand and Toussaint (1980) identified the condensation of monopoles at the critical point as being the physical mechanism responsible for this phase transition.

The critical properties of spin systems depend crucially upon the dimensionality of the lattice, and in view of the deep analogies between gauge theories and spin systems, one expects the existence of critical dimensions for gauge theories. In particular, the U(1) model in four dimensions has a continuum limit describing free massless photons, as we would expect. The question is whether d=4 is the critical dimension for gauge theories. It seems that for d<4, the pure U(1) theory confines photons, of importance for the Schwinger model, and we expect that for d>4, the confining properties of non-Abelian models will be lost.

Investigations of SU(2) and SU(3) have been performed using discrete subgroups. These simulations suggest the absence of a phase transition for the pure SU(2) gauge theory in four dimensions, though in five dimensions, there is evidence of a first order transition. Hence, in four dimensions, SU(2) is confining at all temperatures, though in higher dimensions there is a deconfining transition. This has been rigorously proved (Tomboulis, 1983).

Investigations of SU(3) have proved more difficult, but here too there appears to be no deconfining phase transition in four dimensions.

Mention was made earlier of the string tension which measures the large distance attractive force felt by two static quarks. This is obtained from measurements of the Wilson loop, using (1.17). In practise, one calculates :

$$\chi(I,J) = -\ln\left(\frac{W(I,J)\,W(I-1,J-1)}{W(I,J-1)\,W(I-1,J)}\right) \qquad (1.46)$$

where W(I,J) is a Wilson loop of dimensions I and J in the two directions. The above expression is used in an attempt to eliminate the dependence on size, the true string tension

being obtained in the limit of large I and J, though of course in practice quite small values of I and J have to be used. The results, obtained initially by Creutz (1980) and subsequently reproduced by others, give a string tension, K(g), which follows strong coupling results for small β and then, for larger β follows a scaling behaviour :

$$K(g) = \sigma a^2(g) = \frac{\sigma}{\Lambda^2} (\beta_0 g^2)^{\beta_1/2\beta_0^2} \exp(\tfrac{1}{2}\beta_0 g^2) \qquad (1.47)$$

For larger values of β, one obtains the perturbative behaviour:

$$K(g) \propto \text{constant} \times \beta^{-1} \qquad (1.48)$$

In fact, rather than determining the string tension, by assuming it to be a basic observable, we fix the value of Λ^{latt}, setting the scale for all the physical quantities of the theory.

A second quantity of interest is the mass gap. In a confining theory, where there are no long range forces, one expects the absence of massless mediating particles, and so the mass spectrum of the theory should begin with the first state above the vacuum having some positive mass, m_g, the mass gap of the theory. This represents the mass of a well-defined particle like excitation of the pure gauge system, called a glueball, and in the absence of fermions, the lowest lying such state must be stable, although clearly the state could be broadened by coupling to fermions.

Numerical simulations to calculate this quantity are performed by choosing some operator $O(\underline{x},t)$ that has a non-zero overlap with the required state and then calculating the connected correlation function:

$$G_T(\underline{x},t;\underline{x}',0) = \langle \hat{O}(\underline{x},t)\, \hat{O}(\underline{x}',0) \rangle - \langle \hat{O} \rangle^2 \qquad (1.49)$$

This may be expanded by inserting a complete set of energy-momentum eigenstates, $|n\rangle$, and assuming translational invariance:

$$G(\underline{x},t;\underline{x}',0) = \sum_{n\neq 0} \langle 0|\hat{O}|n\rangle\langle n|\hat{O}|0\rangle e^{-E_n t - i\underline{P}_n(\underline{x}-\underline{x}')} \tag{1.50}$$

Summing over the spatial directions picks out the zero momentum state, and gives:

$$G_c'(t) = \sum_{n\neq 0} |\langle n|\hat{O}|0\rangle|^2 e^{-m_n t} \tag{1.51}$$

where m_n is the mass of the state $|n\rangle$. For sufficiently large t, only the lightest state remains:

$$\lim_{t\to\infty} G_c'(t) \propto e^{-m_g t} \tag{1.52}$$

and m_g may be measured from the exponential fall-off of the propagator.

Measurements are complicated by the fact that higher mass states also in general have a non-zero overlap with $O(\underline{x},t)$, and consequently contribute to $G_c(t)$. Hence, to see a clear glueball mass, we need to go to large times. However, as the correlation length of the glueball state, $1/m_g$, is quite small over the range of couplings for which the Monte Carlo calculations may be performed, the propagator falls off very quickly and becomes of the same order as the statistical fluctuations after only three or four lattice spacings. Numbers have been obtained for the glueball mass (Ishikawa, Teper and Schierholz, 1982; Berg and Billoire, 1982 a and b ; Michael and Teesdale, 1982), and there is a broad

agreement on a lightest glueball mass:

$$m_g \simeq 750 \pm 50 \text{ MeV} \qquad (1.53)$$
$$(\Lambda^{\overline{mom}} = 200 \text{ MeV})$$

Various other interesting calculations have been performed in lattice theories: the quark potential has been measured; the restoration of rotational symmetry in the continuum limit has been investigated; and topological charges have been measured. However, of most interest here are the particle mass calculations that have been performed using Monte Carlo methods. These masses are calculated by first generating a set of gauge field configurations, either according to a 'quenched' action in which the effects of dynamical fermions (i.e. the effects of internal fermion loops) are neglected, or according to an action in which dynamical fermions are included, according to some scheme. Next, some lattice operator is written down that has the quantum numbers of the particle whose mass we wish to measure. For mesons, this operator consists of a quark-antiquark operator, together with some matrices giving the operator its appropriate flavour, parity, etc.. For baryons it consists of some totally anti-symmetric combination of three quarks, again with appropriate matrices. It should be noted that in general such a lattice operator will not represent a unique continuum state, but rather will have a non-zero overlap with a whole series of states with the same quantum numbers, but differing in energy. The calculation proceeds by finding the correlation function of the appropriate lattice operator, and averaging this over configurations of the gauge field. Clearly, a knowledge of the correlation function of meson and baryon operators requires a knowledge of the correlation functions of the individual quarks, that is of the quark propagators, and it is these that are calculated for each gauge

configuration, and put together to form the various particle propagators. Following an identical argument as for the glueball mass calculations, one can show that particle propagators, when summed over the spatial directions, should fall off exponentially with the mass of the particle. Again, one is interested in the behaviour of this so-called 'time slice propagator' at large times, where one expects the lightest particle state to be exposed. Of course, if one is interested in particles of even moderate mass, their correlation lengths will be quite small, and hence the propagator quickly disappears into statistical noise. In summary, then one calculates:

$$\lim_{t \to \infty} \sum_{\underline{n}} \langle \hat{A}(n) \hat{A}(0) \rangle \sim e^{-m_A t} \qquad (1.54)$$

where A is an operator with the correct quantum numbers, m_A is the mass of the state of interest, and ∞ is a few lattice spacings.

Mass calculations are subject to an array of problems, stemming from finite size effects and statistical errors, but nevertheless many essential features of QCD emerge. The pion appears as the lightest meson, and may thus be interpreted as a Goldstone boson by a suitable extrapolation to vanishing quark mass. The fermion condensate, $\langle \bar{\psi}\psi \rangle$, measuring chiral symmetry breaking in the theory has been measured, and the rho is measured to be heavier than the pion, with a mass that remains finite in the limit of vanishing pion mass.

However it is clear that many features of the finite lattice approximation have an important effect upon the measurements which need to be better understood. The small lattices on which simulations are presently performed present an immediate problem when their physical size is

considered: in most cases they are about the size of a proton. Correlations between successive gauge configurations present problems in obtaining good statistical data, and the number of configurations averaged over is generally rather small. The algorithms used for finding quark propagators are often slow in the region of small quark masses, and as a result it is usually necessary to perform some extrapolation to zero mass, possibly introducing more error.

Finally, we note that some work has also been done with two dimensional systems, with various gauge groups, including both U(1) and SU(2). It is clearly easier to do simulations with such models than with four dimensional theories. Also, analytical results are often available for comparison. In the context of four dimensional QCD, for instance, most work has been done in the quenched approximation, where internal quark loops are neglected, but if we wish to work with smaller quark masses, nearer their physical values, then we need to be able to include the effects of dynamical fermions. Such effects are obviously more easily considered in two dimensions than in four. The computer time required for a two dimensional simulation will in general be less, and finite size effects cause less problems, because there is a smaller proportion of lattice sites on the boundary. In the work presented here, we perform numerical simulations for one such two dimensional system (and generalisations of it): the Schwinger model. In the next chapter we present continuum results for this model, and in subsequent chapters present the lattice version and the numerical results we have obtained.

CHAPTER TWO

THE CONTINUUM SCHWINGER MODEL

The Schwinger model (Schwinger, 1962) is quantum electrodynamics of a massless fermion with charge g in 1+1 dimensions. It is exactly soluble. The massive theory is not, although some of its properties are known.

The model displays many of the features of 3+1 dimensional QCD in a relatively simple form. In particular it displays both asymptotic freedom and confinement of the fundamental charges ('quarks'). One hopes, then, that the methods developed for an an investigation of the Schwinger model may be of use in an investigation of QCD.

2.1 The Massless One Species Schwinger Model.

The model may be described by the Lagrangian density:

$$\mathcal{L} = \bar{\psi} i\gamma_\mu \partial^\mu \psi - \frac{1}{4} F_{\mu\nu} F^{\mu\nu} - g\bar{\psi}\gamma_\mu \psi A^\mu \qquad (2.1)$$

with

$$\begin{aligned} &x = (x^0, x^1) \\ &g^{00} = -g^{11} = 1 \qquad g^{01} = g^{10} = 0 \\ &\varepsilon^{10} = -\varepsilon^{01} = -1 \qquad \varepsilon^{00} = \varepsilon^{11} = 0 \\ &\{\gamma_\mu, \gamma_\nu\} = 2 g_{\mu\nu} \\ &\psi = \begin{pmatrix} \psi^1 \\ \psi^2 \end{pmatrix} \qquad \bar{\psi} = \psi^\dagger \gamma_0 \qquad \gamma_5 = \gamma_0 \gamma_1 \end{aligned} \qquad (2.2)$$

The equations of motion are given by:

$$\gamma_\mu (i\partial^\mu - gA^\mu)\psi = 0$$
$$j_\mu \equiv g\bar{\psi}\gamma_\mu\psi = \partial^\nu F_{\nu\mu} \qquad (2.3)$$

The coupling constant g has dimensions of mass and the model is consequently super-renormalisable. No infinite renormalisations are necessary apart from a trivial renormalisation of the zero point energy. Both g and m are finite (though bare) parameters.

Following Schwinger, alternative solutions of the massless model have been given by Casher, Kogut and Susskind (1974); by Coleman, Jackiw and Susskind (1975); and by Baaquie (1982) amongst others.

Casher, Kogut and Susskind solve the model in terms of the degrees of freedom of the Lagrangian given above (this is not necessary: an alternative solution in terms of bosonic fields is outlined below). They are able to show that the single fermion Green's function for a right moving particle, in the Coulomb gauge, is given by:

$$\langle 0|\psi_R^\dagger(x_1,x_0)\psi_R(0,0)|0\rangle = \langle 0|\chi_R^\dagger(x_1,x_0)\chi_R(0,0)|0\rangle e^{K(x_1,x_0)} \qquad (2.4)$$

with

$$K(x_1,x_0) = \text{const}\times\int[e^{i(kx_1-\omega_k x_0)}-1]\frac{(\omega_k-k)^2}{k^2\omega_k}\,dk \qquad (2.5)$$

where χ_R satisfies the free field equation for a right mover:

$$\left(\frac{\partial}{\partial x_0} + \frac{\partial}{\partial x_1}\right)\chi_R = 0 \qquad (2.6)$$

For $x_0=0$, the integral defining $K(x_1,x_0)$ converges and tends to zero as x_1 tends to zero. In this limit, the propagator looks like a free field propagator. For $x_0\neq 0$ the integral diverges for all values of x_1, and the propagator vanishes. Thus there are no real asymptotic fermions in the theory.

It is further shown that:

$$\begin{aligned} T^{\mu\nu}_{free}(x) &= -i\langle 0|T\, j^{\mu}(x)\, j^{\nu}(x)|0\rangle \\ &= \frac{g^2}{\pi}\left(g^{\mu\nu}\Box - \partial^{\mu}\partial^{\nu}\right)\Delta_F(m^2,x^2) \end{aligned} \qquad (2.7)$$

where Δ_F is the Feynman propagator, and $m^2=g^2/\pi$, and j_μ is given in (2.3).

Thus the particle spectrum contains only one boson of mass $m^2=g^2/\pi$.

Baaquie (1982) similarly solves the model in terms of the original degrees of freedom in Euclidean space, using a functional approach. In this approach, the gauge field A_μ is decomposed into a gauge invariant pseudoscalar field and a gauge dependent scalar field:

$$A_\mu(x) = \varepsilon_{\mu\nu}\partial^{\nu}S(x) + \partial_\mu\varphi(x) \qquad (2.8)$$

Gauge transformations may be be performed on the Fermi fields to eliminate the scalar field φ, although this limits calculations in the Fermi sector of the theory to gauge invariant quantities.

Baaquie shows that the Ward identity for the vector field is satisfied:

$$\langle \partial_\mu j^\mu(x) \rangle = 0 \tag{2.9}$$

but that there is an axial anomaly:

$$\langle \partial_\mu j_5^\mu(x) \rangle = \langle \partial_\mu \bar{\psi}(x) \gamma_\mu \gamma_5 \psi(x) \rangle = \partial^2 S(x)/\pi \tag{2.10}$$

The coupling of the gauge field to the fermions is shown to be via this anomaly.

Baaquie's approach also makes it possible to calculate the Wilson loop integral for the gauge field in the interacting theory. Let C denote a circular contour of radius L, enclosing a unique area. Then:

$$e^{W(C)} \equiv \langle \exp\left(i \oint_C A_\mu \, dx^\mu\right) \rangle \tag{2.11}$$

where Z is the partition function:

$$Z \equiv \prod_x \int dS(x) \, d\bar{\psi}(x) \, d\psi(x) \, e^A \tag{2.12}$$

for the action, A:

$$A = \frac{-1}{4g^2} \int F_{\mu\nu} F^{\mu\nu} \, d^2x + \int (\bar{\psi} \not{\partial} \psi + \bar{\psi} \gamma_\mu \gamma_5 \psi \partial^\mu S) \, d^2x \tag{2.13}$$

Then, in the Landau gauge ($\partial_\mu A_\mu = 0$):

$$W = -\pi (gL)^2 I_1(mL) K_1(mL) \qquad (2.14)$$

where I and K are the associated Bessel functions of the first and second kind. This expression is exact, and has the following asymptotic behaviour:

$$\lim_{L\to\infty} W \sim \begin{cases} -L^2 & g^2 = 0 \\ -L & g^2 > 0 \end{cases} \qquad (2.15)$$

For $g>0$, there is a perimeter law rather than the area law which is the usual confinement criterion for pure gauge theories. The area law applies only in the absence of fermions, i.e. $g=0$. Baaquie thus interprets the results in the following way: if the loop integral shows area law behaviour for the pure gauge field, then when this gauge field is coupled to fermions the fermions are confined, although area law behaviour is not expected for the interacting case. Hence, the Wilson loop has no direct interpretation in terms of virtual paths for fermions.

Coleman, Jackiw and Susskind solve the model by making a correspondence with a boson theory. The correspondences between boson and fermion theories in 1+1 dimensions have been investigated by Coleman, by Kogut and Susskind, by Mandelstam (1975) and by Bander (1976). The correspondence for the Schwinger model is as follows: ψ is a Dirac field with chiral components

$$\psi = \begin{pmatrix} \psi_1 \\ \psi_2 \end{pmatrix} \qquad (2.16)$$

satisfying

$$i\left(\frac{\partial}{\partial x_0}+\frac{\partial}{\partial x_1}\right)\psi^1 = i\partial_+\psi^1 = 0$$
$$i\left(\frac{\partial}{\partial x_0}-\frac{\partial}{\partial x_1}\right)\psi^2 = i\partial_-\psi^2 = 0 \qquad (2.17)$$

φ is a massless boson field, with canonical momentum π, and partition function:

$$\mathcal{Z} = \int \mathcal{D}\varphi\mathcal{D}\pi \exp i\int d^2x\left(\pi\partial_0\varphi - \tfrac{1}{2}[\pi^2+\partial_1\varphi^2]\right) \qquad (2.18)$$

with

$$\partial_0 = \frac{\partial}{\partial x_0} \qquad \partial_1 = \frac{\partial}{\partial x_1} \qquad (2.19)$$

Then, identify:

$$\psi^{1,2}(x) = \left(\frac{\Lambda}{2\pi\gamma}\right)^{1/2} \exp\left(-i\sqrt{\pi}\int_{-\infty}^{x_1} d\xi\, e^{\xi/R}[\pi(x_0,\xi)\pm\partial_1\varphi(x_0,\xi)]\right) \qquad (2.20)$$

where R is a spatial cut-off, introduced to keep the integrals finite, and set to infinity at the end of the calculation; Λ is a momentum cut-off, which is also allowed to go to infinity, and γ is Euler's constant. In order to construct an interacting theory with massive fermions, we also need correspondences for composite operators. In particular:

$$:\bar{\psi}\gamma_\mu\psi: \;=\; \frac{\varepsilon_{\mu\nu}}{\sqrt{\pi}}\partial^\nu\varphi$$

$$:\bar{\psi}\psi: \;=\; c\,m\,N_m \cos(2\sqrt{\pi}\varphi)$$
$$c \;=\; \frac{e^{\gamma}}{2\pi} \qquad (2.21)$$

N_m here means normal ordering with respect to mass m (Coleman, 1975). This has the effect of replacing the divergent loop integral of figure 2.1 according to:

$$\int \frac{d^2k}{k^2+\mu^2} \rightarrow \int d^2k \left[\frac{1}{k^2+\mu^2} - \frac{1}{k^2+m^2}\right] \qquad (2.22)$$

If m^2 is set to equal to μ^2, the usual prescription, the graph is cancelled completely.

In the Coulomb gauge, $A_1=0$, we have, from (2.1):

$$A_0 = -\frac{e}{\partial_1^2}\bar{\psi}\gamma_0\psi \qquad (2.23)$$

so that the effective Lagrangian for fermions is:

$$\mathcal{L}_{eff} = i\bar{\psi}\not{\partial}\psi - \frac{e^2}{2}\bar{\psi}\gamma_0\psi\,\frac{1}{\partial_1^2}\,\bar{\psi}\gamma_0\psi \qquad (2.24)$$

and hence by making the correspondence with the scalar field:

$$\mathcal{L} = \pi_0\partial_0\varphi - \frac{\pi^2}{2} - \frac{(\partial_1\varphi)^2}{2} - \frac{e^2}{2\pi}(\partial_1\varphi)\frac{1}{\partial_1^2}(\partial_1\varphi) \qquad (2.25)$$

This may be simplified to the action for a massive boson of mass $m^2=g^2/\pi=\mu^2$:

$$\mathcal{L} = \pi\partial_0\varphi - \frac{\pi^2}{2} - \frac{(\partial_1\varphi)^2}{2} - \frac{\mu^2}{2}\varphi^2 \qquad (2.26)$$

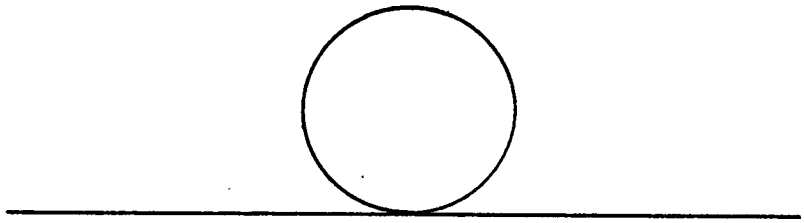

Fig 2.1
Tadpole diagram for the Bose
form of the Shwinger model.

In summary then the massless model is exactly soluble and possesses the following properties. Local electric charge conservation is spontaneously broken but no Goldstone boson appears as the Goldstone mode may be gauged away. Global chiral symmetry is also spontaneously broken and the vacuum is infinitely degenerate. Different vacua may be labelled by an angle $\theta\varepsilon[0,2\pi]$, and global chiral transformations rotate one vacuum into another. Again no Goldstone boson appears, as the axial current is afflicted with an anomaly. The parameter θ may be identified with a constant background electric field. This field could be introduced into 4-dimensional QED but here the vacuum would suffer dielectric breakdown. In 4-dimensions it is always energetically favourable for the vacuum to emit pairs until the background field is brought down to zero. In one spatial dimension, however, the energetics of pair production are different, and it is not energetically favourable for the vacuum to produce a pair if the background field F is such that $|F|\leqslant e/2$. If $|F|>e/2$, pairs will be produced until $|F|\leqslant e/2$. Physics is thus a periodic function of F, with period e, and θ may be identified as

$$\theta = \frac{2\pi F}{e} \qquad (2.27)$$

2.2 The Massive One Species Model.

The model so far considered may be extended by giving the fermions a mass:

$$\mathcal{L} \rightarrow \mathcal{L} - m\bar{\psi}\psi \qquad (2.28)$$

The model is no longer exactly soluble, but it is possible to do perturbation theory in the mass parameter (Kogut and Susskind, 1974; Coleman, Jackiw and Susskind, 1975). In terms of the boson theory, adding a mass term for the fermions changes the Lagrangian to:

$$\mathcal{L} = \frac{1}{2}(\partial\varphi)^2 - \frac{1}{2}\mu^2\varphi^2 - \frac{m\Lambda}{\pi\gamma}\cos(2\sqrt{\pi}\varphi) \qquad (2.29)$$

The massive model is still dependent upon the parameter θ of the massless model, labelling different vacua. The mass term of course explicitly breaks the chiral invariance, so that the vacua are no longer degenerate, but all the vacua remain stable as a result of the absence of Goldstone bosons. This is unusual: generally, when one adds a symmetry breaking term to a theory that displays spontaneous symmetry breaking, the symmetry breaking term removes the degeneracy of the vacua of the original theory (as here) and all the vacua other than the one of lowest energy become unstable, decaying through the emission of Goldstone bosons.

Although the Lagrangian has been written in terms of boson fields, this does not immediately imply that the spectrum of the theory contains no free fermions. Both weakly coupled φ^4 and the sine-Gordon equation are counter examples. However, Coleman, Jackiw and Susskind show that the interaction energy between two widely separated external charges of charge Q is:

$$E = L\left[\varepsilon\left(\theta - \frac{2\pi Q}{e}\right) - \varepsilon(\theta)\right] + \cdots \qquad (2.30)$$

where $\varepsilon(\theta)$ is the vacuum energy per unit length, and L is the distance between the charges. Thus there is no long range force between the charges if Q is an integral multiple of g (remember that physics is periodic in θ, with period 2π), independent of perturbation theory. On the other hand, for arbitrary Q the long range force is present, at least in mass perturbation theory. The disappearance of the long range force is connected with the easy polarisability of the vacuum, and hence with the absence of free fermions from the mass spectrum.

From henceforth we consider only the case $\theta=0$.

For $m \ll g$ the Lagrangian describes a heavy quantum interacting with itself through a weak attractive φ^4 interaction (this comes from expanding the cosine in (2.29); the term in φ^2 shifts the mass of the meson)(Carroll, Kogut, Sinclair, and Susskind, 1976). The model always contains at least one particle, the original pseudoscalar meson of mass:

$$M^- = \frac{g}{\sqrt{\pi}} + me^{\gamma} + O(m^2) \qquad (2.31)$$

Any other particles present will be weakly bound n-mesons of mass nM^- (plus corrections). In particular, the next particle is a scalar meson of mass:

$$M^+ = 2M^- - 2\pi^2 e^{2\gamma} \frac{m^2}{M^-} + O(m^2) \qquad (2.32)$$

As m tends to infinity, the fermion decouples from the theory, and the model reduces to a pure U(1) gauge theory which may be solved by transfer matrix methods. A suitable

gauge transformation shows the pure gauge theory to be equivalent to a set of independent one-dimensional XY spin models, with free energy:

$$F = \ln I_0(2\beta) - 2\beta \tag{2.33}$$

and average plaquette energy (proportional to energy density):

$$\langle 1 - \cos\theta_{\mu\nu} \rangle = \frac{1}{2} E = -\frac{1}{2} \frac{\partial F}{\partial \beta} \tag{2.34}$$

where $\theta_{\mu\nu}$ is the directed sum of links around a plaquette. In this confining theory, a square Wilson loop Γ, enclosing the unique area A is:

$$W(\Gamma) = [I_1(2\beta) / I_0(2\beta)]^A \tag{2.35}$$

and the string tension is:

$$T = \ln [I_0(2\beta) / I_1(2\beta)] \tag{2.36}$$

with

$$T = \begin{cases} \ln \beta + O(\beta^2) & \beta \ll 1 \\ \frac{1}{4\beta} + O\left(\frac{1}{\beta^2}\right) & \beta \gg 1 \end{cases} \tag{2.37}$$

For $m<g$, strong coupling expansions provide a systematic and simple method for calculating the particle spectrum of the theory (Banks, Susskind and Kogut, 1976; Carroll, Kogut,

Sinclair and Susskind, 1976; Kenway and Hamer, 1978). The expansion parameter is (1/ga) (a is the lattice spacing) and when this is small, the kinetic terms may be treated as a perturbation on the static terms. The strong coupling limit is confining, and in order to extract continuum results it is necessary to extrapolate to the weak coupling regime. In order that the extrapolation be smooth, it is necessary that there be no intermediate phase transition. Monte Carlo simulations of the pure gauge theory and approximate renormalisation group analysis (Migdal, 1975; Kadanoff, 1976) both appear to show that this is so. Applied to the Schwinger model, these methods provide good agreement with continuum results, where they can be compared (in many cases to 2 or 3%)

2.3 The Two Species Schwinger Model.

The generalisation of the Schwinger model to a model with flavour was first introduced by Coleman (1975). The new model is described by the Lagrangian density:

$$\mathcal{L} = \sum_{i=1}^{2} \bar{\psi}_i \left(i\partial\!\!\!/ - m_i - g A\!\!\!/ \right) \psi_i - \frac{1}{4} F_{\mu\nu} F^{\mu\nu}$$

$$F_{\mu\nu} = \partial_\mu A_\nu - \partial_\nu A_\mu \qquad (2.38)$$

When the fermions are given equal masses, the model has an internal global SU(2) symmetry, called isospin. The Dirac field ψ forms an isodoublet whereas the gauge field is an isosinglet. In two dimensions there is no spontaneous breakdown of continuous internal symmetries unless the Higgs mechanism occurs or the current conservation equations are afflicted with anomalies (Coleman, 1973).

Neither happens here and so the particles of the theory reside in isomultiplets.

Doubling the number of fermion flavours has some odd dynamical consequences. In particular, the massless model does not confine quarks. Only the charges coupled to the gauge field are confined. The fundamental flavour representation appears among the physical states as electrically neutral isospin one-half particles. The introduction of the mass term, however, filters out these states (except for special values of the background field which will not be discussed here).

Coleman finds that for $m \ll g$, the lowest mass particles reside in a pseudoscalar isotriplet, even when the isospin symmetry of the Lagrangian is explicitly broken by giving the quarks different masses. The next state is a scalar isosinglet, lying a factor $\sqrt{3}$ higher in mass.

For weak coupling, the results are generalisations of those of the one-flavour model. There are four times as many particles, arranged in isotriplets and isosinglets. The lowest lying states are the pseudoscalars with isospin one and zero. Above them are the scalars. In the passage from weak to strong coupling, the $I^P = 0^-$ and 0^+ levels cross.

The results for the 1^- and 0^+ are:

$$\frac{M_{1^-}}{g} \xrightarrow[\frac{m}{g} \to 0]{} 2.066 \left(\frac{m}{g}\right)^{2/3}$$

$$\frac{M_{0^+}}{g} \xrightarrow[\frac{m}{g} \to 0]{} 3.578 \left(\frac{m}{g}\right)^{2/3}$$

$$\frac{M_{0^+}}{M_{1^-}} \xrightarrow[\frac{m}{g} \to 0]{} \sqrt{3}$$

2.4 The Massive One Species Schwinger Model in the Quenched Approximation.

The quenched Schwinger model corresponds to an approximation in which the internal fermion loops contributing to any physical process are neglected. The approximation has been previously investigated for the massless theory by van den Doel (1984). We (Carson and Kenway, 1984) investigate the massive model in the strong coupling regime by means of the replica trick, which consists of generalising the model to one containing N identical fermion species, and taking the limit $N \to 0$ at the end of the calculation. This removes the fermionic determinant that arises from the fermion integration in the partition function and, significantly, works regardless of whether the fermion has a mass (van den Doel subtracts out the known determinant for massless fermions).

We begin with the continuum N species model, described by the Euclidean action:

$$S = \int d^2x \left[-\frac{1}{4} F_{\mu\nu} F^{\mu\nu} + \sum_{\alpha=1}^{N} \bar{\psi}_\alpha (\not{\partial} + m) \psi_\alpha + ig \sum_{\alpha=1}^{N} \bar{\psi}_\alpha \gamma_\mu \psi_\alpha A^\mu \right] \quad (2.40)$$

with

$$F_{\mu\nu} = \partial_\mu A_\nu - \partial_\nu A_\mu = \varepsilon_{\mu\nu} F_{01} \quad (2.41)$$

We next make the correspondence with the Bose theory, using (2.21) (the first of these gets a minus sign in Euclidean space). We then use the equations of motion to eliminate the gauge fields, and finally obtain:

$$S = \int d^2x \, N_m \left[-\frac{1}{2} \sum_{\alpha,\beta=1}^{N} \varphi_\alpha \left(\frac{g^2}{\pi} - \partial^2 \delta_{\alpha\beta} \right) \varphi_\beta + cm^2 \sum_{\alpha=1}^{N} \cos\left(2\sqrt{\pi}\varphi_\alpha\right) \right] \quad (2.42)$$

The quenched approximation to the one species model corresponds to setting N=0 in φ_1 Green functions.

We compute the properties of the theory defined by (2.42) in the strong coupling regime as a perturbative expansion in m/g. First consider the massless theory. The momentum space propagator for the scalar field φ is:

$$G^{(0)}_{\alpha\beta} = \frac{\delta_{\alpha\beta}}{p^2} + \frac{g^2/\pi}{p^2\left(p^2 + \frac{Ng^2}{\pi}\right)} \qquad (2.43)$$

$$= \frac{\delta_{\alpha\beta} - \frac{1}{N}}{p^2} + \frac{1}{N}\frac{1}{p^2 + \frac{Ng^2}{\pi}}$$

The superscript indicates that we are at zeroth order in perturbation theory. Thus, we recover the result of Schwinger for $\langle\varphi\varphi\rangle = G^{(0)}_{11}$ when N=1, and the result of van den Doel when N=0, that is, in the quenched approximation:

$$\langle\varphi\varphi\rangle_{N=0} = \frac{p^2 - g^2/\pi}{(p^2)^2} \qquad (2.44)$$

which is infrared divergent.

To expand in powers of m/g, it is best to re-normal order the cosine interaction in (2.42) with respect to the scalar field propagator. First introduce an infrared regulator, μ:

$$G^{(0)}_{\alpha\beta}(p;\mu) = G^{(0)}_{\alpha\beta}(p^2+\mu^2) \qquad (2.45)$$

Now undo the normal ordering with respect to the ordinary scalar propagator (N=1):

$$m N_m \cos(2\sqrt{\pi}\varphi_\alpha) = \left(\frac{1}{ca^2}\right)^{1/2} \cos(2\sqrt{\pi}\varphi_\alpha) \qquad (2.46)$$

where a is a short distance cut-off, and the ordinary scalar propagator in configuration space is:

$$G^{(0)}_{\alpha\alpha}(x=0;m;a)\big|_{N=1} = \frac{-1}{4\pi} \ln cm^2a^2 + O(m^2a^2) \qquad (2.47)$$

Finally, normal order with respect to (2.43), denoting this by $\mathcal{N}_\mu$:

$$m N_m \cos(2\sqrt{\pi}\varphi_\alpha) = \left(\frac{1}{ca^2}\right)^{1/2} \exp\left[-2\pi G^{(0)}_{\alpha\alpha}(x^2=0;\mu)\right] \times \mathcal{N}_\mu \cos(2\sqrt{\pi}\varphi_\alpha) \qquad (2.48)$$

In configuration space, the scalar propagator is:

$$G^{(0)}_{\alpha\beta}(x;\mu) = \left(\delta_{\alpha\beta} - \frac{1}{N}\right)\frac{1}{2\pi} K_0\left(\mu\sqrt{x^2+a^2}\right) + \frac{1}{2\pi N} K_0\left(\sqrt{\mu^2 + \frac{Ng^2}{\pi}}\sqrt{x^2+a^2}\right) \qquad (2.49)$$

K_0 is the associated Bessel function of the second kind. Assuming $\mu a << 1$, we have:

$$G^{(0)}_{\alpha\alpha}(0;\mu) \simeq \frac{-1}{4\pi N} \ln\left[(c\mu^2a^2)^N \left(1 + \frac{Ng^2}{\pi\mu^2}\right)\right] \qquad (2.50)$$

Substituting in (2.48):

$$m N_m \cos(2\sqrt{\pi}\varphi_\alpha) = \mu\left(1+\frac{Ng^2}{\pi\mu^2}\right)^{1/2N} \mathcal{N}_\mu \cos(2\sqrt{\pi}\varphi_\alpha) \qquad (2.51)$$

From this, we may obtain the order parameter for chiral symmetry breaking in the massless Schwinger model:

$$\begin{aligned} \langle \bar{\psi}\psi \rangle_{N=1} &= \lim_{\mu \to 0} \langle c m N_m \cos(2\sqrt{\pi}\varphi_1) \rangle \\ &= \lim_{\mu \to 0} c\mu \left(1 + \frac{g^2}{\pi\mu^2}\right)^{1/2} \\ &= \frac{cg}{\sqrt{\pi}} \end{aligned} \tag{2.52}$$

and for the quenched approximation:

$$\begin{aligned} \langle \bar{\psi}\psi \rangle_{N=0} &= \lim_{\mu \to 0} \lim_{N \to 0} \langle c m N_m \cos(2\sqrt{\pi}\varphi_1) \rangle \\ &= \lim_{\mu \to 0} \lim_{N \to 0} c\mu \left(1 + \frac{N g^2}{\pi \mu^2}\right)^{1/2N} \\ &= \lim_{\mu \to 0} c\mu \exp\left(\frac{g^2}{2\pi\mu^2}\right) \end{aligned} \tag{2.53}$$

which is the infrared divergence discovered by van den Doel. This divergence may be traced to massless propagation in the tadpole diagrams.

The properly organised action for an expansion in m/g is:

$$\begin{aligned} S = \int d^2x \Big[&-\frac{1}{2} \sum_{\alpha,\beta=1}^{N} \varphi_\alpha \left(\frac{g^2}{\pi} - (\partial^2 - \mu^2)\,\delta_{\alpha\beta} \right) \varphi_\beta \\ &+ c m \mu \left(1 + \frac{N g^2}{\pi \mu^2}\right)^{1/2N} \sum_{\alpha=1}^{N} N_\mu \cos(2\sqrt{\pi}\varphi_\alpha) \Big] \end{aligned} \tag{2.54}$$

Note that the effective expansion parameter diverges for $\mu \to 0$ when $N < 1$, and so studying the quenched approximation in this way is likely to lead to failure. It is easy to write down the scalar field propagator to first order in m/g:

$$G^{(1)}_{\alpha\beta}(p;\mu) = G^{(0)}_{\alpha\beta}\left(p^2 + \mu^2 + 4\pi c m \mu \left(1 + \frac{N g^2}{\pi \mu^2}\right)^{1/2N}\right) \tag{2.55}$$

For the unquenched one species model, we set N=1 and μ=0, and find the pole in the scalar propagator at:

$$\frac{M}{g} = \frac{1}{\sqrt{\pi}} + \frac{2\pi cm}{g} + O\left(\frac{m}{g}\right)^2 \qquad (2.56)$$

which is the familiar result.

The quenched approximation suffers from infrared divergences. Taking the limit N→0 before μ→0, we have:

$$\langle \phi\phi \rangle_{N=0} = \frac{p^2+\mu^2+4\pi cm\mu e^{g^2/2\pi\mu^2} - g^2/\pi}{\left(p^2+\mu^2+4\pi cm\mu e^{g^2/2\pi\mu^2}\right)^2}$$

$$\xrightarrow{\mu\to 0} \frac{e^{-g^2/2\pi\mu^2}}{4\pi cm\mu} \qquad (2.57)$$

Note that the momentum dependence drops out as the infrared regulator is removed. In this limit, all the fermions become trapped in local minima of the gauge field potential, and are thus localised.

Perturbation theory in m/g assumes that massless particles are propagating around the tadpole diagrams, and is clearly not a good approximation for the situation we have described. Hence we take account of these localisations (i.e. the tendency for the scalar field to acquire a large mass) in a self-consistent way as follows: re-normal order (2.55) with respect to $G_{\alpha\beta}^{(0)}(p;\lambda)$, where λ is chosen such that:

$$\lambda^2 = \mu^2 + 4\pi cm\lambda\left(1+\frac{Ng^2}{\pi\lambda^2}\right)^{1/2N} \qquad (2.58)$$

This makes $G_{\alpha\beta}^{(0)}(p;\lambda)$ the scalar propagator to order m/g, and also the propagator used for normal ordering the interaction. Thus, λ is the scalar particle mass. For N=1, this gives the same result to first order in m/g as before (2.57). For N=0, however, we have:

$$\langle \varphi \varphi \rangle_{N=0} = \frac{p^2 + \lambda^2 - g^2/\pi}{(p^2+\lambda^2)^2} \qquad (2.59)$$

with

$$\lambda^2 = \mu^2 + 4\pi c m \lambda e^{g^2/2\pi\lambda^2} \qquad (2.60)$$

This has a unique solution, as is clear from figure 2.2, satisfying $0<\lambda<\infty$, even for $\mu=0$, and so we can remove the cut-off without encountering any infrared divergences, provided that m>0. The expansion parameter is now small ($\sim(m\lambda/g)$) so perturbation theory is valid. We conclude that the pseudoscalar particle exists in the quenched approximation with mass:

$$M^-_{N=0} = \lambda = 4\pi c m e^{g^2/2\pi\lambda^2} \qquad (2.61)$$

The order parameter for chiral symmetry breaking is:

$$\langle \bar{\psi}\psi \rangle_{N=0} = c\lambda e^{g^2/2\pi\lambda^2} \qquad (2.62)$$

These equations may be solved numerically, to obtain M^-/g and $\langle\bar{\psi}\psi\rangle/g$ as functions of m/g. The results are shown in figures 2.3 and 2.4. Also, in the limit $m/g \to 0$, we have:

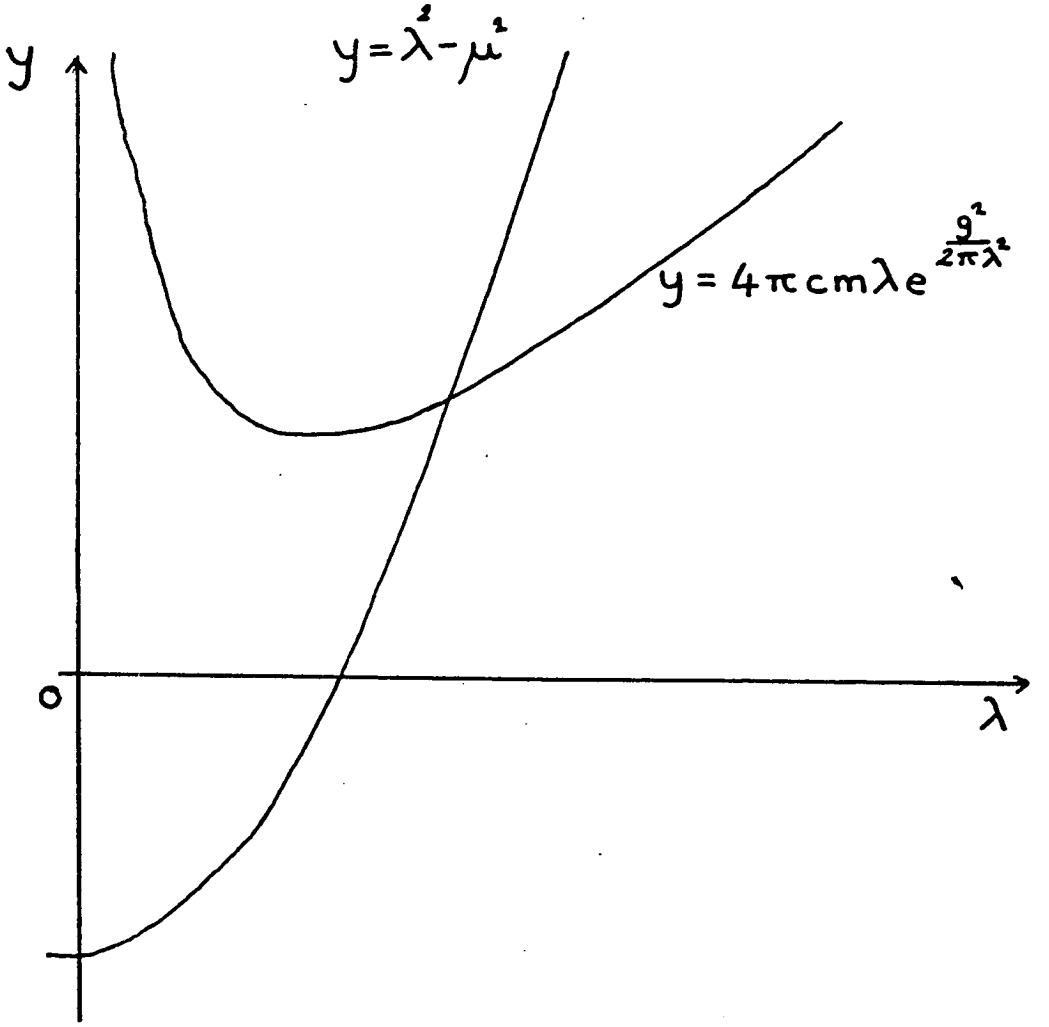

Fig 2.2

Showing that equation (2.60) has a unique solution.

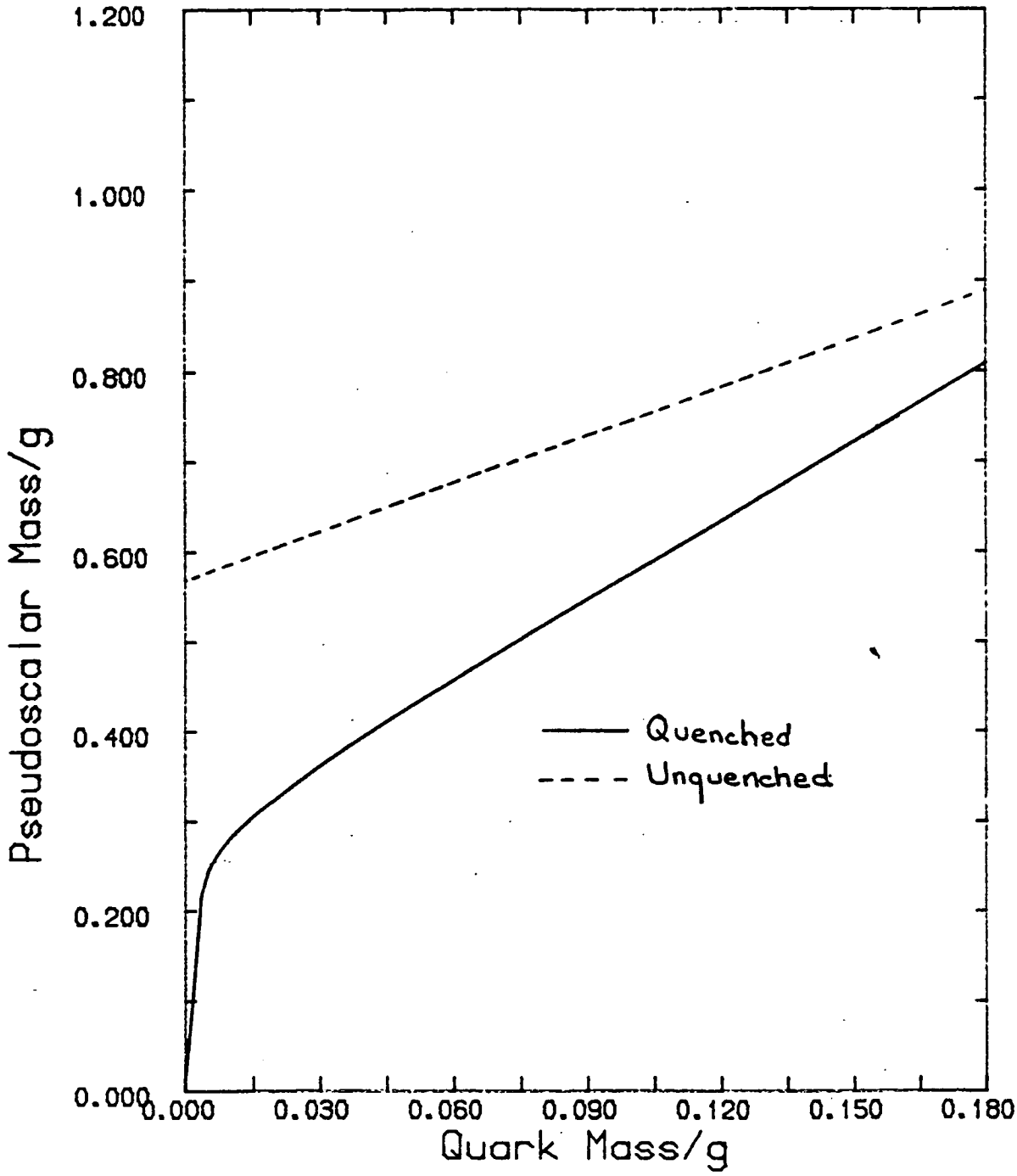

Fig 2.3

Pseudoscalar Mass as a function of quark mass in the one species model.

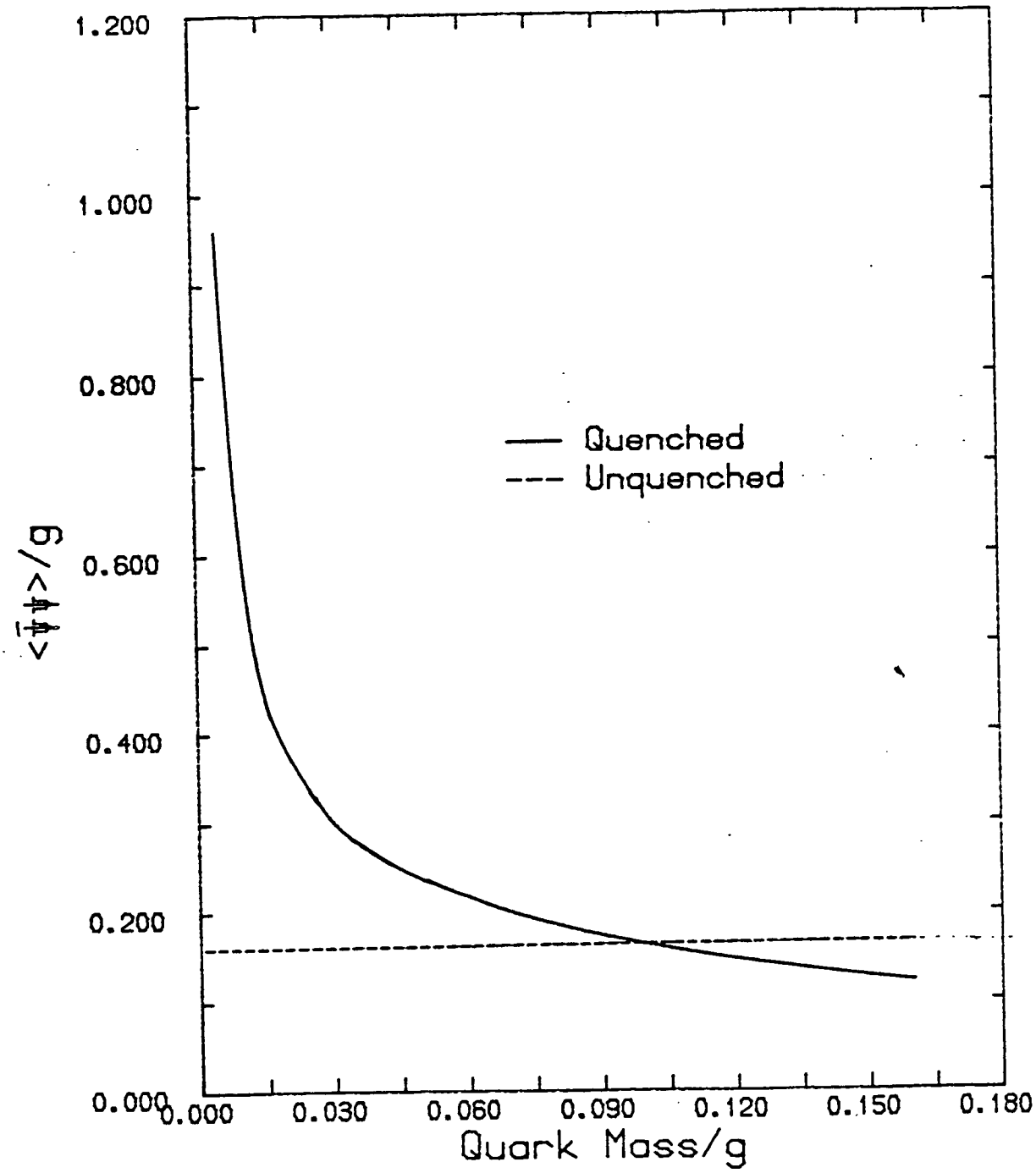

Fig 2.4

Fermionic Condensate as a function of quark mass in the one species model.

$$\frac{M}{g}_{N=0} \xrightarrow[\frac{m}{g}\to 0]{} \frac{1}{\sqrt{\left[-2\pi \ln\left(\sqrt{2\pi}\, 4\pi \frac{cm}{g}\right)\right.}} \qquad (2.63)$$

so that the pseudoscalar mass vanishes slowly, and the massless quenched theory agrees with that of van den Doel. However, the divergence in $\langle\bar{\psi}\psi\rangle_{N=0}$ as $m/g \to 0$ is much weaker than van den Doel's result. As m/g increases, we note that the result for $N=0$ and $N=1$ are becoming similar. This is to be expected: as the fermion mass becomes greater, the effects of internal loops become less important.

CHAPTER THREE

THE LATTICE SCHWINGER MODEL

In this chapter, we shall formulate the Schwinger model on a lattice, paying attention not only to how to formulate the basic Lagrangian, but also to how to form the mesonic operators from the fundamental fields of the Lagrangian.

Before going into details about the lattice Schwinger model, we need first to consider how to put the Dirac equation on the lattice.

3.1 Lattice Fermions.

Consider the action for free fermions in the continuum:

$$S_F = \int d^d x \, \bar{\psi} (\not{\partial} + m) \psi \qquad (3.1)$$

in d-dimensional Euclidean space. This action represents one fermion of mass m. We discretise the action by making the replacement :

$$\partial_\mu \psi(x) \to \frac{1}{2a} [\psi(\underline{n} + a\underline{e}_\mu) - \psi(\underline{n} - a\underline{e}_\mu)] \qquad (3.2)$$

where $\underline{n}$ represents a site of the four dimensional Euclidean lattice, $\underline{e}_\mu$ is a unit vector in the μ direction, and a is the lattice spacing. The lattice action is then :

$$S_F = \frac{1}{2a} \sum_{n,\mu} \{\bar{\psi}(n)\gamma_\mu[\psi(n+a\hat{e}_\mu)-\psi(n-a\hat{e}_\mu)\} + \sum_n m\bar{\psi}(n)\psi(n) \tag{3.3}$$

for free fermions. From this action we can calculate the momentum space propagator :

$$G(p) = \frac{1}{m + \frac{i}{a}\sum_\mu \gamma_\mu \sin p_\mu a} \tag{3.4}$$

For free massless fermions, it is clear that G(p) has poles for $p_\mu=0$ or π/a, and hence represents 2^d fermion species. Even in a system initially containing particles corresponding to only one pole, the introduction of gauge fields causes the other allowed particles to be pair produced and so contribute to intermediate processes. For instance, in a perturbative expansion all internal fermion loops contribute with a factor 2^d times their continuum counterparts (Guerin and Kenway, 1980; Sharatchandra, Thun and Weisz, 1981). This causes the loss of asymptotic freedom for the SU(2) colour group, and its near loss for SU(3).

This species doubling has been overcome completely, and without loss of chiral invariance, by a method due to Drell, Weinstein and Yankielowicz (1976). The naive lattice discretisation of the Dirac operator is replaced by a highly non-local term by first going to momentum space:

$$\partial_\mu \psi(n) = \sum_p i p_\mu e^{ip\cdot n} \tilde{\psi}(p) \tag{3.5}$$

where :

$$\tilde{\psi}(p) = \frac{1}{V} \sum_n e^{-ip\cdot n} \psi(n) \tag{3.6}$$

V is the volume of the lattice (a=1 here). Being highly non-local, this so-called SLAC derivative is of no use in

Monte Carlo simulations, and moreover fails to recover locality or Lorentz invariance in the continuum limit (Karsten and Smit, 1979).

Wilson has invented a method whereby the unwanted fermion species are given a mass of order (1/a), and hence disappear in the continuum limit. This is done by adding to the naive fermionic action a term which is of order the cut-off - such terms clearly disappear as a→0. In particular, add a term corresponding to the lattice version of the second derivative of the fermion field, multiplied by an arbitrary factor, r. The modified action is then:

$$S_F = \frac{1}{2a} \sum_{\underline{n},\mu} [\bar{\psi}(\underline{n})(\gamma_\mu - r\,1)\psi(\underline{n}+a\underline{e}_\mu) - \bar{\psi}(\underline{n})(\gamma_\mu + r\,1)\psi(\underline{n}-a\underline{e}_\mu)] + \sum_{\underline{n}} \left[m + \frac{4r}{a}\right] \bar{\psi}(\underline{n})\psi(\underline{n}) \qquad (3.7)$$

The momentum space propagator is:

$$G(p) = \frac{1}{(m+\frac{4r}{a}) + \frac{1}{a}\sum_\mu i\gamma_\mu \sin p_\mu a - \frac{r}{a}\sum_\mu \cos p_\mu a} \qquad (3.8)$$

and the only remaining non-zero mass pole is that at $p_\mu = 0$. Note that for the special case r=1, $(\gamma_\mu - 1)$ and $(\gamma_\mu + 1)$ are just projection operators, and that for a→0, we have the correct continuum proagator:

$$G(p) \xrightarrow[a\to 0]{} \frac{1}{i\not{p} + m} \qquad (3.9)$$

The Wilson fermion method, although it does solve the doubling problem, has the disadvantage that chiral symmetery is explicitly broken, even for m=0. This is important because chiral invariance is an approximate symmetry of QCD, one of the consequences of which is the small pion mass.

We now turn our attention to the method of Susskind (1977). Here, the fermion degeneracy is reduced from 2^d to $2^{d/2}$ in d Euclidean dimensions. The resulting lattice action possesses a continuous remnant of chiral symmetry, and this makes lattice studies of the mechanism for the spontaneous chiral symmetry breaking sensible: no tuning of the bare quark mass is necessary to recover a massless pion, as it is for Wilson fermions.

The method consists of reducing the fermion degrees of freedom at any given site by distributing them on sublattices. To thin the degrees of freedom, we spin diagonalise the naive lattice action by defining a field χ as follows (Kawamoto and Smit, 1981):

$$\psi(\underline{n}) = \gamma_1^{n_1}\gamma_2^{n_2}\cdots\gamma_d^{n_d}\chi(\underline{n}) \tag{3.10}$$

where n_i, i=1,...,d, are the components of the vector $\underline{n}$ labelling lattice sites. Independently:

$$\bar{\psi}(\underline{n}) = \bar{\chi}(\underline{n})\gamma_d^{n_d}\cdots\gamma_2^{n_2}\gamma_1^{n_1} \tag{3.11}$$

Rewriting the action (3.3) in terms of the fields $\bar{\chi}$ and χ we have:

$$S_F = \frac{1}{2a}\sum_{\underline{n},\mu}\bar{\chi}^\alpha(\underline{n})\eta_\mu(\underline{n})\left[\chi^\alpha(\underline{n}+a\underline{e}_\mu)-\chi^\alpha(\underline{n}-a\underline{e}_\mu)\right] + m\sum_{\underline{n}}\bar{\chi}^\alpha(\underline{n})\chi^\alpha(\underline{n}) \tag{3.12}$$

where

$$\eta_\mu(\underline{n}) = (-1)^{n_1+n_2+\cdots+n_\mu} \tag{3.13}$$

and the index α labels the Dirac components of the original fermion fields, and runs from 1 to $2^{d/2}$. We see then that the action has been diagonalised in spin space, that is, it has completely decoupled into $2^{d/2}$ identical spinor copies. All but one of these may be thrown away, and the degeneracy in the continuum is reduced from 2^d to $2^{d/2}$. Kluberg-Stern et al. have pointed out that all transformations like (3.10) and (3.11) that diagonalise the action are equivalent. The diagonalisation may alternatively be carried out in momentum space (Sharatchandra, Thun and Weisz, 1981). Retaining only one copy of the action, then:

$$S_F = \frac{1}{2a}\sum_{\underline{n},\mu}\bar{\chi}(\underline{n})\eta_\mu(\underline{n})\left[\chi(\underline{n}+a\underline{e}_\mu)-\chi(\underline{n}-a\underline{e}_\mu)\right] + m\sum_{\underline{n}}\bar{\chi}(\underline{n})\chi(\underline{n}) \tag{3.14}$$

This action has a global U(1)⊗U(1) symmetry if m=0, which is a remnant of the chiral symmetry of the continuum theory. This symmetry arises from the fact that χ fields situated at odd (even) sites are only coupled to $\bar{\chi}$ fields at even (odd) sites. It is explicitly broken down to its diagonal subgroup, U(1), by the mass term, which couples two fermions at the same site. The propagator for the single component Susskind fermions on an N^4 periodic lattice is given by:

$$G_F(\underline{n},\underline{m}) \equiv \langle\bar{\chi}(\underline{m})\chi(\underline{n})\rangle = \sum_{p=1}^{N} e^{i\underline{p}\cdot(\underline{m}-\underline{n})\frac{\pi}{N}} \frac{\left\{m - i\sum_\mu \eta_\mu(\underline{n})\sin\left(\frac{p_\mu\pi}{N}\right)\right\}}{m^2 + \sum_\mu \sin^2\left(\frac{p_\mu\pi}{N}\right)} \tag{3.15}$$

and we see that translational invariance by one lattice spacing is lost, but that translational invariance by two lattice spacings in a given direction is retained. This is a reflection of the fact that physical quark fields should be identified with combinations of the Susskind fields around 2^d hypercubes, as we show below. Note also that the poles of the momentum space propagator occur in the same places as for the naive propagator (p_μ=0 or N), the difference being that the spinor degrees of freedom have been thinned.

So far we have failed to construct a lattice theory of free fermions with just one fermion and continuous chiral symmetry, with a covariant continuum limit. The reason is intimately connected with the Adler-Bell-Jackiw anomaly (Adler, 1969; Bell and Jackiw, 1969; Karsten and Smit, 1981): the doubling occurs in such a way that even if we put a single left handed spinor on the lattice, it would reappear doubled with a right handed counterpart in the continuum limit, and is thus no longer chiral. The connection between doubling and chirality is formalised in the Nielson-Ninomiya theorem (1981).

Because we wish to investigate the spectrum and chiral symmetry properties of the Schwinger model at light quark masses, we choose to work with the Susskind formulation. We have shown that, in two dimensions, the Susskind action for free fermions represents two continuum flavours. It is more natural, then, in the lattice formulation of the Schwinger model, to consider first its two species generalisation, whose continuum version was considered in the last chapter.

3.2 The Lattice Two Species Schwinger Model.

Our starting point in this section is the lattice action for free Susskind fermions in two dimensions. We shall consider the introduction of gauge fields later. The action, then, is:

$$S_F = \frac{1}{2}\sum_{\underline{n}} \bar{\chi}(\underline{n})\left[\{\chi(\underline{n}+a\underline{e}_1)-\chi(\underline{n}-a\underline{e}_1)\} + (-1)^{n_1}\{\chi(\underline{n}+a\underline{e}_2)-\chi(\underline{n}-a\underline{e}_2)\}\right] \qquad (3.16)$$
$$+ m\sum_{\underline{n}} \bar{\chi}(\underline{n})\chi(\underline{n})$$

$\bar{\chi}$ and χ are one-component spinor fields placed on sites $\underline{n}$ of the lattice, and $\underline{e}_1$ and $\underline{e}_2$ are unit vectors in the two directions. We know that this action describes two continuum flavours, but it is not immediately obvious how one should identify them.

We follow Kluberg-Stern et. al. (1983) and construct Dirac fields with two components, out of the fields $\bar{\chi}$ and χ, for which the propagator has only one pole in momentum space. These new Dirac fields are governed by an action that goes to the continuum action for Dirac fermions with two flavours and a flavour invariant mass term in the limit $a\to 0$. Relabel $\bar{\chi}(\underline{n})$ and $\chi(\underline{n})$:

$$\chi(2\underline{n}) \equiv \chi_\phi(\underline{y}) \qquad \chi(2\underline{n}+\underline{e}_1) \equiv \chi_1(\underline{y})$$
$$\chi(2\underline{n}+\underline{e}_2) \equiv \chi_2(\underline{y}) \qquad \chi(2\underline{n}+\underline{e}_1+\underline{e}_2) \equiv \chi_{12}(\underline{y}) \qquad (3.17)$$

Next define first and second order derivatives on the new lattice of spacing 2a formed by the sites $2\underline{n}=\underline{y}$:

$$\Delta_\mu f(\underline{y}) = \frac{1}{4a}\left[f(\underline{y}+2a\underline{e}_\mu)-f(\underline{y}-2a\underline{e}_\mu)\right] \xrightarrow[a\to 0]{} \partial_\mu f(\underline{y}) \qquad (3.18)$$

$$\delta_\mu f(\underline{y}) = \frac{1}{4a^2}\left[f(\underline{y}+2a\underline{e}_\mu)-2f(\underline{y})+f(\underline{y}-2a\underline{e}_\mu)\right] \xrightarrow[a\to 0]{} \partial_\mu^2 f(\underline{y}) \qquad (3.19)$$

Finally define (H=φ,1,2,12):

$$\Gamma^{\mu}_{HK} = \frac{1}{2} Tr\left(\Gamma_H^{\dagger} \gamma_\mu \Gamma_K\right) \tag{3.20}$$

$$\tilde{\Gamma}^{\mu}_{HK} = \Gamma^{\mu}_{HK} \left(\delta_{\underline{e}_K, \underline{e}_H - \underline{e}_\mu} - \delta_{\underline{e}_H, \underline{e}_K - \underline{e}_\mu}\right) \tag{3.21}$$

with:

$$\Gamma_\varphi = \mathbb{1} \qquad \Gamma_1 = \gamma_1 \qquad \Gamma_2 = \gamma_2 \qquad \Gamma_{12} = \gamma_1\gamma_2 = \gamma_5$$

$$\{\gamma_\mu, \gamma_\nu\} = 2\delta_{\mu\nu} \qquad \gamma_\mu^{\dagger} = \gamma_\mu \tag{3.22}$$

Then the free massless action may be written as:

$$S_F = \sum_{\underline{n},\mu} \sum_{H,K} \bar{\chi}_H(\underline{y}) \left\{\Gamma^{\mu}_{HK} \Delta_\mu + \tilde{\Gamma}^{\mu}_{HK} \delta_\mu\right\} \chi_K(\underline{y}) \tag{3.23}$$

We wish now to define quark fields such that the kinetic term is of the form $\bar{q}\gamma_\mu\Delta_\mu q$, and so from (3.23), we define:

$$q^{\alpha a}(\underline{y}) = \frac{1}{\sqrt{2}} \sum_H \Gamma_H^{\alpha a} \chi_H(\underline{y})$$

$$\bar{q}^{\alpha a}(\underline{y}) = \frac{1}{\sqrt{2}} \sum_H \bar{\chi}_H(\underline{y}) \Gamma_H^{*\alpha a} \tag{3.24}$$

which may be inverted to give:

$$\chi_H(\underline{y}) = \frac{1}{\sqrt{2}} \sum_{\alpha,a} \Gamma_H^{*\alpha a} q^{\alpha a}(\underline{y})$$

$$\bar{\chi}_H(\underline{y}) = \frac{1}{\sqrt{2}} \sum_{\alpha,a} \bar{q}^{\alpha a}(\underline{y}) \Gamma_H^{\alpha a} \tag{3.25}$$

Inserting these expressions into the free lattice action

(3.16), we have:

$$S_F = \sum_{y,\mu} \{ \bar{q}(y)(\gamma_\mu \otimes 1)\Delta_\mu q(y) + a\bar{q}(y)(\gamma_5 \otimes \gamma_\mu^T \gamma_5^T)\delta_\mu q(y)\} + m\sum_y \bar{q}(y)(1 \otimes 1) q(y) \quad (3.26)$$

In the quark bilinears, the first matrix acts in spinor space (Greek indices), the second in flavour space (Latin indices). Note that the second term, involving second order lattice derivatives, is formally of order a with respect to the first, and lifts the flavour degeneracy. Hence the flavour symmetry of the continuum theory is lost on the lattice. From (3.26), we can write the free momentum space quark propagator:

$$G_q(p) = \frac{a}{2(a^2m^2 + \sum_\mu \sin^2 p_\mu a)} \{ i\sum_\mu \sin(2p_\mu a)(\gamma_\mu \otimes 1) + \sum_\mu (\cos(2p_\mu a) - 1)(\gamma_5 \otimes \gamma_\mu^T \gamma_5^T) - 2m(1 \otimes 1)\} \quad (3.27)$$

The momentum p lies in the first Brillouin zone associated with the lattice of spacing 2a, that is:

$$-\frac{\pi}{2a} \leq p_\mu \leq \frac{\pi}{2a} \quad (3.28)$$

so that $\Sigma_\mu \sin^2(2ap_\mu)$ in the denominator disappears only for p=0 in the allowed range of momentum.

The action (3.26) is in fact equivalent to a natural discretisation of the Kahler-Dirac equation (Rabin, 1982; Becher, 1981; Becher and Joos, 1982; Banks, Dothan and Horn, 1982; Kahler, 1962). This is a geometric formulation of the Dirac equation in the language of differential forms, which can be reduced in the continuum into $2^{d/2}$ decoupled Dirac

equations, as a result of the underlying Clifford algebra, for which the four matrices, Γ_H (in two dimensions), form a representation. The Kahler-Dirac equation has a rather natural lattice formulation that has the same flavour degeneracy as the continuum equation, although the decoupling can only be done in momentum space. Although for free fermions, the lattice form of the Kahler-Dirac equation and the Kogut-Susskind form of the Dirac equation are equivalent, in the interacting case they are not. In the Kahler-Dirac formulation all Dirac components of the quark fields transform in the same way under gauge transformations, being associated with the same spacetime point, whereas in the Kogut-Susskind formulation the Dirac components are at different spacetime points and so transform differently. We have chosen to work with the Kogut-Susskind formulation of lattice fermions, and hence wish to construct lattice operators from the fields $\bar{\chi}$ and χ appearing in the action (3.16) rather than the $\bar{q}$ and q fields appearing in (3.26). Before considering lattice particle operators, however, we first consider the introduction of gauge fields into the action.

Gauge fields are introduced into the fermionic action in such a way as to make the action gauge invariant. As we chose to work with the Kogut-Susskind formulation we should introduce these fields on the original lattice of spacing a. Hence, (3.16) becomes:

$$S_F = \frac{1}{2a} \sum_{\underline{n}} \bar{\chi}(\underline{n}) \{ \eta_\mu(\underline{n}) [U_\mu(\underline{n}) \chi(\underline{n} + a\underline{e}_\mu) - U_\mu^\dagger(\underline{n} - a\underline{e}_\mu) \chi(\underline{n} - a\underline{e}_\mu)] \} + m \sum_{\underline{n}} \bar{\chi}(\underline{n}) \chi(\underline{n}) \qquad (3.29)$$

The definition of the physical quark fields may be generalised to:

$$q^{\alpha a}(y) = \frac{1}{\sqrt{2}} \sum_H \Gamma_H^{\alpha a} U_H(y) \chi_H(y)$$

$$\bar{q}^{\alpha a}(y) = \frac{1}{\sqrt{2}} \sum_H \bar{\chi}_H(y) U_H^\dagger(y) \Gamma_H^{*\alpha a} \qquad (3.30)$$

where $U_H(\underline{y})$ is the product of link variables $U_\mu(\underline{n})$ along any definite path going from $2\underline{n}$ to $2\underline{n}+\underline{e}_H$. With this definition, the fields $\bar{q}$ and q transform under the gauge group transformation associated with the site $2\underline{n}$.

We now have all the expressions we need to identify mesonic operators on the lattice. A meson is a bound $\bar{q}q$ state with definite quantum numbers, and hence we may write a general lattice meson in terms of the physical quark fields as:

$$M_{AB}(y) = \bar{q}(y)(\Gamma_A \otimes \Gamma_B) q(y) \qquad (3.31)$$

where Γ_A and Γ_B are 2x2 matrices which may be formed from the four matrices of the Clifford algebra, the first matrix acting in spinor space, the second in flavour space. As we shall work in the Kogut-Susskind formulation of the theory, we need to translate (3.31) into an operator written in terms of the fields $\bar{\chi}$ and χ of the 'small' lattice. Using (3.24), and writing indices explicitly for clarity:

$$M_{AB}(y) = \frac{1}{2} \sum_{H,K} \bar{\chi}_H(y) \Gamma_H^{*\alpha a} \Gamma_A^{\alpha\beta} \Gamma_B^{ab} \Gamma_K^{\beta b} \chi_K(y)$$

$$= \sum_{H,K} \bar{\chi}_H(y) C_{HK} \chi_K(y) \qquad (3.32)$$

$$C_{HK} = \frac{1}{2} \mathrm{Tr}\left(\Gamma_H^\dagger \Gamma_A \Gamma_K \Gamma_B^T\right) \qquad (3.33)$$

Mesons with particular quantum numbers may now be

explicitly constructed, by appropriate choices of Γ_A (defining parity), and Γ_B (defining isospin). The form of C_{HK} is dependent on choice of γ matrices, because the isospin (Pauli) matrices are fixed. The isosinglet state is generated by:

$$\Gamma_B = \mathbb{1} \tag{3.34}$$

and the three members of the isotriplet by:

$$\Gamma_B = \begin{cases} \sigma_+ = \begin{pmatrix} 0 & 1 \\ 0 & 0 \end{pmatrix} & I_3 = +1 \\ \sigma_3 = \begin{pmatrix} 1 & 0 \\ 0 & -1 \end{pmatrix} & I_3 = 0 \\ \sigma_- = \begin{pmatrix} 0 & 0 \\ 1 & 0 \end{pmatrix} & I_3 = -1 \end{cases} \tag{3.35}$$

The matrices of the Clifford algebra may now be chosen to make the mesonic operators as local as possible, for convenience in Monte Carlo calculations. For instance, choosing γ_5 diagonal, the π^0 state, $(I,I_3)^P=(1,0)^-$, is given by:

$$(1,0)^- = \sum_{HK} \bar{\chi}_H C_{HK}^{(1,0)^-} \chi_K \tag{3.36}$$

$$C_{HK}^{(1,0)^-} = \frac{1}{2} Tr\left(\Gamma_H^\dagger \gamma_5 \Gamma_K \sigma_3^T\right)$$
$$= i \begin{pmatrix} -1 & 0 & 0 & 0 \\ 0 & 1 & 0 & 0 \\ 0 & 0 & 1 & 0 \\ 0 & 0 & 0 & -1 \end{pmatrix} \qquad (3.37)$$

and so the π^0 operator is local:

$$M_{\pi^0}(y) = -i \sum_H \varepsilon_H \bar{\chi}_H(y) \chi_H(y) \qquad (3.38)$$

where

$$\varepsilon_H = (-1)^{e_{H_1} + e_{H_2}}$$

If on the other hand γ_2 had been chosen diagonal, then

$$C_{HK}^{(1,0)^-} = \begin{pmatrix} 0 & -1 & 0 & 0 \\ 1 & 0 & 0 & 0 \\ 0 & 0 & 0 & -1 \\ 0 & 0 & 1 & 0 \end{pmatrix} \qquad (3.39)$$

and the operator is thus one link. These two possible definitions for the pion are compared in chapter five. The 0^+ operator is always local; the 0^- is always two-link; and the $(1,\pm1)^\pm$ operators are either a mixture of local and two link pieces, or purely one link, depending upon the choice of the representation of the Clifford algebra.

We have chosen to make γ_2 diagonal, and hence, cataloguing the possible C_{HK} :

$$C^{0^+}_{HK} = \frac{1}{2}\mathrm{Tr}\left(\Gamma_H^\dagger \mathbb{1} \Gamma_K \mathbb{1}\right) = \begin{pmatrix} 1 & 0 & 0 & 0 \\ 0 & 1 & 0 & 0 \\ 0 & 0 & 1 & 0 \\ 0 & 0 & 0 & 1 \end{pmatrix} \tag{3.40}$$

$$C^{(1,0)^+}_{HK} = \frac{1}{2}\mathrm{Tr}\left(\Gamma_H^\dagger \mathbb{1} \Gamma_K \sigma_3\right) = \frac{1}{2}\mathrm{Tr}\left(\Gamma_H^\dagger \mathbb{1} \Gamma_K \gamma_2\right)$$
$$= \begin{pmatrix} 0 & 0 & 1 & 0 \\ 0 & 0 & 0 & 1 \\ 1 & 0 & 0 & 0 \\ 0 & 1 & 0 & 0 \end{pmatrix} \tag{3.41}$$

$$C^{(1,\pm 1)^+}_{HK} = \frac{1}{2}\mathrm{Tr}\left(\Gamma_H^\dagger \mathbb{1} \Gamma_K \sigma_\pm\right) = \frac{1}{2}\mathrm{Tr}\left(\Gamma_H^\dagger \mathbb{1} \Gamma_K \tfrac{1}{2}[\gamma_1 \mp \gamma_5]\right)$$
$$= \frac{1}{2}\left\{\begin{pmatrix} 0 & 1 & 0 & 0 \\ 1 & 0 & 0 & 0 \\ 0 & 0 & 0 & -1 \\ 0 & 0 & -1 & 0 \end{pmatrix} \mp \begin{pmatrix} 0 & 0 & 0 & -1 \\ 0 & 0 & -1 & 0 \\ 0 & 1 & 0 & 0 \\ 1 & 0 & 0 & 0 \end{pmatrix}\right\} \tag{3.42}$$

$$C^{0^-}_{HK} = \frac{1}{2}\mathrm{Tr}\left(\Gamma_H^\dagger \gamma_5 \Gamma_K \mathbb{1}\right) = \begin{pmatrix} 0 & 0 & 0 & -1 \\ 0 & 0 & 1 & 0 \\ 0 & -1 & 0 & 0 \\ 1 & 0 & 0 & 0 \end{pmatrix} \tag{3.43}$$

$$C^{(1,0)^-}_{HK} = \frac{1}{2}\mathrm{Tr}\left(\Gamma_H^\dagger \gamma_5 \Gamma_K \gamma_2\right) = \begin{pmatrix} 0 & -1 & 0 & 0 \\ 1 & 0 & 0 & 0 \\ 0 & 0 & 0 & -1 \\ 0 & 0 & 1 & 0 \end{pmatrix} \tag{3.44}$$

$$C^{(1,\pm 1)^-}_{HK} = \frac{1}{2}\mathrm{Tr}\left(\Gamma_H^\dagger \gamma_5 \Gamma_K \sigma_\pm\right) = \frac{1}{2}\mathrm{Tr}\left(\Gamma_H^\dagger \gamma_5 \Gamma_K \tfrac{1}{2}[\gamma_1 \mp \gamma_5]\right)$$
$$= \left\{\begin{pmatrix} 0 & 0 & 1 & 0 \\ 0 & 0 & 0 & -1 \\ -1 & 0 & 0 & 0 \\ 0 & 1 & 0 & 0 \end{pmatrix} \mp \begin{pmatrix} -1 & 0 & 0 & 0 \\ 0 & 1 & 0 & 0 \\ 0 & 0 & 1 & 0 \\ 0 & 0 & 0 & -1 \end{pmatrix}\right\} \tag{3.45}$$

Having made this identification of particle operators for free fermions, we now introduce the gauge fields in the obvious way to make them gauge invariant (Kluberg-Stern et. al., 1983):

$$\bar{\chi}_H(y)\chi_K(y) \to \bar{\chi}_H(y)\, U_{HK}(y)\, \chi_K(y) \tag{3.46}$$

where $U_{HK}(y)$ is the product of gauge variables along any path linking $\bar{\chi}$ and χ.

3.3 The One Species Schwinger Model

We wish now to modify the lattice action so that only one species is produced in the continuum. We shall do this by introducing a mass term that gives the two continuum species different masses, and then we shall let the mass of one of the species become very large so that it decouples from the theory (Mitra and Weisz, 1983; Mitra, 1983; Burkitt and Kenway, 1983; Burkitt, Kenway and Kenway, 1983). In the next chapter, we present numerical evidence that this procedure indeed causes one of the flavours to disappear from the theory.

Consider the free action (3.26) We can introduce different masses for the two fermion flavours by making the replacement:

$$\begin{aligned} m \sum_y \bar{q}(y)(\mathbb{1}\otimes\mathbb{1})\, q(y) \\ = m \sum_y \bar{q}^{\alpha a}(y)\, q^{\alpha a}(y) \\ \longrightarrow \sum_y m_a \bar{q}^{\alpha a}(y) q^{\alpha a}(y) \end{aligned} \tag{3.47}$$

sums on repeated indices being understood. We next write:

$$\begin{aligned} \mathcal{M} &= \sum_{a,\alpha} m_a \bar{q}^{\alpha a}(y) q^{\alpha a}(y) \\ &= \mathrm{Tr}\,(\bar{q} M q) \end{aligned} \tag{3.48}$$

where:

$$\begin{aligned} M_{ab} &= \sum_c m_c P_{ab}^{(c)} \\ P_{ab}^{(c)} &= \delta_{ac}\,\delta_{bc} \end{aligned} \tag{3.49}$$

Let the two quark flavours be called up (u) and down (d). Then, if we make γ_2 diagonal, we have:

$$P^{(u)} = \tfrac{1}{2}(\mathbb{1} + \gamma_2) \qquad P^{(d)} = \tfrac{1}{2}(\mathbb{1} - \gamma_2) \tag{3.50}$$

where $p^{(u)}$ and $p^{(d)}$ are projection operators for the up and down quarks respectively, and:

$$M = \tfrac{1}{2}\left[\mathbb{1}(m_u + m_d) + \gamma_2(m_u - m_d)\right] \tag{3.51}$$

Now use (3.24) to write this mass term in terms of the lattice fields $\bar{\chi}(\underline{n})$ and $\chi(\underline{n})$:

$$\begin{aligned} \mathcal{M} &= \tfrac{1}{2}\bar{\chi}_H(y)\,\mathrm{Tr}\left(\Gamma_K M \Gamma_H^\dagger\right)\chi_K(y) \\ &= \bar{\chi}_H\, m_{HK}\,\chi_K(y) \end{aligned} \tag{3.52}$$

where

$$m_{HK} = \tfrac{1}{2}\begin{pmatrix} m_u+m_d & 0 & m_u-m_d & 0 \\ 0 & m_u+m_d & 0 & m_u-m_d \\ m_u-m_d & 0 & m_u+m_d & 0 \\ 0 & m_u-m_d & 0 & m_u+m_d \end{pmatrix} \tag{3.53}$$

Hence, the Susskind action for non-degenerate flavours is:

$$\begin{aligned} S_F = &\sum_{\underline{n}} \tfrac{1}{2a}\bar{\chi}(\underline{n})\eta_\mu(\underline{n})\left[U_\mu(\underline{n})\chi(\underline{n}+a\underline{e}_\mu) - U_\mu^\dagger(\underline{n}-a\underline{e}_\mu)\chi(\underline{n}-a\underline{e}_\mu)\right] \\ &+ \sum_{\underline{n}} \left(\tfrac{m_u+m_d}{2}\right)\bar{\chi}(\underline{n})\chi(\underline{n}) \\ &+ \sum_{\underline{n}} \left(\tfrac{m_u-m_d}{2}\right)\bar{\chi}(\underline{n})\left\{\left(\tfrac{1+(-1)^{n_2}}{2}\right)U_2(\underline{n})\chi(\underline{n}+a\underline{e}_2) + \left(\tfrac{1-(-1)^{n_2}}{2}\right)U_2^\dagger(\underline{n}-a\underline{e}_2)\chi(\underline{n}-a\underline{e}_2)\right\} \end{aligned} \tag{3.54}$$

Note that this action is not unique. Choosing γ_2 diagonal results in a one link mass term in the two direction, but we could have chosen equivalently γ_1 diagonal, giving a one link mass term in the one direction. Choosing γ_5 diagonal results in a two link mass term, with m_{HK} given by:

$$M_{HK} = \frac{1}{2}\begin{pmatrix} m_u+m_d & 0 & 0 & i(m_d-m_u) \\ 0 & m_u+m_d & i(m_d-m_u) & 0 \\ 0 & -i(m_d-m_u) & m_u+m_d & 0 \\ -i(m_d-m_u) & 0 & 0 & (m_u+m_d) \end{pmatrix} \quad (3.55)$$

We have chosen γ_2 diagonal, as a one link mass term is clearly easier for numerical simulations than a two link term. However, this has some disadvantages for lattice particle propagators, as we shall see below, as well as destroying discrete O(2) invariance on the lattice.

With the action (3.54), we are able to give the two continuum flavours different masses. We simulate the one species model by giving one of the flavours a mass:

$$m = \frac{1}{a} \quad (3.56)$$

whilst the other flavour remains light. The heavy quark is hopefully so heavy that it decouples entirely from the theory. This procedure is not entirely satisfactory, as in the limit in which the mass of the heavy species goes to ∞ (although it is not clear what it means to give a particle a mass greater than the cut-off), it appears that the number of the light poles in the free propagator doubles again (Verstegen, 1984). We demonstrate this numerically in the next chapter.

Now consider mesonic operators for the one species model. We can still define operators according to (3.31), but clearly Γ_B now has no meaning. If the d quark is made heavy, then all useful mesonic operators must have a $\langle\bar{u}u\rangle$ piece in their definition. Thus, according to the particular identification scheme given above for the two species model, only those operators with $I_3=0$ are useful in the simulation

of the one species model, and only their parity is important.

3.4 Correlation Functions.

In chapter one, we argued that sums on spatial directions of particle propagators (time slice propagators) should decay exponentially in Euclidean time with the mass of the particle. In this section we discuss the basic correlation functions and time slice propagators for both the two species and one species models.

Consider first the two species model. Equation (3.31) tells us how to identify the mesonic operators. In a representation where the γ matrices are real, mesonic propagators are given by:

$$P_{AB}(y,\underline{o}) = \langle \bar{M}_{AB}(y)\, M_{AB}(\underline{o})\rangle$$
$$= \langle \bar{q}(y)(\Gamma_A^T \otimes \Gamma_B^T) q(y) \bar{q}(\underline{o})(\Gamma_A \otimes \Gamma_B) q(\underline{o})\rangle \qquad (3.57)$$

Expanding this and putting in Dirac and flavour indices explicitly:

$$P_{AB}(y,\underline{o}) = \{\langle \bar{q}^{\alpha a}(y) q^{\delta d}(\underline{o})\rangle\langle \bar{q}^{\gamma c}(\underline{o}) q^{\beta b}(y)\rangle - \langle \bar{q}^{\alpha a}(y) q^{\beta b}(y)\rangle\langle \bar{q}^{\gamma c}(\underline{o}) q^{\delta d}(\underline{o})\rangle\}$$
$$\times (\Gamma_A^T)^{\alpha\beta} (\Gamma_B^T)^{ab} (\Gamma_A)^{\gamma\delta} (\Gamma_B)^{cd} \qquad (3.58)$$

The action, (3.26), contains a term that breaks the flavour symmetry of the continuum action, but is formally of order a (the lattice spacing) with respect to the other terms. If, then, we are near the continuum limit, we can consider only flavour conserving currents, and we have:

$$P_{AB}(y,0) \simeq \langle \bar{q}^{\alpha a}(y) q^{\delta a}(0) \rangle \langle \bar{q}^{\gamma b}(0) q^{\beta b}(y) \rangle \Gamma_A^{\beta\alpha} \Gamma_A^{\gamma\delta} \left(\Gamma_B^{ba}\right)^2$$
$$- \langle \bar{q}^{\alpha a}(y) q^{\beta a}(y) \rangle \langle \bar{q}^{\gamma c}(0) q^{\delta c}(0) \rangle \Gamma_A^{\beta\alpha} \Gamma_A^{\gamma\delta} \Gamma_B^{aa} \Gamma_B^{cc} \qquad (3.59)$$

Hence, the flavour non-singlet states (I=1) get no contribution from the second term in (3.59), because if $m_u=m_d$ then $\langle\bar{u}u\rangle=\langle\bar{d}d\rangle$, and Γ_B is traceless. Notice also that it is exactly the second term that causes the splitting between the I=0 and the $(I,I_3)=(1,0)$ states, because $(\Gamma_B^{ab})^2$ is identical for both states. This is consistent with Coleman's comments (1976), who states that in the continuum two species model, it is the annihilation diagrams that lift the degeneracy of the isosinglet and isotriplet states. These diagrams are shown in figure 3.1. They are those in which two fermion loops are connected by photons, and are non-zero in the continuum only for those states with $I_3=0$ (because the photon is an isosinglet), although both scalar and pseudoscalar states get contributions as the photon is a pseudoscalar. Pseudoscalar states are connected by an odd number of photons and scalar states by an even number.

Particle masses may now be calculated by inserting appropriate gauge fields into (3.59) in order to make the correlation functions gauge invariant.

The above system of particle identification yields mesonic operators that have well-defined quantum numbers. However as these operators are often non-local, they must be multiplied by gauge fields in order to make them gauge invariant. As far as Monte Carlo calculations are concerned, this has the adverse effect of worsening statistical errors. It is possible to define local operators on a single site of the lattice, but these no longer describe single particles with well-defined quantum numbers. However, as these are

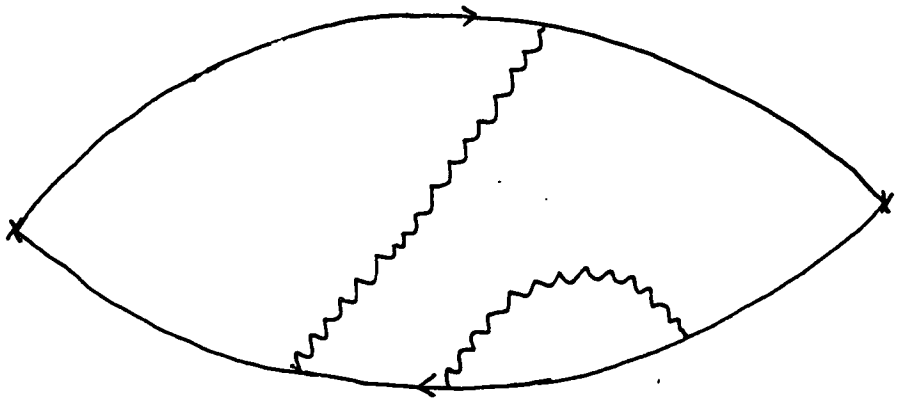

(a)

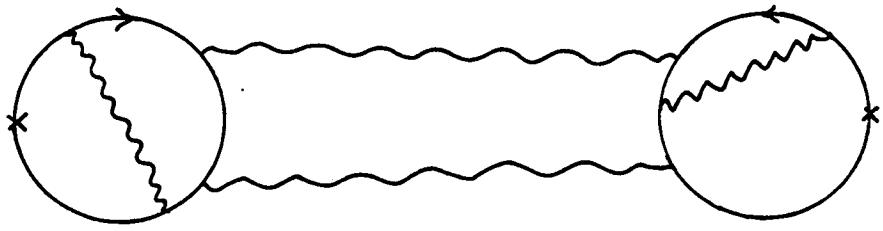

(b)

Fig 3.1

The two types of diagram contributing to meson propagation. Fig 3.1(b) represents the annihilation terms that lift the degeneracy between I=0 and I=1 states.

by far the easiest operators to use in a Monte Carlo calculation, we consider them here.

Mesonic operators are defined by (3.31):

$$M_{AB}(y) = \bar{q}(y)\,(\Gamma_A \otimes \Gamma_B)\,q(y) \qquad (3.31)$$

these are local if $\Gamma_A=\Gamma_B$:

$$M_A(y) = \bar{q}(y)\,(\Gamma_A \otimes \Gamma_A)\,q(y) \qquad (3.60)$$

Clearly then in two dimensions, there are four local operators of this type, given by:

$$\begin{aligned} \Gamma_A &= \mathbb{1} \\ \Gamma_A &= \gamma_1 \\ \Gamma_A &= \gamma_2 \\ \Gamma_A &= \gamma_1\gamma_2 = \gamma_5 \end{aligned} \qquad (3.61)$$

In Euclidean space, we are free to choose either direction as time. This choice determines the parity of the mesonic operators: if time is the 1-direction, then $\Gamma_A=1$ or γ_1 yields a scalar, whereas $\Gamma_A=\gamma_2$ or γ_5 yields a pseudoscalar. The isospin of the local operators depends on the choice of γ matrices. Choosing γ_2 diagonal, we have:

$$\gamma_1 = \begin{pmatrix} 0 & 1 \\ 1 & 0 \end{pmatrix} \qquad \gamma_2 = \begin{pmatrix} 1 & 0 \\ 0 & -1 \end{pmatrix} \qquad (3.62)$$

and so in terms of the Pauli matrices (noting that it is Γ_A^T that is important according to (3.33)):

$$\gamma_1^T = \sigma_+ + \sigma_- \qquad \gamma_2^T = \sigma_3 \qquad \gamma_5^T = \sigma_+ - \sigma_- \tag{3.63}$$

Thus $\Gamma_A=1$ yields the isoscalar, whereas the other particles all have I=1. Choosing γ_5 diagonal produces a different identification of the quantum numbers, causing mixing among the isotriplet members with respect to the above identification.

Now consider operators of the form:

$$M_{loc}(\underline{n}) = \varepsilon \overline{\chi}(\underline{n}) \chi(\underline{n}) \tag{3.64}$$

These are the most convenient for Monte carlo calculations. They are defined on a <u>single</u> lattice site. ε is some phase, and $\overline{\chi}$ and χ have no H subscript as $\underline{n}$ here labels sites of the original lattice. As we shall want to sum over the sites in the spatial direction in order to extract meson masses (as we discussed in chapter one), define (having chosen time to be the one direction):

$$\begin{aligned}
M_S(t) &= \sum_{n_2} (-1)^{n_2+t} \left| G(\underline{o}; n_2, t) \right|^2 \\
M_{PS}(t) &= \sum_{n_2} \left| G(\underline{o}; n_2, t) \right|^2 \\
M_{L1}(t) &= \sum_{n_2} (-1)^{t} \left| G(\underline{o}; n_2, t) \right|^2 \\
M_{L2}(t) &= \sum_{n_2} (-1)^{n_2} \left| G(\underline{o}; n_2, t) \right|^2
\end{aligned} \tag{3.65}$$

where $t=n_1$ and $G(\underline{o},\underline{n})=\langle \chi(\underline{n})\chi(\underline{o}) \rangle$. These operators exhaust the possibilities for the phase in two dimensions.

Correlation functions for the local mesons M_A defined in (3.60), when summed over the spatial direction, give:

$$M_\phi(t) = \sum_{n_2} \{\bar{q}(y)(1\otimes 1)q(y)\,\bar{q}(\underline{o})(1\otimes 1)q(\underline{o})\}$$

$$M_1(t) = \sum_{n_2} \{\bar{q}(y)(\gamma_1\otimes\gamma_1)q(y)\,\bar{q}(\underline{o})(\gamma_1\otimes\gamma_1)q(\underline{o})\} \qquad (3.66)$$

$$M_2(t) = \sum_{n_2} \{\bar{q}(y)(\gamma_2\otimes\gamma_2)q(y)\,q(\underline{o})(\gamma_2\otimes\gamma_2)q(\underline{o})\}$$

$$M_{12}(t) = \sum_{n_2} \{\bar{q}(y)(\gamma_5\otimes\gamma_5)q(y)\,\bar{q}(\underline{o})(\gamma_5\otimes\gamma_5)\bar{q}(\underline{o})\}$$

We note that $G_{HK}(\underline{o},\underline{n})=G(\underline{e}_H,2\underline{n}+\underline{e}_K)=(-1)^{e_{H_1}+e_{H_2}+e_{K_1}+e_{K_2}}G_{HK}(\underline{n},\underline{o})$ and invoking translational invariance, we have:

$$M_\phi(t) = 2\sum_{n_2}(-1)^{e_{K_2}}\{2|G(\underline{o};n_2,2t)|^2-|G(\underline{o};n_2,2t+1)|^2-|G(\underline{o};n_2,2t-1)|^2\}$$

$$M_1(t) = 2\sum_{n_2}\{2|G(\underline{o};n_2,2t)|^2-|G(\underline{o};n_2,2t+1)|^2-|G(\underline{o};n_2,2t-1)|^2\} \qquad (3.67)$$

$$M_2(t) = 2\sum_{n_2}(-1)^{e_{K_2}}\{2|G(\underline{o};n_2,2t)|^2+|G(\underline{o};n_2,2t+1)|^2+|G(\underline{o};n_2,2t-1)|^2\}$$

$$M_{12}(t) = 2\sum_{n_2}\{2|G(\underline{o};n_2,2t)|^2+|G(\underline{o};n_2,2t+1)|^2+|G(\underline{o};n_2,2t-1)|^2\}$$

In writing the first of these expressions, we have neglected the annihilation diagrams whose importance for the singlet state was noted earlier. Hence, we cannot expect to extract a reliable estimate of the mass of the 0^+ state from any local operators. With this caveat in mind, however, we proceed to extract masses. (Similar calculations by Gilchrist et. al.(1984) in four dimensions for the ε meson produced unsatisfacory results.) The time slice propagators are expected to behave like exponentials in the meson masses. Hence we may assume (remembering the degeneracy of the isotriplet):

$$M_\phi(t) = K_{0+}\left\{e^{-m_{0+}2t} + e^{-m_{0+}(T-2t)}\right\}+\cdots$$

$$M_1(t) = K_{1+}\left\{e^{-m_{1+}2t} + e^{-m_{1+}(T-2t)}\right\}+\cdots$$

$$M_2(t) = K_{1-}\left\{e^{-m_{1-}2t} + e^{-m_{1-}(T-2t)}\right\}+\cdots \qquad (3.68)$$

$$M_{12}(t) = K'_{1-}\left\{e^{-m_{1-}2t} + e^{-m_{1-}(T-2t)}\right\}+\cdots$$

T is the temporal extent of the lattice. We notice that:

$$M_{\substack{L1\\L2}}(2t\pm1) = -M_{\substack{PS\\S}}(2t\pm1)$$

$$M_{\substack{L1\\L2}}(2t) = +M_{\substack{PS\\S}}(2t) \qquad (3.69)$$

and hence write:

$$M_\phi(t) = 2\left[2M_S(2t) + M_S(2t+1) + M_S(2t-1)\right]$$

$$M_1(t) = 2\left[2M_{PS}(2t) - M_{PS}(2t+1) - M_{PS}(2t-1)\right]$$

$$M_2(t) = 2\left[2M_S(2t) - M_S(2t+1) - M_S(2t-1)\right] \qquad (3.70)$$

$$M_{12}(t) = 2\left[2M_{PS}(2t) + M_{PS}(2t+1) - M_S(2t-1)\right]$$

these may be solved for M_S and M_{PS}. We find

$$\begin{aligned} M_S(t) = {} & \frac{K_{0+}(1+\cosh m_{0+})}{16\cosh m_{0+}}\left\{e^{-m_{0+}t} + e^{-m_{0+}(T-t)}\right\} \\ & - \frac{K_{1-}(1-\cosh m_{1-})}{16\cosh m_{1-}}\left\{e^{-m_{1-}t} + e^{-m_{1-}(T-t)}\right\} \\ & + (-1)^t\left[\frac{K_{1-}(1+\cosh m_{1-})}{16\cosh m_{1-}}\left\{e^{-m_{1-}t} + e^{-m_{1-}(T-t)}\right\}\right. \\ & \left. - \frac{K_{0+}(1-\cosh m_{0+})}{16\cosh m_{0+}}\left\{e^{-m_{0+}t} + e^{-m_{0+}(T-t)}\right\}\right] \end{aligned} \qquad (3.71)$$

$$M_{PS}(t) = \frac{K_{1-}'(1+\cosh m_{1-})}{16\cosh m_{1-}} \left\{ e^{-m_{1-}t} + e^{-m_{1-}(T-t)} \right\}$$
$$- \frac{K_{1+}(1-\cosh m_{1+})}{16\cosh m_{1+}} \left\{ e^{-m_{1+}t} + e^{-m_{1+}(T-t)} \right\} \qquad (3.72)$$
$$+ (-1)^t \left[\frac{K_{1+}(1+\cosh m_{1+})}{16\cosh m_{1+}} \left\{ e^{-m_{1+}t} + e^{-m_{1+}(T-t)} \right\} \right.$$
$$\left. - \frac{K_{1-}'(1-\cosh m_{1-})}{16\cosh m_{1-}} \left\{ e^{-m_{1-}t} + e^{-m_{1-}(T-t)} \right\} \right]$$

Similar expressions have been obtained in four dimensions (Gilchrist et. al., 1984). In the continuum limit, a→0, these expressions reduce to:

$$M_S(t) = \frac{1}{8}\left[K_{0+} \left\{ e^{-m_{0+}t} + e^{-m_{0+}(T-t)} \right\} + (-1)^t K_{1-} \left\{ e^{-m_{1-}t} + e^{-m_{1-}(T-t)} \right\} \right] \qquad (3.73)$$

$$M_{PS}(t) = \frac{1}{8}\left[K_{1-}' \left\{ e^{-m_{1-}t} + e^{-m_{1-}(T-t)} \right\} + (-1)^t K_{1+} \left\{ e^{-m_{1+}t} + e^{-m_{1+}(T-t)} \right\} \right] \qquad (3.74)$$

Note that M_{PS} propagates both the 1^+ and 1^- states, which is not the case in four dimensions. Also note that the 0^- state does not mix with any of these simple local operators. This is because it is not possible to find any representation of the Clifford algebra in which the 0^- operator has any local pieces. This is always possible for the 0^+, 1^+ and 1^- states. Hence the mass of the 0^- particle may only be calculated using non-local mesonic operators.

Now consider correlation functions for the one species model. Meson propagators are still given by (3.31), but to ensure that the propagator contains a $\langle\bar{u}u\rangle$ piece, we require that Γ_B be diagonal. Note that now $\langle\bar{u}u\rangle \neq \langle\bar{d}d\rangle$ and hence that the second term (the annihilation term) in (3.59) is important for all meson operators. However, Coleman

(1976) argues that the annihilation force is negligible for weak coupling in the one species model, and at least does not alter the qualitative features of the mesonic spectrum at strong coupling.

Now consider the definition of local particles for the one species model. In the derivation of equations (3.73) and (3.74) given above, we used the fact that:

$$G_{HK}(\underline{o},\underline{n}) = (-1)^{e_{H_1}+e_{H_2}+e_{H_3}+e_{K_2}} G_{KH}(\underline{n},\underline{o}) \qquad (3.75)$$

This relation is only true for the two species model: the one link mass term in the action invalidates this equation, although had we chosen a two link mass term to lift the degeneracy, (3.75) would still have been valid. The relation is used to enable us to find G^T, the transpose of the quark Green function, from G. In the one species model, we are forced to calculate both G and G^T separately. Then, we can form:

$$(-1)^{n_1+n_2} G(\underline{o},\underline{n}) G(\underline{n},\underline{o}) \qquad (3.76)$$

which is the analogue of $|G(\underline{n},\underline{o})|^2$ for the two species model. Note that if γ_2 is diagonal, $M_1(t)$ and $M_{12}(t)$ are meaningless for the one species model, and hence only $M_S(t)$ retains any usefulness, mixing the scalar and pseudoscalar particles. Again, note that had we chosen γ_5 diagonal, then $M_1(t)$ and $M_2(t)$ would have become meaningless, so that $M_S(t)$ and $M_{PS}(t)$ would both have propagated only a single state, $M_S(t)$ the scalar, and $M_{PS}(t)$ the pseudoscalar. However, it must be noted that any local definition of mesonic operators for the one species model necessarily neglects the annihilation terms, and hence produces unreliable results.

CHAPTER FOUR

NUMERICAL TECHNIQUES

In chapter three, we showed how to formulate the Schwinger model on a lattice, and how to lift the mass degeneracy of the naive discretisation of the action with a one-link mass term. We can proceed now in two ways: either by performing strong or weak coupling expansions for the physical quantities of interest, or by simulating the system numerically. We shall perform numerical simulations of the theory, for the one and two species models, and for the quenched and unquenched models. Some Monte Carlo results already exist for the Schwinger model (Marinari, Parisi and Rebbi, 1981; Ranft, 1983), though only quenched results exist for the particle masses (Carpenter, 1983). Some strong coupling results have also appeared (Hamer and Kenway, 1981; Carroll et al., 1976)

In this chapter, we shall present the numerical techniques used in this work: the Metropolis algorithm, which was used for updating the gauge fields (the faster heat bath method would not have been suitable because of the technique we used to simulate the effects of dynamical fermions in the unquenched model); the pseudofermion heat bath technique, used to produce unquenched gauge configurations, and also used in the calculation of $\langle\bar{\psi}\psi(m)\rangle$, the fermion condensate; and the conjugate gradient method, used for the calculation of the quark Green functions within a given gauge field configuration. As well as defining the algorithms, we shall emphasise how they may be efficiently implemented on a parallel machine, in particular, the ICL Distributed Array Processor (DAP), the machine actually used in all these calculations. As a simple introduction to the

special features of a parallel processor a short appendix appears at the end of this work.

We also present in this chapter a few free fermion results, as examples of the use of the pseudofermion and conjugate gradient programmes, and as examples of the importance of fermionic boundary conditions.

4.1 Generalities

As we have already seen, the expectation value of a physical observable in a quantum field theory is given by the functional integral:

$$\langle \hat{O} \rangle = \int \mathcal{D}\varphi \, \hat{O}(\varphi) \, e^{-S(\varphi)} \qquad (4.1)$$

where φ denotes generically the dynamical field variables in the theory. The idea of the Monte Carlo method is to replace this integral by an average over field configurations, C_i:

$$\langle \hat{O} \rangle = \frac{\sum_i \hat{O}(C_i)}{\sum_i 1} = \frac{1}{N} \sum_i \hat{O}(C_i) \qquad (4.2)$$

At equilibrium, the configurations, C_i, are distributed with the Boltzmann factor, exp(-S), and hence the field configurations with large action will not contribute significantly to the sum (4.2). We are faced, then, with the problem of somehow generating a representative sample of equilibrium configurations that contribute significantly to the quantum average (4.2).

The Monte Carlo technique is designed to generate such a set of configurations. One begins with some arbitrary field

configuration, C, and from this generates a new configuration, C′. The passage from one configuration to the next is determined by the transition matrix, P(C→C′), satisfying the constraints of stochastic matrices:

$$P(C \to C') \geq 0$$

$$\sum_{C'} P(C \to C') = 1 \qquad (4.3)$$

Generally, one implements Monte Carlo algorithms by updating just one dynamical variable at a time - in the case of gauge theories, one updates a particular link variable, $U_\mu(\underline{n}) \to U_\mu'(\underline{n})$, and then moves on to the next, eventually updating all links and completing one sweep through the lattice. Hence, one does not define a single transition matrix, P(C→C′), but rather a whole collection, $P_{\underline{n},\mu}(C \to C')$, coinciding with the transition probability $P(U_\mu(\underline{n}) \to U_\mu'(\underline{n}))$, the other dynamical variables being kept fixed. In what follows, we leave the indices on P implicit.

One wishes, then to define a stochastic sequence such that, once statistical equilibrium is reached, the probability of finding any configuration C becomes proportional to exp{-S(C)}. A sufficient (but not necessary) condition for this is that each step of the transition matrix should satisfy detailed balance:

$$e^{-S(C)} P(C \to C') = e^{-S(C')} P(C' \to C) \qquad (4.4)$$

It is now easy to show that e^{-S} is an eigenvector of the stochastic process:

$$\sum_C e^{-S(C)} P(C \to C') = \sum_C e^{-S(C')} P(C' \to C) \qquad (4.5)$$

$$= e^{-S(C')} \quad \text{by (4.3)}$$

To study the convergence to the Boltzmann distribution, define a distance between two ensembles of configurations, E and E′, each containing many configurations, as:

$$\| E - E' \| = \sum_C | P(C) \to P'(C) | \qquad (4.6)$$

where P(C) and P′(C) are the probability density for configuration C in E and E′ respectively, and the sum runs over all possible configurations. Now suppose that E′ resulted from the application of a Monte Carlo algorithm satisfying (4.4) to E. Then:

$$P'(C) = \sum_{C'} P(C' \to C)\, P(C') \qquad (4.7)$$

If E_{eq} is an equilibrium ensemble, then:

$$\begin{aligned} \| E' - E_{eq} \| &= \sum_C \Big| \sum_{C'} P(C' \to C)\,(P(C') - P_{eq}(C')) \Big| \\ &\leq \sum_{C,C'} P(C' \to C)\, |P(C') - P_{eq}(C')| = \| E - E_{eq} \| \end{aligned} \qquad (4.8)$$

If P(C→C′) never vanishes, the inequality is strict, unless we are already in equilibrium, and hence the algorithm always takes us closer to equilibrium.

The detailed balance condition does not uniquely determine the transition probabilities, and we go on now to consider the Metropolis algorithm, used for updating the gauge fields.

4.2 The Metropolis Algorithm

Consider a gauge field configuration, {U}. From this, we wish to generate a new configuration, {U'}, by updating a single link, $U_\mu(\underline{n})$. This is done by selecting arbitrarily a new variable, $\tilde{U}_\mu(\underline{n})$, giving a new configuration, $\{\tilde{U}\}$. Next calculate the change in the action, ΔS:

$$\Delta S = S(\{\tilde{U}\}) - S(\{U\}) \tag{4.9}$$

If $\Delta S \leq 0$, the change is accepted, and we have $U'_\mu(\underline{n}) = \tilde{U}_\mu(\underline{n})$ and $\{U'\} = \{\tilde{U}\}$. If $\Delta S > 0$, the new configuration is accepted with the conditional probability, $\exp(-\Delta S)$. In practice, this is done by choosing a pseudorandom number, r, selected in the interval $0 < r < 1$, with uniform probability distribution. If

$$r \leq e^{-\Delta S} \tag{4.10}$$

the change is accepted, and $\{U'\} = \{\tilde{U}\}$. Otherwise the change is rejected and $\{U'\} = \{U\}$. We have in summary, then:

$$P(\{U\} \to \{U'\}) = \begin{cases} 1 & \text{if } S(\{U\}) > S(\{U'\}) \\ e^{-[S(\{U'\}) - S(\{U\})]} & \text{if } S(\{U\}) < S(\{U'\}) \end{cases} \tag{4.11}$$

and so:

$$\frac{P(\{U'\} \to \{U\})}{P(\{U\} \to \{U'\})} = e^{+[S(\{U'\}) - S(\{U\})]} \tag{4.12}$$

which is the condition for detailed balance. To specify the Metropolis algorithm completely, one needs now to specify how to choose a new link variable, $\tilde{U}_\mu(\underline{n})$. In the case of models like gauge theories, where the dynamical variables belong to continuous groups, we must invent a procedure that can cover the gauge group space uniformly, thus respecting the Haar measure of the partition function. For an SU(3) theory, one can generate a table of random SU(3) matrices, and their Hermitian adjoints, and use these to change a particular link variable by multiplication, finally executing the standard algorithm, outlined above. Repeated applications of matrices chosen from this table to any arbitrary SU(3) matrix takes one arbitrarily close to any other member of the group (Wilson, 1980).

In the work presented here, with a U(1) gauge group, the choice of new link variables is made particularly simple:

$$U_\mu(\underline{n}) = e^{i\theta_\mu(\underline{n})} \tag{4·13}$$

where $\theta_\mu(\underline{n})$ is some angle in the range $[0,2\pi)$. A new gauge field variable is then selected by generating random numbers in the interval $[0,1)$, and multiplying these by 2π to obtain a value for $\tilde{\theta}_\mu(\underline{n})$. In practise, $\tilde{\theta}_\mu(\underline{n})$ is chosen close to $\theta_\mu(\underline{n})$, for reasons that will become obvious below.

We now turn our attention to the implementation of the algorithm on a parallel machine. The action for the pure gauge theory:

$$S_G(U) = \beta \sum_{\underline{n},\mu,\nu} U_\mu(\underline{n}) U_\nu(\underline{n}+a\underline{e}_\mu) U_\mu^\dagger(\underline{n}+a\underline{e}_\nu) U_\nu^\dagger(\underline{n}) \tag{4·14}$$

is local: each link variable interacts only with those variables with which it forms elementary plaquettes. The

change in the action, ΔS, caused by updating any particular link, depends only on those links with which it interacts, all other terms in the sum on $\underline{n}$ of the action cancelling out. It should be obvious then that we can simultaneously update all those variables which are not connected by the action. It is clearly important to find the largest such subset of non-interacting variables to update at the same time. In a two dimensional lattice gauge theory with the Wilson form of the action (4.14), it is easy to see that the optimum pattern is achieved by updating link variables in any one direction in a chessboard pattern. Thus, half the link variables in a particular direction may be simultaneously updated, clearly saving much of the time required on an ordinary serial machine, where only one link may be updated at a time.

Finally, before leaving the Metropolis algorithm, we note that it can be considerably improved, for the pure gauge system, by repeating the algorithm more than once on the same link before proceeding to the next Monte Carlo step. As the number of 'hits' made on one particular link is increased, this modified Metropolis algorithm tends to the heat bath algorithm, discussed below for fermionic degrees of freedom. This method is not suitable if we wish to include dynamical fermions, as we discuss below.

4.3 Dynamical Fermions and Monte Carlo Methods.

The gauge field action given above (4.14) represents only a pure gauge system, and if one generates configurations of the gauge field with this action, in any subsequent calculation (e.g. of particle masses) one will be neglecting the effects of dynamical fermions, that is, in terms of Feynman diagrams, one will be neglecting internal fermion loops. Although it is argued that internal quark loops

should not be very important in QCD (Barbour, 1983) as the quark mass is decreased in numerical simulations in an attempt to reach physical quark mass values, these loops clearly become increasingly important. Hence, to make reliable extrapolations to zero quark masses, one would like to include fermions dynamically in lattice gauge theory calculations. The introduction of anticommuting variables directly in a computer simulation is well nigh impossible, since, on a lattice with N sites, the N anticommuting variables span an algebra with 2^N generators. One would like then to devise some approximation in order to obtain useful results within acceptable computer time.

The standard Euclidean action for a gauge theory with dynamical fermions is:

$$S(\bar{\psi}, \psi, U) = S_G(U) + \sum_{\underline{n},\underline{m}} \bar{\psi}(\underline{n}) \Delta_{\underline{n}\underline{m}}(U) \psi(\underline{m}) \qquad (4.15)$$

where $S_G(U)$ is the pure gauge action (4.13), $\underline{n}$ and $\underline{m}$ label lattice sites, and $\Delta_{\underline{n}\underline{m}}(U)$ is the lattice version of the the Dirac operator (in either its simple form, describing $2^{d/2}$ flavours, or with the flavour symmetry breaking mass term). To simulate the effect of the fermionic part of the action, one first eliminates the Grassmann variables, $\bar{\psi}$ and ψ . This is done analytically using the standard Matthews-Salam formulae (Matthews and Salam, 1954,1955):

$$\int \mathcal{D}\bar{\psi}\, \mathcal{D}\psi\, e^{-S(\bar{\psi},\psi,U)+\bar{\psi}\eta+\bar{\eta}\psi} = \det[\Delta(U)]\, e^{-S(U)-\bar{\eta}\Delta^{-1}\eta} \qquad (4.16)$$

If det{Δ(U)} does not change sign as afunction of U, it can be absorbed into an effective action for the bosonic gauge field, U:

$$S_{eff}(U) = S_G(U) - Tr\, ln\, \{\Delta(U)\} \qquad (4.17)$$

However, even this purely bosonic action is no good for Monte Carlo calculations: it is non-local, due to the determinant of the Dirac operator that appears. Direct evaluation of the determinant is not practical, since the matrix $\Delta_{\underline{nm}}(U)$ is NxN, where N is the number of lattice sites. In fact, the determinant consists of $\sim N^3$ terms, and is produced by cancellation between them. To deal with this non-local determinant, many approximate methods have been developed, that make use of the sparse nature of $\Delta_{\underline{nm}}(U)$ (the Dirac operator couples only nearest neighbours, so that $\Delta_{\underline{nm}}(U)$ is essentially tridiagonal, although periodic or antiperiodic boundary conditions on the fermion fields introduce non-zero elements in the corners of the matrix). One of these methods, the hopping parameter expansion (Lang and Nicolai, 1982; Hasenfratz and Hasenfratz, 1981), is in many respects analogous to the high temperature series expansion used in the study of phase transitions, and has been used in the study of the SU(3) hadron spectrum (Hasenfratz, Hasenfratz, Kunszt and Lang, 1982a,b; Langguth and Montvay, 1984). The hopping parameter is proportional to the amplitude for moving a quark by one lattice spacing, and the order of the expansion is the length of the quark paths considered. So long as the order of the expansion is compatible with the size of the hadron, the results are supposed to be fairly accurate.

A second method proposed by Kuti (1982) is related to the hopping parameter expansion, but generates the quark paths stochastically, so that the quarks perform random walks around the lattice.

There is another method due to Scalapino and Sugar (1981) which requires an initial knowledge of the entire quark Green function, and then makes use of the fact that a

change in gauge variable on a single link induces changes in $\Delta_{\underline{nm}}(U)$ only for those elements near the link. These elements may be updated between successive changes of the gauge field. Rounding errors, which cause $\Delta^{-1}(U)$ to stray from its true value after many iterations are reduced by a correction procedure carried out periodically.

Many other methods also exist (see, e.g. Kogut, 1983), and some have been tested in the context of the Schwinger model (Duncan and Furman, 1981; Martin and Otto, 1982; Ranft and Schiller, 1983; Burkitt, 1983; Ranft, 1983), and we now turn our attention to the pseudofermion method of Fucito, Marinari, Parisi and Rebbi (1980).

Consider the effective action (4.17). First replace (4.17) by:

$$S_{eff}(U) = S_G(U) - \tfrac{1}{2} Tr \ln \{K(U)\} \qquad (4.18)$$

where:

$$K(U) = \Delta^{\dagger} \Delta(U) \qquad (4.19)$$

The problem with using this action directly for Monte Carlo calculations is the non-local nature of the fermionic determinant. Consider updating the gauge field variable on one link, $U_{\mu}(\underline{l})$, say. Then if we wish to implement the Metropolis algorithm discussed in the previous section, we need to find the change in the action:

$$\exp[S_{eff}(U') - S_{eff}(U)] = \exp[S_G(U') - S_G(U)] \frac{\det \Delta(U')}{\det \Delta(U)} \qquad (4.20)$$

If the new link variable is chosen so that it is close to

the old one, we can linearise the expression for the change in the effective action:

$$S_{eff}(\{U'\}) - S_{eff}(\{U\}) = S_G(\{U'\}) - S_G(\{U\}) - \frac{1}{2} \sum_{\underline{n},\underline{m}} K^{-1}_{\underline{n},\underline{m}} \frac{\delta K_{\underline{m},\underline{n}}}{\delta U_\mu(\underline{l})} \delta U_\mu(\underline{l}) + O(\delta U^2) \qquad (4.21)$$

As we are updating only one gauge link, $\delta K/\delta U$ is non-zero only for very few values of $\underline{n}$ and $\underline{m}$, namely for those sites neighbouring the link being updated. Hence, we only need the element of K^{-1} for sites neighbouring this link, rather than the entire Green function. These elements can be calculated in a variety of ways (Burkitt, 1983), but in the pseudofermion method of Fucito et. al. these elements are calculated approximately using a Monte Carlo technique. Note that:

$$K^{-1}_{\underline{n},\underline{m}}(U) = \langle \varphi^*(\underline{m}) \varphi(\underline{n}) \rangle_{PF} = \frac{\int \mathcal{D}\varphi^* \mathcal{D}\varphi \; \varphi^*(\underline{m}) \varphi(\underline{n}) \exp(-S_{PF})}{\int \mathcal{D}\varphi^* \mathcal{D}\varphi \exp(-S_{PF})} \qquad (4.22)$$

where:

$$S_{PF} = \sum_{\underline{n},\underline{m}} \varphi^*(\underline{n}) K_{\underline{n},\underline{m}} \varphi(\underline{m}) \qquad (4.23)$$

S_{PF} is the action for the pseudofermionic variables, φ^* and φ which are complex bosonic fields. Now we can calculate $K^{-1}_{\underline{nm}}$ approximately, for a given gauge configuration, by performing successive updates of the pseudofermion fields, according to the above action, and then using an expression exactly analogous to (4.2):

$$\langle \varphi^*(\underline{m}) \varphi(\underline{n}) \rangle_{PF} \Big|_{\{U\}} = \frac{1}{N_{PF}} \sum_{\{\varphi^*,\varphi\}} \varphi^*(\underline{m}) \varphi(\underline{n}) \Big|_{\{U\}} \qquad (4.24)$$

where N_{PF} is the number of pseudofermion sweeps performed, and $\{\varphi^*,\varphi\}$ denotes the pseudofermion configurations. These values are fed back into the effective action for the gauge fields as these are updated, according to a Metropolis algorithm with action:

$$S_{eff}(U) = S_G(U) - \frac{1}{2}\sum_{\underline{n},\underline{m}} \langle \varphi^*_{\underline{n}} \varphi_{\underline{m}} \rangle K_{\underline{n},\underline{m}}(U) \qquad (4.25)$$

and the pseudofermion fields are again updated several times to obtain values of $\langle \varphi^*_{\underline{n}}, \varphi_{\underline{m}} \rangle_{PF}$ in the new gauge field configuration.

The computer time required for this process is clearly proportional to N_{PF}, the number of pseudofermion sweeps performed between each gauge field update, independently of the lattice size. The exact result, apart from errors proportional to $(\delta U)^2$ is obtained in the limit $N_{PF} \to \infty$. The method then depends on the value of N_{PF} required to give reliable results, which must be found by experiment. In the simulation of the Schwinger model by Marinari, Parisi and Rebbi (1981), it was found that the values of N_{PF} required to extrapolate to ∞ were manageable. However, as one proceeds to smaller masses than those used by Marinari et. al., the convergence of the algorithm deteriorates (Burkitt, 1983), and many more pseudofermion steps are required between each update of the gauge field. The work of Marinari et. al., and that of Burkitt, was performed using a Metropolis algorithm for both gauge fields and pseudofermion fields. Gauge field updates must be done with a Metropolis algorithm, if we are to be able to use the small angle update approximation for linearisation of the effective action, but there is a much more efficient algorithm available for the update of the pseudofermion field : the heat bath. In the next section, we shall show how this algorithm is implemented for the pseudofermion

fields, in the hope that the faster convergence of the algorithm will enable us to generate good unquenched gauge field configurations at lower quark masses than the Metropolis algorithm in a reasonable amount of computer time.

4.4 The Heat Bath Algorithm For Pseudofermions.

Consider the pseudofermionic action, (4.23):

$$S_{PF} = \sum_{\underline{n},\underline{m}} \varphi^*(\underline{n})\, K_{\underline{n},\underline{m}}\, \varphi(\underline{m}) \qquad (4.23)$$

where $K_{\underline{nm}}$ is essentially the square of the lattice Dirac operator. Our aim is to update the pseudofermionic variables in a fixed gauge configuration according to a Boltzmann distribution, $\exp(-S_{PF})$. We could do this by considering the change in the action caused by changing any one pseudofermionic variable and applying the Metropolis algorithm discussed in section 4.2. But we know that using the Metropolis algorithm, unless we choose a new pseudofermionic variable quite close to the old one, the algorithm is likely to reject the update. Hence, the Metropolis algorithm moves only slowly away from an initial configuration, sampling only a small part of the distribution of equilibrium configurations. The heat bath algorithm enables us to choose a new pseudofermionic variable independently of the old one, and hence we can sample equilibrium configurations far away from our original configuration very quickly.

Consider updating a particular pseudofermionic variable, say $\varphi(\underline{r})$. Write the action in terms of $\varphi(\underline{r})$:

$$S_{PF}[\varphi(\underline{r})] = a(\underline{r})\,|\varphi(\underline{r})|^2 + b'(\underline{r})\,\varphi(\underline{r}) + \varphi^*(\underline{r})\,b(\underline{r}) + c(\underline{r}) \qquad (4.26)$$

The coefficient of the quadratic term comes from the part of the action coupling $\varphi(\underline{r})$ to itself, and is independent of $\underline{r}$, apart from a phase; the linear coefficients $b(\underline{r})$ and $b'(\underline{r})$ depend on the pseudofermionic variables to which $\varphi(\underline{r})$ is coupled (nearest neighbours and next nearest neighbours), which are held fixed whilst $\varphi(\underline{r})$ is updated; and $c(\underline{r})$ is independent of $\varphi(\underline{r})$, and arises from interactions between all other pseudofermionic variables on the lattice, which are also held fixed whilst $\varphi(\underline{r})$ is updated (though we relax this constraint when we consider parallel programming below). From (4.23), we see that:

$$b'(\underline{r}) = \sum_{\underline{n}} \varphi^*(\underline{n}) K_{\underline{n},\underline{r}} \qquad (4.27)$$

and

$$b(\underline{r}) = \sum_{\underline{n}} K_{\underline{r},\underline{n}} \varphi(\underline{n})$$

If we write the lattice Dirac operator symbolically as:

$$\Delta_{\underline{n},\underline{m}}(U) = (\not{D} + m)_{\underline{n},\underline{m}} \qquad (4.28)$$

then a consideration of the explicit form of the action (3.18) gives:

$$(\not{D} + m)^{\dagger}_{\underline{n},\underline{m}} = (-\not{D} + m)_{\underline{n},\underline{m}} \qquad (4.29)$$

and hence:

$$K^*_{\underline{n},\underline{m}} = K_{\underline{m},\underline{n}} \qquad (4.30)$$

So, we have:

$$b'(\underline{r}) = b^*(\underline{r}) \qquad (4.31)$$

Writing the complex scalar field as:

$$\varphi(\underline{r}) = \varphi_R(\underline{r}) + i\,\varphi_I(\underline{r}) \tag{4.32}$$

we see that the action is quadratic in both φ_R and φ_I separately:

$$S_{PF}[\varphi_R(\underline{r}) + i\varphi_I(\underline{r})] = a(\underline{r})\varphi_R^2(\underline{r}) + 2b_R(\underline{r})\varphi_R(\underline{r}) + c_R(\underline{r}) + a(\underline{r})\varphi_I^2(\underline{r}) + 2b_I(\underline{r})\varphi_I(\underline{r}) + c_I(\underline{r}) \tag{4.33}$$

where b_R, b_I and c_R and c_I are, respectively, the real and imaginary parts of b and c. Now, because at equilibrium the pseudofermionic variables are distributed with the Boltzmann factor, $\exp(-S_{PF})$, we see that the real and imaginary parts of $\varphi(\underline{r})$ are separately distributed according to a Gaussian distribution, $\exp\{-(1/2\sigma^2)[\varphi(\underline{r})-\bar{\varphi}(\underline{r})]\}$ with:

$$\sigma(\underline{r}) = \frac{1}{\sqrt{2a(\underline{r})}} \tag{4.34}$$

and

$$\bar{\varphi}_{R,I}(\underline{r}) = \frac{-b_{R,I}(\underline{r})}{a(\underline{r})} \tag{4.35}$$

A consideration of the action gives explicitly:

$$\sigma(\underline{r}) = (-1)^{r_1+r_2}\left(\frac{m_d - m_u}{4}\right) + \left(\frac{m_d^2 + m_u^2}{2}\right) + 1 \tag{4.36}$$

The explicit form of b is not particularly illuminating, but consists of both one and two link terms resulting from the application of the Dirac operator and its hermitian conjugate at the site $\underline{r}$.

The heat bath algorithm, then, consists of choosing a pseudo random number with a Gaussian distribution N(1,0) (in the notation $N(\sigma^2,\bar{\varphi})$), and rescaling this to obtain a new pseudofermionic variable with the correct Boltzmann distribution. That is, pick a random number, r, with distribution $\exp(-r^2/2)$, and then define a new pseudofermionic variable according to:

$$\varphi(\underline{r}) = \frac{1}{\sqrt{2a(\underline{r})}} - \frac{b(\underline{r})}{a(\underline{r})} \qquad (4.37)$$

This procedure is carried out independently for both the real and imaginary parts of $\varphi(\underline{r})$.

When we considered updating the gauge fields in section 4.2, we argued that we could simultaneously update any subset of the gauge fields not connected by the action. The same is true of pseudofermionic updates, and hence, as for the gauge fields, we seek the largest such subset of variables, to make the greatest use of the parallelism of the DAP. The simple Kogut-Susskind action for degenerate flavours leads to a pseudofermionic action that couples next nearest neighbours. Hence, although we cannot simultaneously update any given pseudofermionic variable and any of its eight next nearest neighbours, we can simultaneously update the variable and any <u>one</u> of its four immediate neighbours. The introduction of the one link mass term does not change the resulting one in four update pattern, provided that we simultaneously update nearest neighbours in the direction perpendicular to that of the mass term. A two link mass term, however, does destroy the one in four update pattern, a one in six pattern being the best we can do, although, because we work on a 64x64 lattice (the DAP consists of 64x64 processing elements, each representing a site of the lattice), a one in eight update pattern is easier to implement.

In fact, the one in four update pattern, whilst at first sight seeming to waste rather a lot of the power of the DAP, is very efficient. To calculate the coefficients a and b of the heat bath algorithm, we require the action of the operator $\Delta^\dagger\Delta$ on every pseudofermionic variable to be updated. In practice, this was done by calculating at the four nearest neighbour sites the action of the first order operator Δ (the lattice Dirac operator), and then multiplying these quantities by the gauge fields linking them to the update site, weighted to simulate the action of Δ at the update site. The calculation of the action of Δ is the most time consuming part of the programmes, and we note that our one in four update pattern requires a knowledge of the operator at every lattice site, hence exploiting to the full the parallelism of the DAP.

Note too that the expression (4.19) is actually implemented using the expression:

$$\begin{aligned} \delta S_{eff} &= \delta S_G(U) - \tfrac{1}{2}\left[\Delta^{-1}\delta\Delta + (\Delta^\dagger)^{-1}\delta(\Delta^\dagger)\right] + O(\delta U^2) \\ &= \delta S_G(U) - \tfrac{1}{2}\mathrm{Tr}\left[(\not{D}+m)^{-1} - (-\not{D}+m)^{-1}\right]\delta\not{D} + O(\delta U^2) \end{aligned} \tag{4.38}$$

by (4.28) and (4.29). The inverse matrix elements are found using:

$$\begin{aligned} (\not{D}+m)^{-1}_{n,m} &= \frac{1}{Z_{PF}}\int \mathcal{D}\phi^*\mathcal{D}\phi\,[(\not{D}+m)\phi]^*(m)\,\phi(n)\; e^{-S_{PF}} \\ &\simeq \frac{1}{N_{PF}}\sum_{\{\phi^*,\phi\}}[(\not{D}+m)\phi]^*(m)\,\phi(n) \end{aligned} \tag{4.39}$$

and

$$\begin{aligned} [(\not{D}+m)^\dagger]^{-1}_{n,m} = (-\not{D}+m)^{-1}_{n,m} &= \frac{1}{Z_{PF}}\int \mathcal{D}\phi^*\mathcal{D}\phi\;\phi^*(m)[(\not{D}+m)\phi](n) \\ &\quad \times e^{-S_{PF}} \\ &\simeq \frac{1}{N_{PF}}\sum_{\{\phi^*,\phi\}}\phi^*(m)[(\not{D}+m)\phi](n) \end{aligned} \tag{4.40}$$

where Z_{PF} is the pseudofermionic partition function. Hence, we see that the implementation of the Metropolis algorithm for the gauge fields requires a knowledge of the operation of Δ at each end of the update link, and the optimal one in two chessboard update pattern for the gauge fields thus requires the calculation of $\Delta\varphi$ at every site, and is also efficient in exploiting the parallelism of the DAP.

4.5 The Conjugate Gradient Algorithm.

Once we have generated gauge configurations, be they quenched or unquenched, we need to calculate quark Green functions within these configurations, and from these form the mesonic propagators considered in the last chapter. We are interested in the propagator from some fixed site, the origin, out to some site $\underline{n}$:

$$\langle \bar{\chi}(\underline{0})\chi(\underline{n})\rangle = G(\underline{n},\underline{0}) \tag{4.41}$$

The Green function satisfies:

$$\Delta(\underline{n},\underline{m})\,G(\underline{m},\underline{l}) = \delta_{\underline{n},\underline{l}} \tag{4.42}$$

As $\underline{l}$ is fixed in the calculation of interest, we need calculate only one column of the Green function. We are faced, then, with the problem of solving a matrix equation of the type:

$$A\underline{x} = \underline{b} \tag{4.43}$$

for the vector $\underline{x}$. There are many ways of solving this

problem, a common one being the Gauss-Seidel iterative scheme (Bowler, Pawley and Wallace, 1983). We present here the method of conjugate gradients, due to Hestenes and Stiefel (1952; see also Householder, 1964; Reid, 1971; Stoer and Bulirsch, 1980) which we have tested and found to be much faster than the Gauss-Seidel scheme for the sparse matrices of interest.

Let A be symmetric and positive definite. This immediately implies that its inverse is also symmeteric positive definite. Suppose we guess a solution to (4.43), $\bar{\underline{x}}$. Form the vector of residuals, $\underline{r}$:

$$\underline{r} = \underline{b} - A\bar{\underline{x}} \qquad (4.44)$$

From this define the positive error function, h^2:

$$h^2 = (\underline{r}, A^{-1}\underline{r}) \qquad (4.45)$$

This must have a real positive value for all possible vectors $\bar{\underline{x}}$, except the correct solution, $\underline{x}$. Substituting (4.44) into (4.45) we have:

$$h^2 = (\bar{\underline{x}}, A\bar{\underline{x}}) - 2(\underline{b}, \bar{\underline{x}}) + (\underline{b}, A^{-1}\underline{b}) \qquad (4.46)$$

Let $\underline{x}^i$ be some n-dimensional vector in the space in which A acts, and write:

$$\bar{\underline{x}} = \underline{x}^i + \alpha \underline{d}^i \qquad (4.47)$$

$\underline{d}^i$ defines a direction in which we have to move a distance α to reach $\bar{\underline{x}}$. Substituting in h^2, we have:

$$h^2 = (\underline{x}^i + \alpha \underline{d}^i, A[\underline{x}^i + \alpha \underline{d}^i]) - 2(\underline{b}, \underline{x}^i + \alpha \underline{d}^i) + (\underline{b}, A^{-1}\underline{b})$$

$$= (\underline{x}^i, A\underline{x}^i) + \alpha^2 (\underline{d}^i, A\underline{d}^i) + 2\alpha (\underline{d}^i, A\underline{x}^i) \qquad (4.48)$$

$$- 2(\underline{b}, \underline{x}^i) - 2\alpha (\underline{d}^i, \underline{b}) + (\underline{b}, A^{-1}\underline{b})$$

So, h^2 has a local minimum (because A is positive definite) for a value of α given by:

$$\frac{\partial h^2}{\partial \alpha} = 0 = 2\alpha(\underline{d}^i, A\underline{d}^i) + 2(\underline{d}^i, A\underline{x}^i) - 2(\underline{d}^i, \underline{b}) \qquad (4.49)$$

namely:

$$\alpha = \frac{(\underline{d}^i, [\underline{b} - A\underline{x}^i])}{(\underline{d}^i, A\underline{d}^i)} \qquad (4.50)$$

This then suggests the following algorithm: take a starting vector, $\underline{x}_0$, and form the corresponding residual:

$$\underline{r}_0 = \underline{b} - A\underline{x}_0 \qquad (4.51)$$

Set $p_0 = r_0$, and then for i=0,1,2,... find the vectors x^{i+1}, r^{i+1} and p^{i+1}, and the scalars α_i and β_i using:

$$\alpha_i = (\underline{p}^i, \underline{r}^i) / (\underline{p}^i, A\underline{p}^i)$$

$$\underline{x}^{i+1} = \underline{x}^i + \alpha_i \underline{p}^i$$

$$\underline{r}^{i+1} = \underline{b} - A\underline{x}^{i+1} \qquad (4.52)$$

$$\beta_i = (-\underline{r}^{i+1}, A\underline{p}^i) / (\underline{p}^i, A\underline{p}^i)$$

$$\underline{p}^{i+1} = \underline{r}^{i+1} + \beta_i \underline{p}^i$$

stopping if either r^i or p^i is zero. The inner product is the ordinary scalar product:

$$(\underline{x}, \underline{y}) = \underline{x}^T \underline{y} \tag{4.53}$$

The vectors of the algorithm satisfy the orthogonality relations:

$$(\underline{r}^i, \underline{p}^j) = 0 \qquad i > j \tag{4.54}$$

$$(\underline{p}^i, A\underline{p}^j) = 0 \qquad i \neq j \tag{4.55}$$

$$(\underline{r}^i, \underline{r}^j) = 0 \qquad i \neq j \tag{4.56}$$

These may be proved by induction. The method, then consists of choosing a starting point $\underline{x}_0$ and a direction $\underline{p}_0$, and minimising the residuals in this direction. A new direction is then chosen, as nearly as possible the direction of steepest descent from the local minimum, but with the overriding condition that the direction vectors be mutually conjugate, that is, mutually orthogonal with respect to A (4.55).

The orthogonality relations together with the fact that

$$(\underline{r}^i, \underline{r}^i) = (\underline{r}^i, \underline{p}^i) \tag{4.57}$$

which may also be proved by induction, enables us to write a version of the algorithm which is more efficient

computationally, and which is identical in the absence of round-off. Replace (4.52) by:

$$\begin{aligned} \alpha_i &= (\underline{r}^i, \underline{r}^i)/(\underline{p}^i, A\underline{p}^i) \\ \underline{x}^{i+1} &= \underline{x}^i + \alpha \underline{p}^i \\ \underline{r}^{i+1} &= \underline{r}^i - \alpha_i A\underline{p}^i \\ \beta_i &= (\underline{r}^{i+1}, r^{i+1})/(\underline{r}^i, \underline{r}^i) \\ \underline{p}^{i+1} &= \underline{r}^{i+1} + \beta_i \underline{p}^i \end{aligned} \qquad (4.58)$$

This version of the algorithm is preferable as each iteration involves the computation of one less scalar product. Numerical experiments by Reid (1971) suggest that there is very little difference between the accuracy obtained with the two versions, using the same number of iterations.

Strictly speaking, the conjugate gradient method is not an iterative technique (in the absence of round-off). From the recurrences for p^i and r^i, we know that these vectors both lie in the space

$$S_{i+1} = \{\underline{r}_0, A\underline{r}_0, \cdots, A^i\underline{r}_0\} \qquad (4.59)$$

Note that $S_i \subset S_{i+1}$ (i=0,1,2,...) and if m is the smallest integer such that $A^m r_0$ is contained in S_m, then the dimension of S_i is i for i<m and m for i>m. Usually m is equal to the order of A, but if A has any multiple eigenvalues, or if r_0 has a zero component of any eigenvector of A, then m<n. The relation (4.56) tells us that the residuals r^i are the same

vectors as those obtained from the sequence r_0, Ar_0,... by orthogonalisation, and the vectors p^i may similarly be obtained using (4.55). Hence, $p^i, r^i \neq 0$ for $i<m$, and $p^m = r^m = 0$, so that the algorithm is finite and terminates after exactly m steps. Unfortunately, this property no longer holds in the presence of round-off, although in practice many fewer than n iterations are necessary to achieve good accuracy.

Finally we note that all we have said applies only to positive definite symmetric matrices, and the matrix we wish to invert, the lattice Dirac operator, is not positive definite. We get round this in the same way as for the pseudofermionic technique discussed above and solve the normal equations obtained by multiplying through by $A^\dagger$:

$$A^\dagger A \, \underline{x} = A^\dagger \underline{b} \tag{4.60}$$

with the following algorithm:

$$\begin{aligned}
&\underline{r}_0 = \underline{b} - A\underline{x}_0 \,, \qquad \overline{r}_0 = \underline{p}_0 = A^\dagger \underline{r}_0 \\
&\alpha_i = (\overline{r}^i, \overline{r}^i) / (A\underline{p}^i, A\underline{p}^i) \\
&x^{i+1} = \underline{x}^i + \alpha_i \underline{p}^i \\
&\underline{r}^{i+1} = \underline{r}^i - \alpha_i A \underline{p}^i \\
&\beta_i = (\overline{r}^{i+1}, \overline{r}^{i+1}) / (\overline{r}^i, \overline{r}^i) \\
&\underline{p}^{i+1} = \overline{r}^{i+1} + \beta_i \underline{p}^i
\end{aligned} \tag{4.61}$$

The orthogonality relations become:

$$(\underline{r}^{i*}, \underline{p}^{j}) = 0 \qquad i > j \tag{4.62}$$

$$(\underline{r}^{i*}, \underline{r}^{j}) = 0 \qquad i \neq j \tag{4.63}$$

$$(A\underline{p}^{i*}, A\underline{p}^{j}) = 0 \qquad i \neq j \tag{4.64}$$

We now have all the algorithms we need to calculate particle masses in the Schwinger model.

4.6 Free Fermion Results.

In this section we use free fermion results to illustrate the programmes developed for an investigation of the Schwinger model, and to provide guidelines for the investigation of the fully interacting theory.

Consider first the fermionic Green function, $G(\underline{n},\underline{m})$. This was calculated using both the conjugate gradient algorithm discussed above, and the more widely used Gauss-Seidel scheme, with relaxation. This scheme solves a system of equations:

$$A\underline{x} = \underline{b} \tag{4.65}$$

by an iterative method, whereby, from an initial guess at the vector $\underline{x}$, successively better approximations are generated according to the formula:

$$\underline{x}^{i+1} = x_i + \varepsilon(\underline{b} - A\underline{x}^{i}) \tag{4.66}$$

The parameter ε is varied until, empirically, some optimum value is found. It was found that the conjugate gradient method converged much more quickly than the Gauss-Seidel scheme, even though a single iteration for the latter was much quicker. For example, in the free two species model, where both quark masses were set equal to 0.10 (in units of the reciprocal lattice spacing), each Gauss-Seidel iteration took 0.028 seconds, whilst each conjugate gradient step took 0.070 seconds. However, to achieve eight figure accuracy in the time slice quark propagator required only about 70 conjugate gradient iterations, compared with 5000 Gauss-Seidel steps with ε=0.02.

In figure 4.1, we show the time slice propagator for the fundamental fermion fields in the Lagrangian, $\bar{\chi}$ and χ, in the two species model with $m_u=m_d=0.10$. The oscillation in the Green function can be traced to the finiteness and (anti)periodicity of the lattice. It is reassuring that this oscillation does not appear in the free propagator of the continuum Kahler-Dirac fields u and d, constructed according to:

$$q^{\alpha a}(y) = \begin{pmatrix} u_1(y) & d_1(y) \\ u_2(y) & d_2(y) \end{pmatrix} = \frac{1}{\sqrt{2}} \begin{pmatrix} \chi_\phi(y)+\chi_2(y) & \chi_1(y)-\chi_{12}(y) \\ \chi_1(y)+\chi_{12}(y) & \chi_\phi(y)-\chi_2(y) \end{pmatrix} \tag{4.67}$$

in the notation of chapter three. This is illustrated in figure 4.2.

To illustrate the effect of the one-link mass term introduced to enable us to decouple one of the continuum flavours, we present figures 4.3a to 4.3d. In these, the d quark mass is increased from m_d=0.10 up to m_d=90.0, whilst

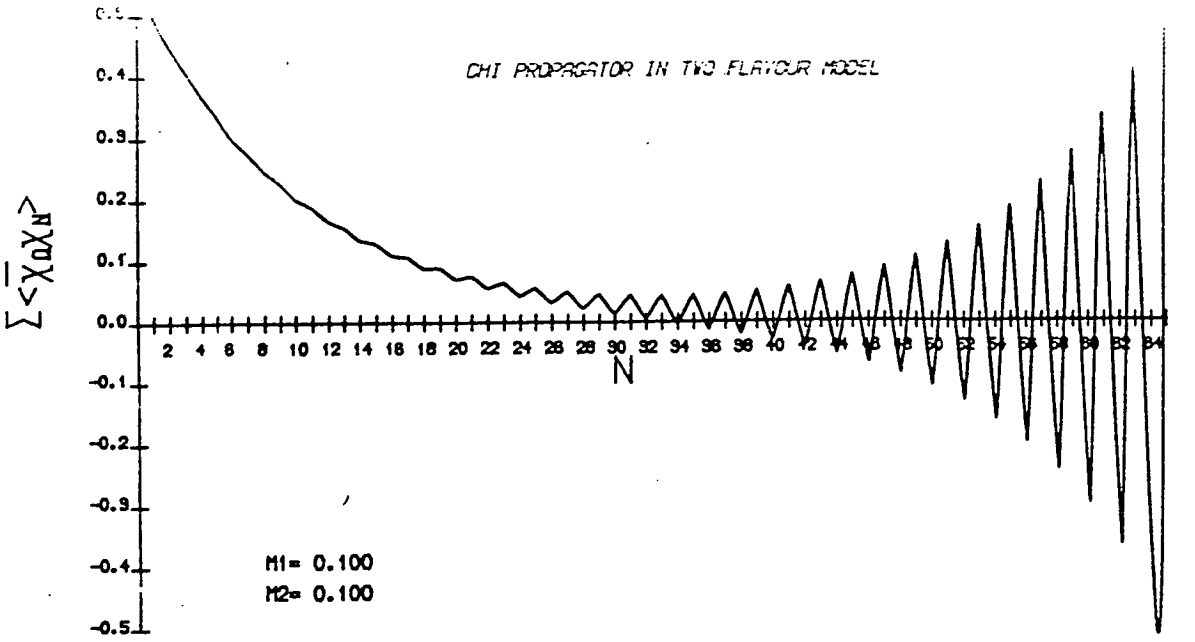

Fig 4.1
Timeslice propagator for the Kogut-Susskind field, χ.
Free case, $m_u=m_d=0.1$

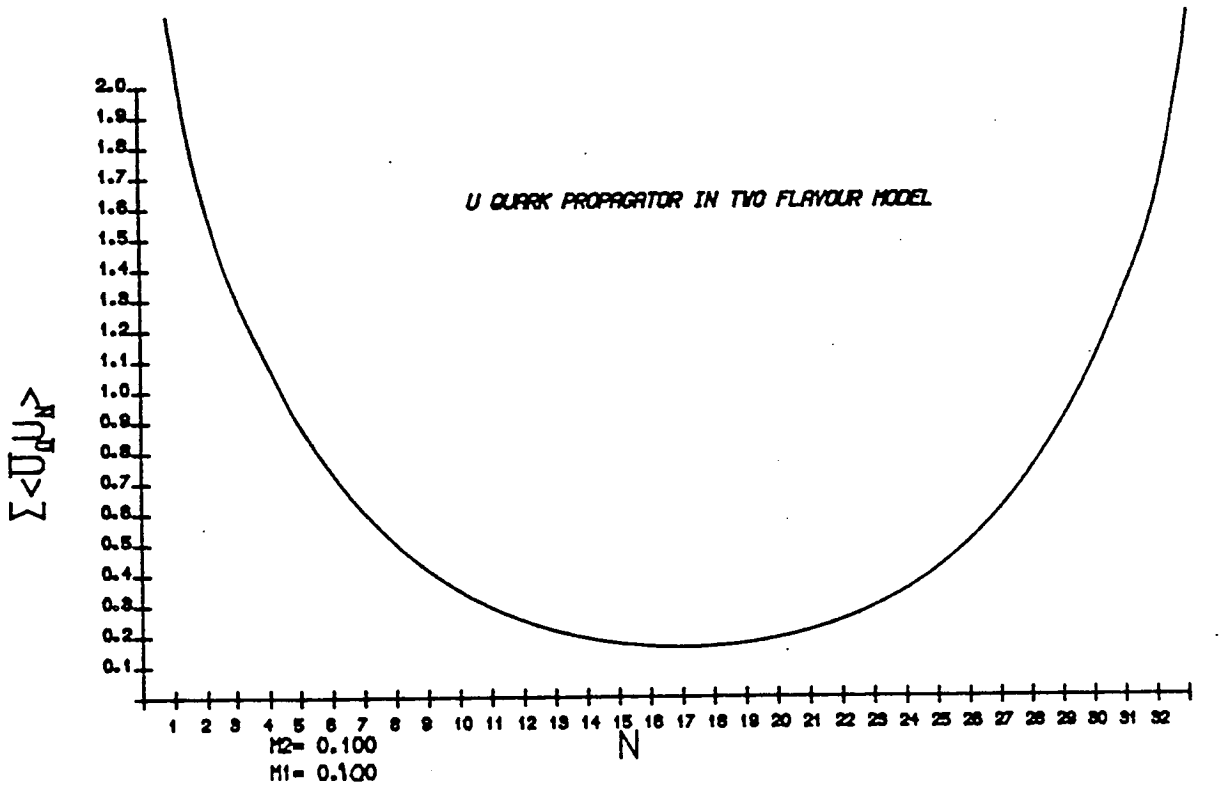

Fig 4.2
Timeslice propagator for the up quark, constructed according to the Kahler Dirac formulation.
Free case, $m_u=m_d=0.1$

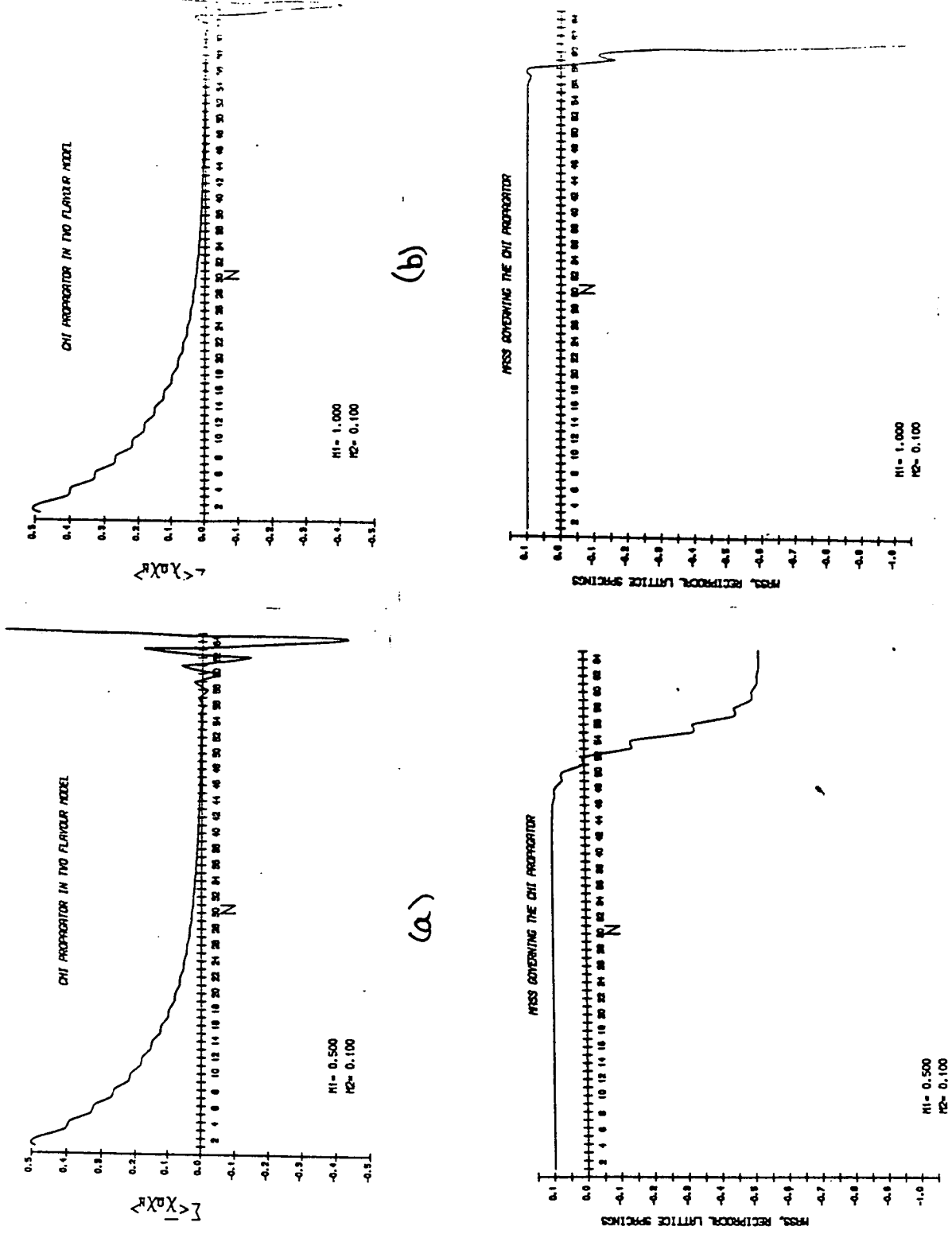

Fig 4.3

Timeslice propagators for the χ field, showing the effect of the one link mass term.

(see also next page.)

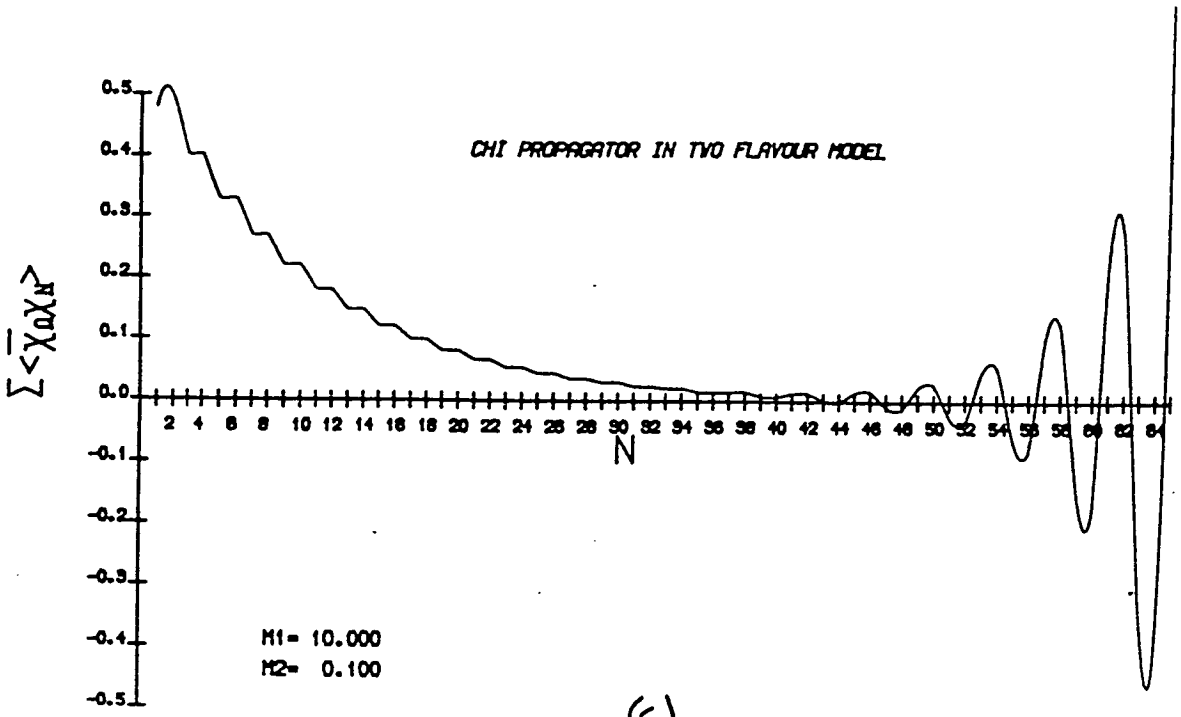
CHI PROPAGATOR IN TWO FLAVOUR MODEL
$\Sigma\bar{<}\chi_0\chi_N>$
N
M1= 10.000
M2= 0.100

(c)

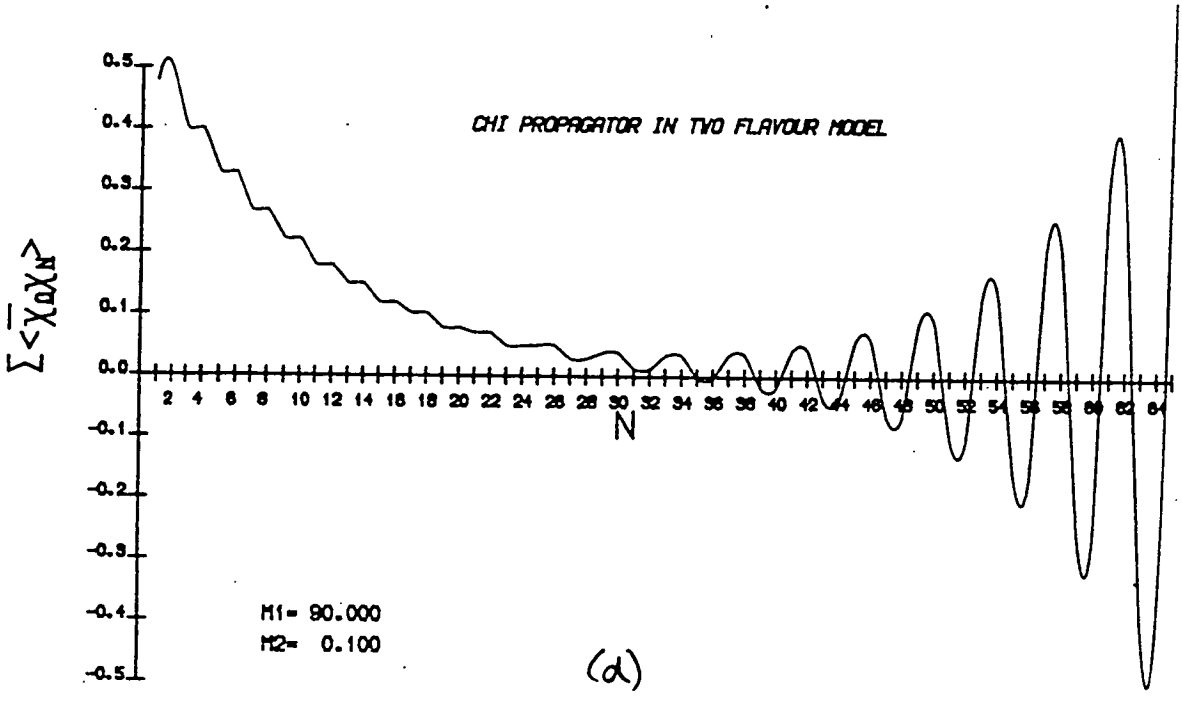
CHI PROPAGATOR IN TWO FLAVOUR MODEL
$\Sigma\bar{<}\chi_0\chi_N>$
N
M1= 90.000
M2= 0.100

(d)

Fig 4.3

the u quark mass is held fixed at $m_u=0.10$. We also show plots of the effective mass:

$$m_{eff} = \ln \left\{ \frac{\Delta(t)}{\Delta(t+1)} \right\} \qquad (4.68)$$

where Δ is the time slice propagator of the χ field, and t labels the time coordinate in lattice spacings. These plots show clearly the two quark masses: the u quark propagating forwards, and the d quark backwards. Again it is reassuring that the u and d quark propagators decay across the lattice with only a single mass.

These figures show that when $m_d=1.0$ (the natural cut-off of the theory), the d quark seems to have decoupled completely, and the propagator decays with the u quark mass right across the lattice, jumping at the end only to satisfy periodicity. Note, though, that when m_d is increased beyond this natural cut-off, we see a second fermion flavour once more beginning to propagate back across the lattice. At very large values of m_d, we seem once again to have fermion flavours, degenerate in the u quark mass. This result was subsequently verified analytically by Verstegen (1984). Note too that as the d quark mass is increased, points in the time slice propagator become associated in pairs, so that the propagator becomes stepped. This is most clearly seen at $m_d=1.0$, and is, of course, due to the coupling between lattice points introduced by the one link mass term, which is proportional to the mass splitting. This also explains why, for very large m_d, although the oscillation in the fermionic time slice propagator returns, it does so with only half the frequency of the oscillations occurring for $m_d<1.0$: the coupling freezes the fields together in pairs along one direction effectively doubling

the lattice spacing.

From the quark Green functions discussed above, we can construct meson propagators according to the local or better defined non-local definitions discussed in chapter three. This is done by multiplying together the appropriate Green functions of the fundamental fermionic fields. Examples of the resulting time slice propagators are shown in figures 4.4 and 4.5. Figures 4.4a and 4.4b show the two possible local mesonic time slice propagators for the two species model. As for the χ propagators, the local mesonic propagators oscillate, because, as we showed in chapter three, these operators mix two of the physical ststes, one with an oscillating phase. Figures 4.5a to 4.5d show the time slice propagators for the non-local (Kahler-Dirac) definition of the mesonic operators. We pointed out in chapter three that if we neglect the annihilation diagrams that contribute to the mesonic propagators, then the states are degenerate in isospin. For the free propagators, of course, the annihilation diagrams do not contribute, and we do indeed see that the isospin states are degenerate. Two alternative definitions of the pion are used. In figure 4.5d, we show the time slice propagator for a pion defined with γ_2 diagonal. In figure 4.5e, we show the operator defined with γ_5 diagonal. This freedom in the definition of particle operators no longer remains in the one species model, where the definition of the mass term determines the choice of the gamma matrices. It is also possible to calculate free propagators for the mesonic states with $I_3 \neq 0$. These states are a mixture of local and two link pieces with γ_2 diagonal, and display behaviour identical with the $I_3=0$ states.

We may similarly calculate free mesonic propagators for the one species model, with $m_d=1.0$.

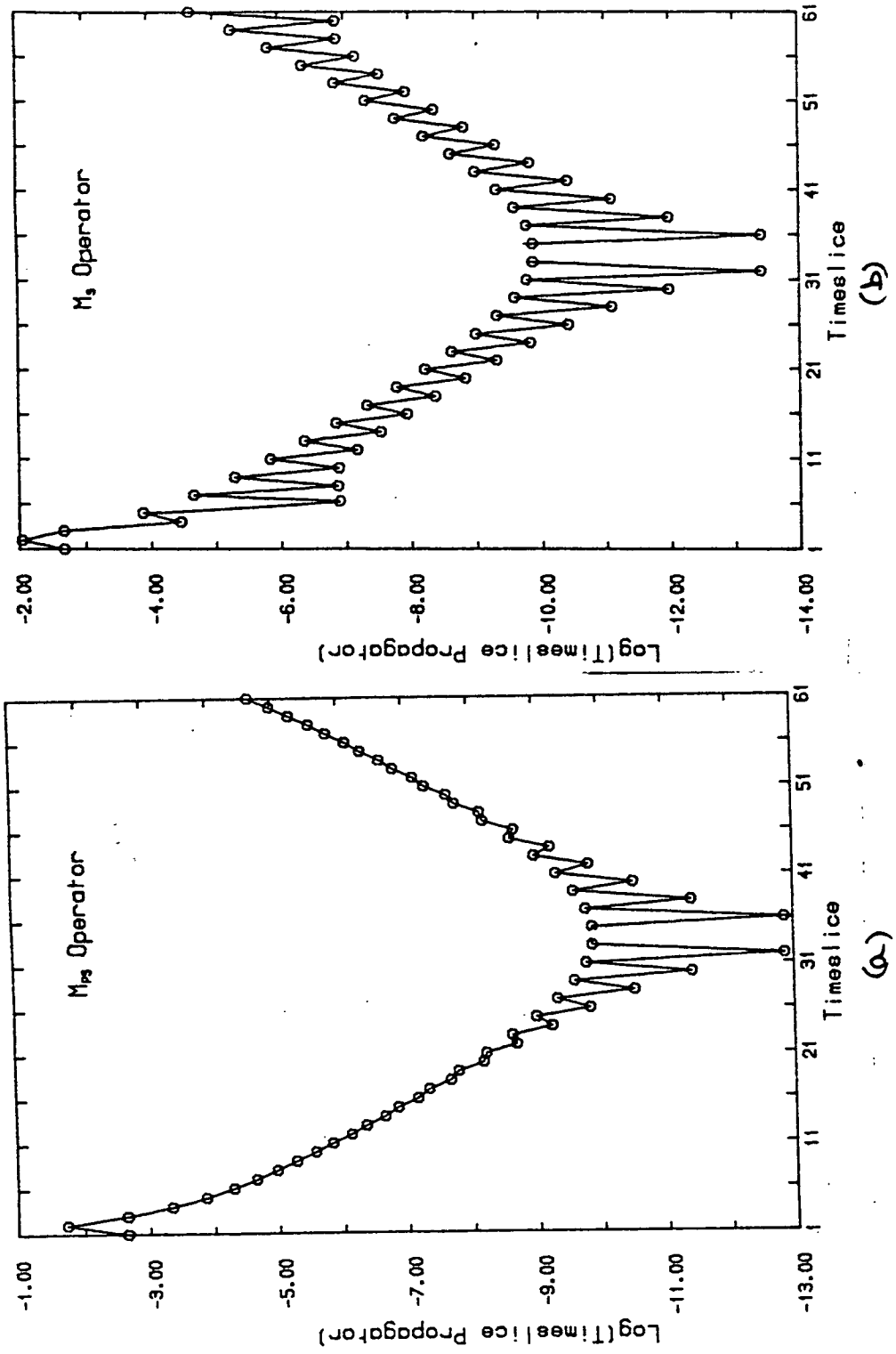

Fig 4.4

Timeslice propagators for the local definition of mesonic particle operators. Free case, $m_u=m_d=0.1$.

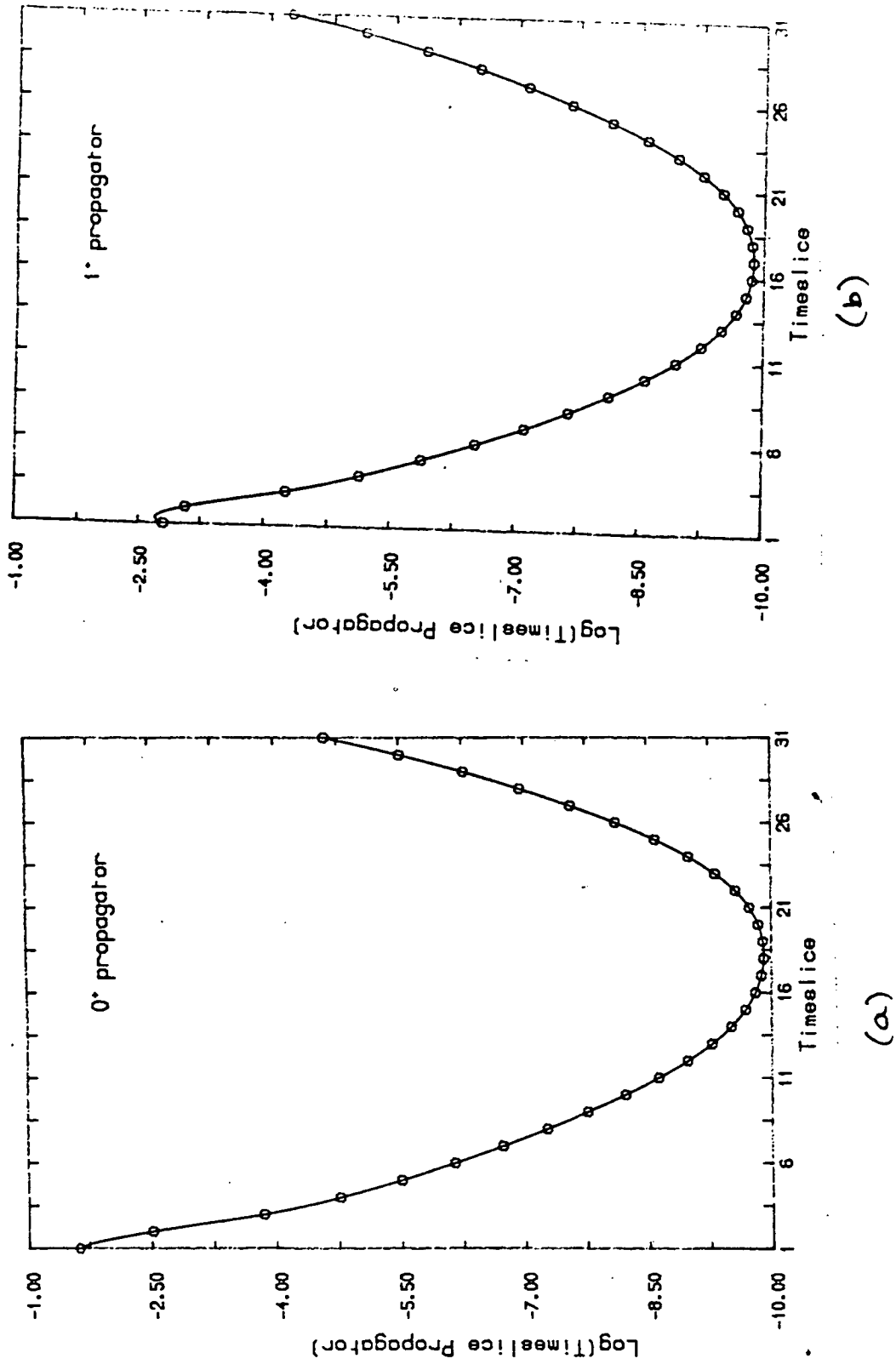

Fig 4.5

Timeslice propagators for the Kahler-Dirac definition of mesonic operators in the two species model.

Free case, $m_u = m_d = 0.1$.

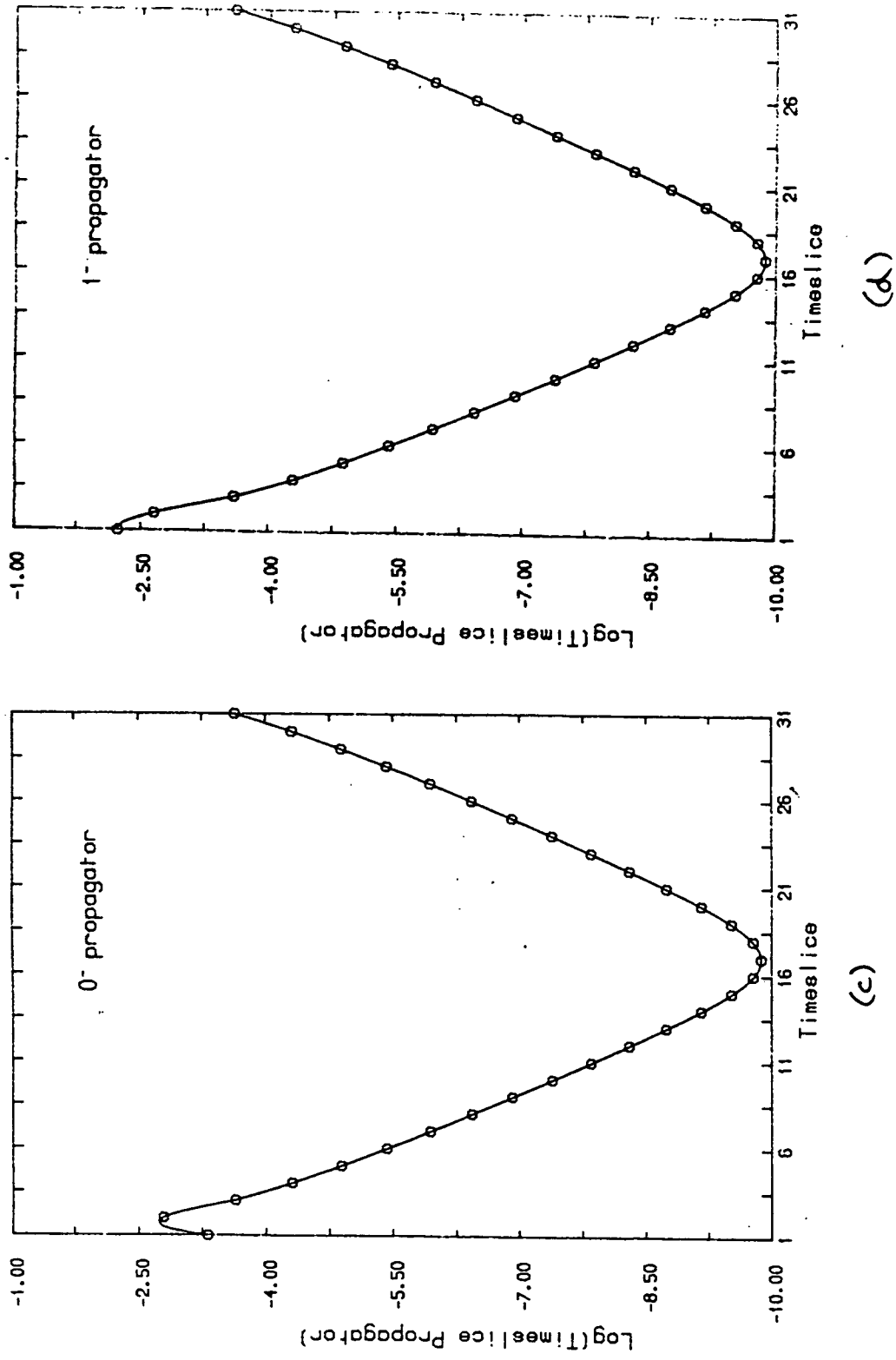

Fig 4.5

Timeslice propagators for the Kahler-Dirac definition of mesonic operators in the two species model. Free case, $m_u=m_d=0.1$.

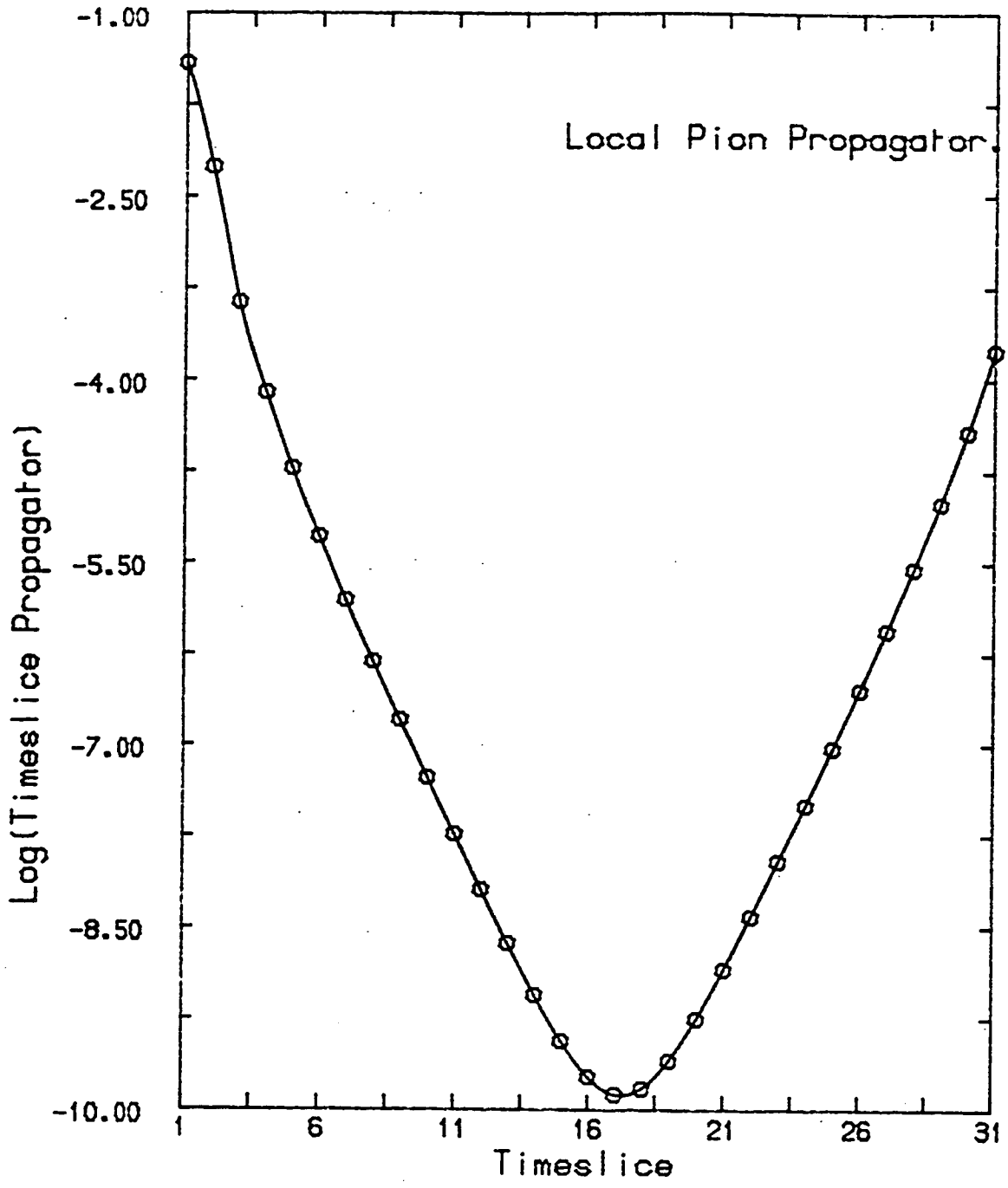

Fig 4.5(e)

Timeslice propagators for the Kahler-Dirac definition of mesonic operators in the two species model.

Free case, $m_u = m_d = 0.1$.

The pseudofermion heat bath programmes may be tested by calculating the fermionic chiral condensate, $\langle\bar{\psi}\psi(m)\rangle$, for the one and two species models and comparing the results with analytical results. This allows us to investigate the effects of boundary conditions for small quark masses. The condensate for the two species model is calculated according to:

$$\frac{1}{N}\sum_{\underline{n}}\langle\bar{u}u\rangle = \frac{1}{N}\frac{\partial}{\partial m_u}\ln Z$$
$$\frac{1}{N}\sum_{\underline{n}}\langle\bar{d}d\rangle = \frac{1}{N}\frac{\partial}{\partial m_d}\ln Z \qquad (4.69)$$

where Z is the partition function of the theory, N the number of lattice sites, and we have averaged over the lattice. Hence:

$$\langle\bar{u}u\rangle = \langle\tfrac{1}{2}\bar{\chi}(\underline{n})\chi(\underline{n})\rangle + \tfrac{1}{2}\left(\frac{1+(-1)^{n_2}}{2}\right)\langle\bar{\chi}(\underline{n})\chi(\underline{n}+a\underline{e}_2)\rangle + \tfrac{1}{2}\left(\frac{1-(-1)^{n_2}}{2}\right)\langle\bar{\chi}(\underline{n})\chi(\underline{n}-a\underline{e}_2)\rangle \qquad (4.70)$$

$$\langle\bar{d}d\rangle = \langle\tfrac{1}{2}\bar{\chi}(\underline{n})\chi(\underline{n})\rangle - \tfrac{1}{2}\left(\frac{1+(-1)^{n_2}}{2}\right)\langle\bar{\chi}(\underline{n})\chi(\underline{n}+a\underline{e}_2)\rangle - \tfrac{1}{2}\left(\frac{1-(-1)^{n_2}}{2}\right)\langle\bar{\chi}(\underline{n})\chi(\underline{n}-a\underline{e}_2)\rangle \qquad (4.71)$$

These quantities are averaged over the entire lattice.

For the two flavour model, $m_u=m_d$, we expect $\langle\bar{u}u\rangle=\langle\bar{d}d\rangle$, and when the algorithm has converged, this is indeed what we find. In figure 4.6 we plot values of $\langle\bar{\psi}\psi\rangle$ for the two species model, where:

$$\langle\bar{\psi}\psi\rangle = \frac{1}{2}\left(\langle\bar{u}u\rangle + \langle\bar{d}d\rangle\right) \qquad (4.72)$$

as a function of the quark mass, for both periodic and antiperiodic boundary conditions. We expect boundary conditions to be important only if the relevant correlation length is larger than the extent of the lattice. For free fermions the correlation length is (1/ma), where m is the quark mass, and hence, we would expect differences to appear between antiperiodic and periodic boundary conditions for values of the quark mass of ma=0.02. This is indeed what we find. At small quark masses, imposition of periodic boundary conditions causes divergence of $\langle\bar{\psi}\psi\rangle$, due to the presence of the zero mode in the propagator. The value of $\langle\bar{\psi}\psi\rangle$ calculated with antiperiodic boundary conditions goes to zero with the quark mass: these boundary conditions exclude the zero mode.

For the one species model, the same picture emerges: periodic boundary conditions result in a divergence of $\langle\bar{u}u\rangle$ at small values of the mass (when the d quark mass is set to unity), whereas for antiperiodic boundary conditions, $\langle\bar{u}u\rangle$ is forced to zero. Again the results begin to separate only for values of the quark mass whose correlation length is comparable with the size of the system.

Which boundary conditions are the correct ones to use is not clear, at least for the one species model. An analytic calculation of $\langle\bar{u}u\rangle$ in the free case on an infinite lattice shows that there is a breaking of chiral symmetry even at zero quark mass, (this is due to the heavy d quark feeding

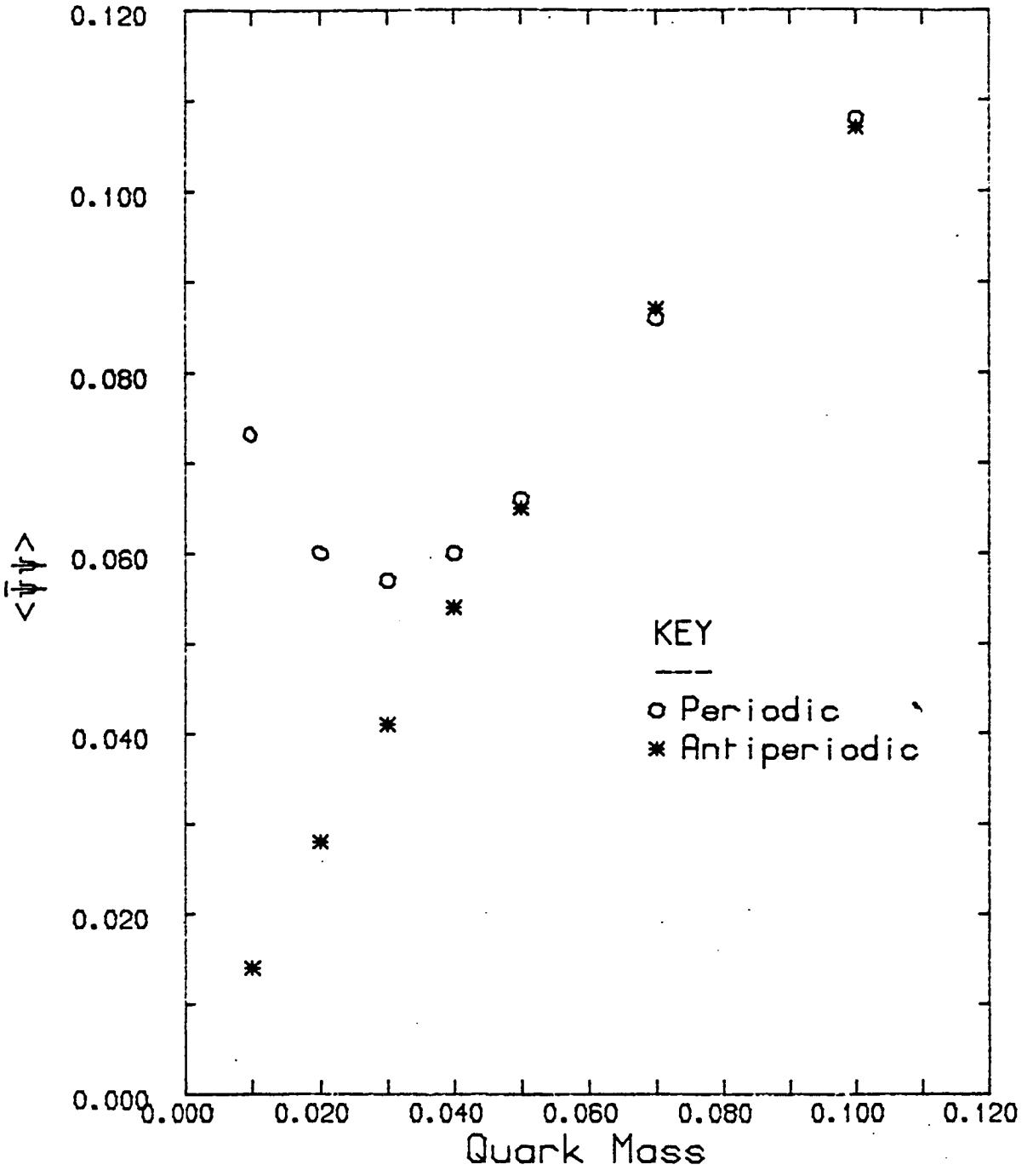

Fig 4.6

Fermionic condensate in the two species model showing the effects of boundary conditions. Free case.

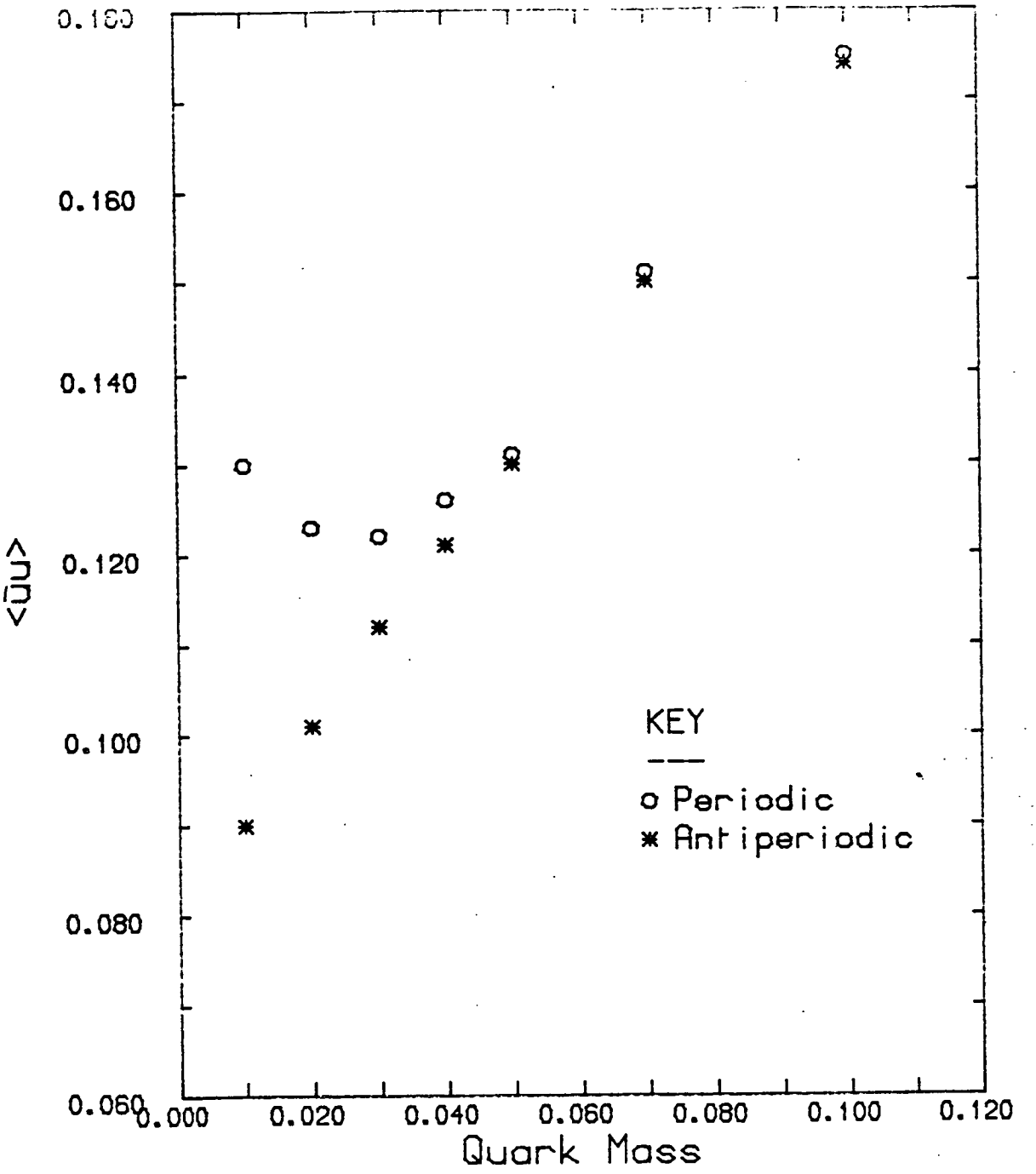

Fig 4.7

Fermion condensate in the one species model, showing the effects of boundary conditions. Free case.

back into the light fermion sector in a similar manner to the way in which the r term of Wilson fermions breaks chiral symmetry) and we see that at small quark masses, the result for periodic boundary conditions rises above the expected infinite lattice result, whereas the antiperiodic result falls below. In the two species model, $\langle\bar{\psi}\psi\rangle$ does go to zero on an infinite lattice, and hence antiperiodic boundary conditions are better. However, in the interacting case, where quarks are confined, boundary conditions are no longer so important, on a big lattice like 64x64, even at the smallest quark masses.

CHAPTER FIVE

NUMERICAL SIMULATION OF TWO DIMENSIONAL QED WITH TWO FLAVOURS

So far, we have presented continuum results and examined how we may hope to reproduce these on the lattice. In the last chapter, we discussed some of the numerical techniques available to us, and we now present the results of the actual simulations. We begin in this chapter with the two flavour model, as it is the more natural to simulate with Kogut-Susskind fermions.

5.1 The Quenched Approximation.

In the quenched approximation, we neglect the effects of internal fermion loops, that is, we generate gauge field configurations with the action (4.16) using the Metropolis algorithm. Because these loops have been neglected, we need only generate one set of configurations which may be used for any fermion mass, and for both the one and two flavour versions of the model. With a maximum update angle of $0.1 \times 2\pi$, and at $\beta=(1/ga)^2=3.0$, approximately 85% of the gauge fields were updated per sweep through the lattice, whereas with an update angle of $0.2 \times 2\pi$, this proportion dropped to approximately 73%. We elected to use an update angle of $0.2 \times 2\pi$, and performed 10250 sweeps through the lattice between configurations, generating 30 configurations. Of these 30, the first six were thrown away, as the gauge fields take some time to come into equilibrium. Figure 5.1 shows how the average plaquette energy approaches equilibrium from a cold start (where all the gauge fields are initially set to $U_\mu(\underline{n})=1$). The value of β used, $\beta=3.0$,

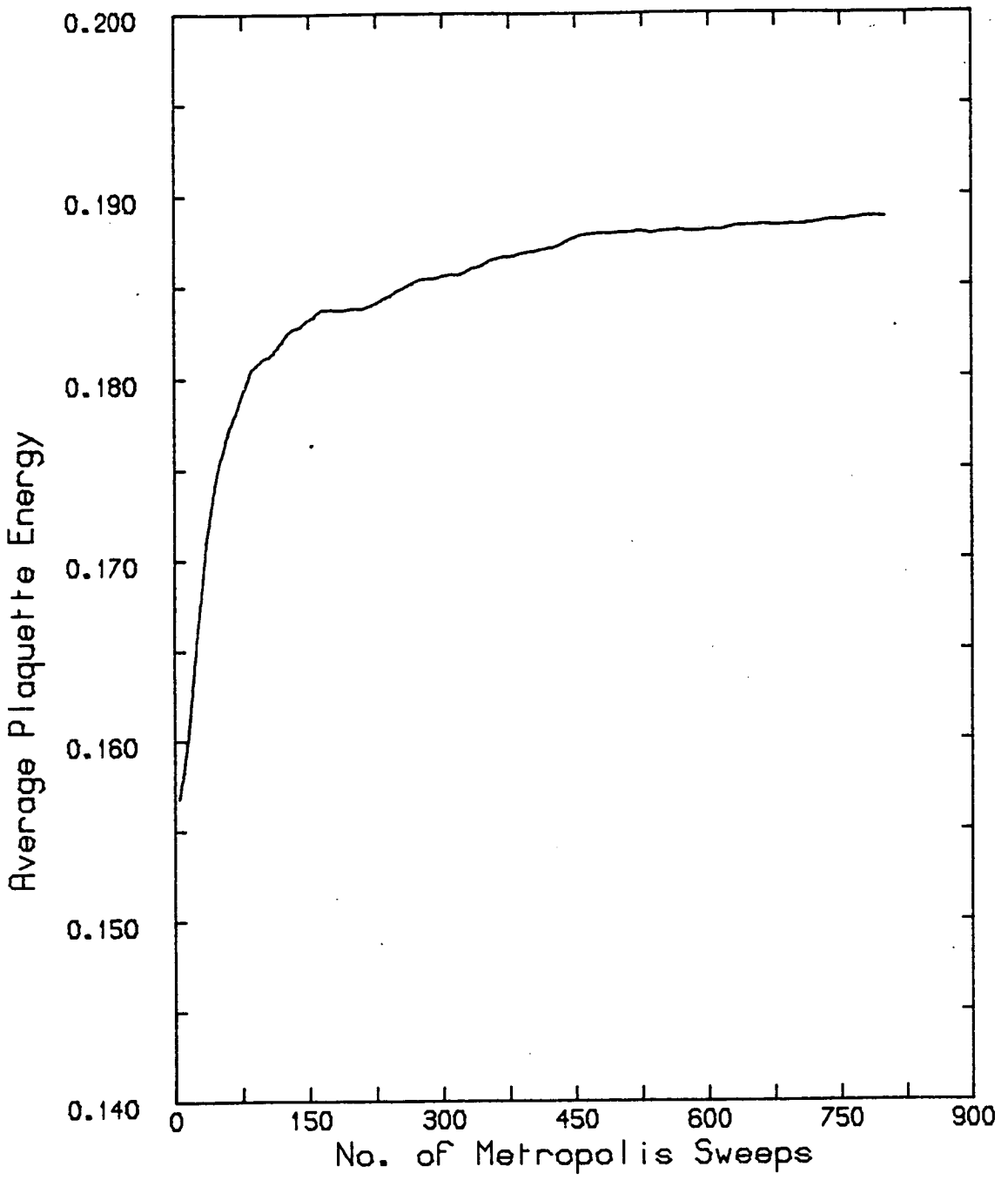

Fig 5.1

Average plaquette energy vs. no. of updates for quenched configurations, demonstrating the approach to equilibrium.

ensures that we are well into the strong coupling regime for the range of quark masses used, where reliable analytical results exist. It also ensures that the the correlation lengths of the physical particles are greater than the lattice spacing, and that the lattice is sufficiently large to accomodate all the physical states with ease. Having generated these configurations, we may use them to calculate the fermionic condensate $\langle\bar{\psi}\psi\rangle$, and the particle masses.

The fermionic condensate was calculated using the pseudofermionic technique discussed in chapter four. The pseudofermions were first allowed to come into equilibrium with a given gauge field configuration by updating many times, and then a value of $\langle\bar{u}u\rangle$ and $\langle\bar{d}d\rangle$ was calculated and averaged over all subsequent updates, before being finally averaged over the entire lattice. To test for equilibration, the process is repeated for the same gauge field configuration, using the final pseudofermionic configuration of the first calculation as the starting point of the second. We also used other pseudofermionic configurations, generated at different quark masses, as the starting point, to allow the pseudofermions to come into equilibrium from above and from below, as a further check on equilibration. In practise, $\langle\bar{\psi}\psi\rangle$ was averaged over about 5000 pseudofermionic sweeps, after about 5000 sweeps for equilibration. At the large quark masses ($m_u=m_d=0.10$) a few hundred sweeps would probably have been sufficient, but at small quark masses, equilibration is very slow, and at least a thousand sweeps are needed for good equilibration. This process is then repeated for other gauge configurations. We found that $\langle\bar{\psi}\psi\rangle$ varied by only a few percent (5% at most) from configuration to configuration, and in general, we averaged over only two widely seperated configurations, to obtain an estimate of the errors. This whole process was repeated for both periodic and antiperiodic boundary conditions at

seven values of the quark mass. The results are shown in figure 5.2. It is clear first that the importance of boundary conditions is much smaller than for free fermions, the difference being only about 7 or 8% at even the smallest quark mass values. This is not surprising: we know that in two dimensions, QED is confining, so that the quarks are unaware of the finiteness of the system. Secondly, we see that $\langle\bar{\psi}\psi\rangle$ diverges at small values of the quark mass for both periodic and antiperiodic boundary conditions, a result that we do not expect to find in the unquenched case.

If we are truly near the continuum limit, then our results should be independent of the lattice spacing, a. To check that this is so, we need to vary the lattice spacing, by varying the value of the dimensionless coupling, ag; to shrink the lattice spacing, we increase β. Setting $\beta=\infty$ freezes out the gauge fields, and gives us the free theory on the lattice, and so we cannot just set $\beta=\infty$. In fact, we are very limited in the range of β values available to us. The larger the value of β, the smaller the change in the gauge fields that will be accepted by the Metropolis algorithm, so that longer equilibration times are required by the gauge fields. Also, as we wish to compare our quenched results with unquenched results, we want to work at as small a value of (m/g) as possible, so that the difference between the two cases is as large as possible. Unfortunately, as we shall see, the pseudofermion method used for producing unquenched configurations converges more slowly the lower the quark mass. If we reduce the value of the dimensionless lattice coupling, ag, then to maintain a constant value of (m/g), we need to reduce the dimensionless mass parameter, am, and hence encounter equilibration problems. Also, as we shall show later, pseudofermion programmes that have antiperiodic boundary conditions imposed on them equilibrate much more slowly than periodic programmes. In fact we found that at least

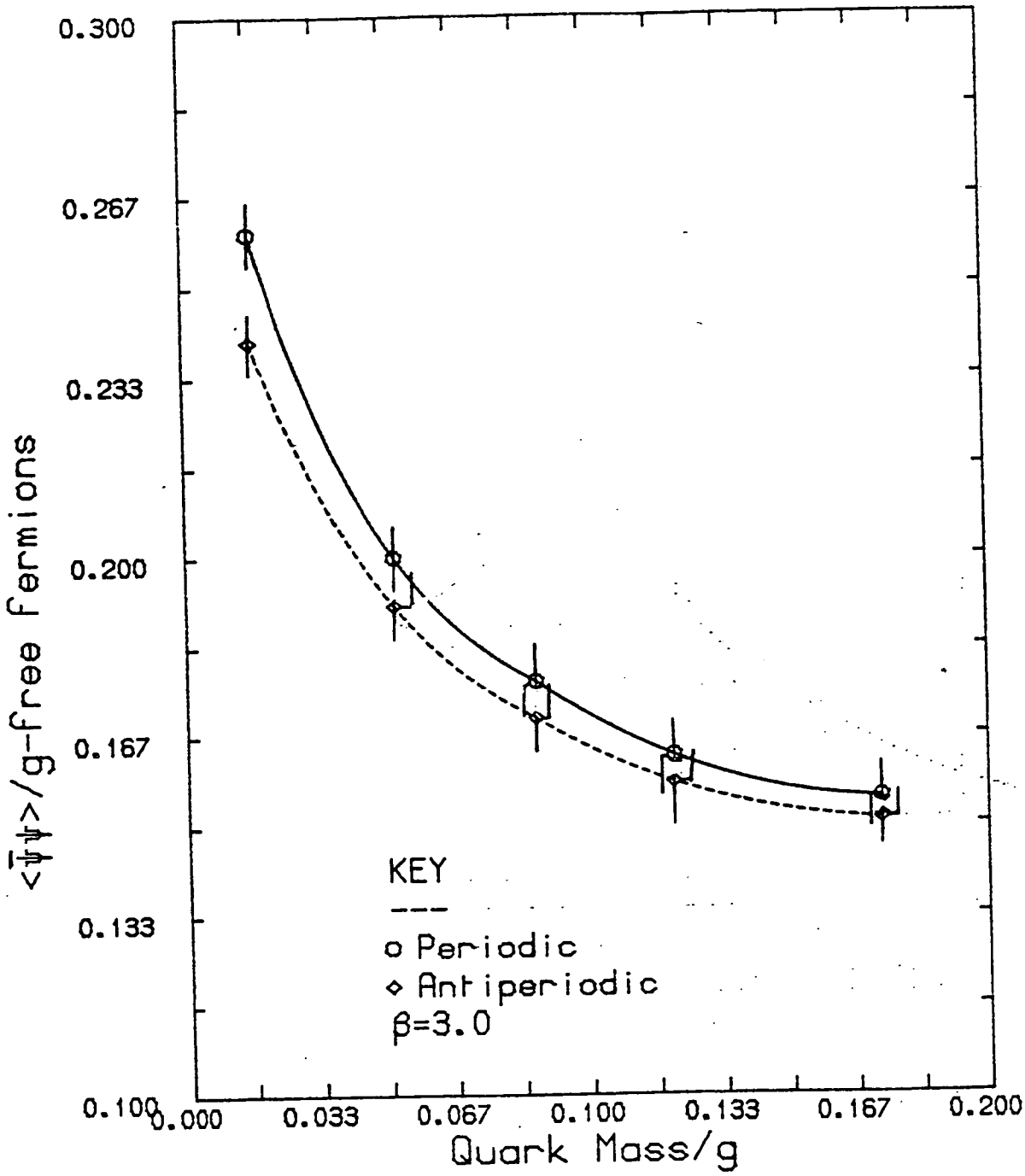

Fig 5.2

Fermionic condensate in the quenched two species model showing the effects of boundary conditions.

in the quenched case boundary conditions have no observable effect on particle masses, but if we are to use periodic boundary conditions in the unquenched case and be sure of avoiding finite size effects, we cannot realistically work with quark masses less than about 0.02. Reducing the value of ag does have one positive effect: the analytical results show that reducing ag increases the correlation lengths of the particles, and hence the signal in the time slice propagators should stand out from the statistical noise for more lattice spacings.

For the two species model, then, we have chosen to work at two alternative values of the coupling: β=0.25 and β=8.0. The first of these has the advantage that as β is smaller than the previous value, the gauge fields equilibrate faster, and working at a quark mass of 0.035 (which corresponds to a mass of about 0.010 at β=3.0), the pseudofermion technique converges quite quickly and we avoid problems from finite size effects. However, the lattice is rather coarse at this value, and in fact the correlation lengths of the 1^+ and 0^- states shrink to less than one lattice spacing, making calculations of their masses rather meaningless.

A value of β=8.0 takes nearer the continuum limit by shrinking the lattice spacing, but involves us with the equilibration problems outlined above.

At both these new values of the coupling, 16 configurations were generated, with 10250 sweeps through the lattice separating each one, after discarding the first few for equilibration. At β=0.25 an update angle of $0.2\times2\pi$ was used, and at β=8.0, an update angle of $0.08\times2\pi$. Again the pseudofermion technique was used to calculate $\langle\psi\psi\rangle$, in four of the configurations. Results are shown in figure 5.3. The results for $\langle\bar{\psi}\psi\rangle$ agree well with theory. We believe that in the quenched case, the one and two species models

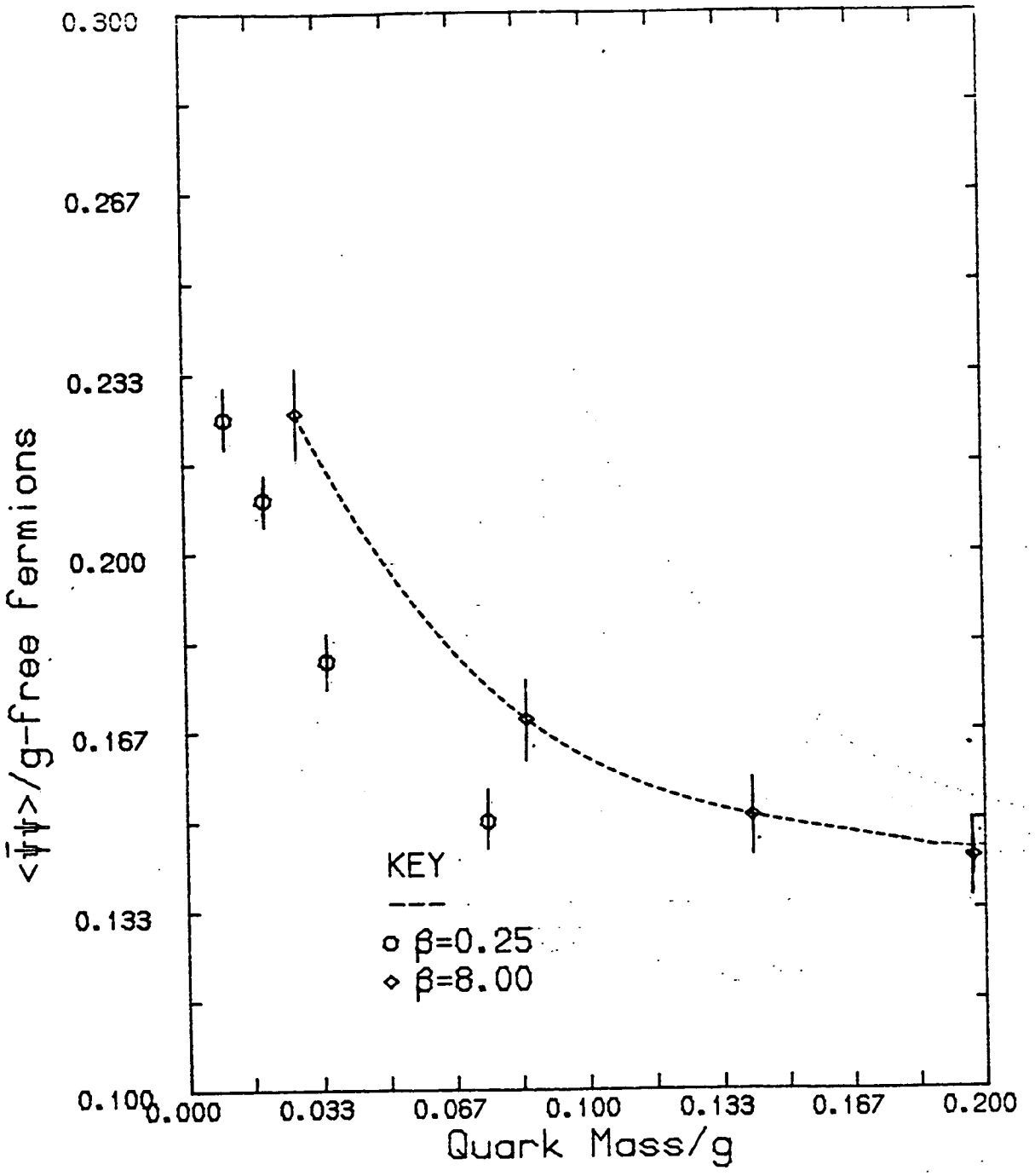

Fig 5.3

Fermionic condensate in the quenched two species model at β=0.25 and β=8.0.

should be very similar, and at least for this calculation, this is true. Figures 5.2 and 5.3 should be compared with figures 6.1 and 6.2 showing the fermion condensate in the quenched one species model at the same values of the coupling. Note that whilst results at β=3.0 and β=8.0 are in very good agreement, those at β=0.25, though still showing a divergence in $\langle\bar{\psi}\psi\rangle$ in the limit of zero quark mass, differ slightly. This may be an indication that we are moving away from the continuum limit.

We now turn to the calculation of the particle masses. We have seen that there are two ways of defining mesonic operators on the lattice: we may either use local operators, which are the modulus squared of the quark Green functions, multiplied by some appropriate phase, and which mix two of the physical states, or we can use the Kahler-Dirac form of the operators, and hopefully form a purer operator.

In either case, the first step is to calculate the quark Green functions, using the conjugate gradient technique. To obtain good accuracy, we iterated the algorithm until the error function defined in (4.5) was 10^{-70} or smaller. This value was more than sufficient to ensure that even the smallest element of the quark Green function did not change within machine accuracy on further iteration. Having obtained the quark Green functions, we multiply them together, with gauge fields if necessary, to form gauge invariant operators. The resulting mesonic operators are then summed over the spatial direction (the choice of which is arbitrary), and the resulting time-slice propagators are averaged over 24 configurations.

We now face a major difficulty in trying to extract masses for the isosinglet states. As we noted in chapter three, to obtain good estimates of the masses of these

states, we need to include annihilation diagrams. In terms of the quark Green functions, these have the form:

$$\sum_{HKH'K'} C_{HK} C_{H'K'} G_{HK}(\underline{e},\underline{e}) G_{H'K'}(\underline{y},\underline{y}) = \sum_{HKH'K'} C_{HK} C_{H'K'} G(\underline{e}_H, \underline{e}_K) G(2\underline{n}+\underline{e}_{H'}, 2\underline{n}+e_{K'}) \quad (5.1)$$

and it is clear that the conjugate gradient method is going to be of no use here, because we need to know all the elements of the propagator matrix along a diagonal band and the use of conjugate gradient would therefore require a calculation of the entire Green function, rather than of a particular row or column. This would require hours of computer time at the lightest quark mass values for even a single gauge field configuration (at $m_u=m_d=0.01$, approximately 2500 conjugate gradient steps were required to achieve the required accuracy). The pseudofermionic technique does allow us to calculate these diagrams, as it allows calculation of any element of the Green function. However, the method is subject to large statistical errors (being a Monte Carlo technique, rather than an essentially exact technique like conjugate gradient), as we shall see when we consider the unquenched model, and produces disappointing results. The computer time required for the calculation, although less than that which would be required were we to use the conjugate gradient algorithm, is considerable. We have already seen that several thousand sweeps were required to produce reliable estimates for $\langle\bar{\psi}\psi\rangle$, even when it was possible to average over the lattice, and when calculating particle masses we need to average over many configurations. We therefore neglect the annihilation terms and can realistically calculate masses only for the isotriplet states, 1^+ and 1^-. Even here there is a problem for the states with $I_3\neq 0$, because on the lattice, as we showed in chapter three, there is a flavour breaking term in the

action, so that annihilation terms should contribute to the propagation of these states (the annihilation terms cancel for the $I_3=0$ states). Hence for these states we impose flavour symmetry artificially, by neglecting the annihilation terms, and so perhaps force the theory nearer the continuum limit, where the flavour symmetry is exact.

Having calculated the time slice propagators, we need to extract masses. We do this by fitting the data to exponentials. In chapter one, we showed that the time slice propagator was expected to fall off exponentially in Euclidean time with the mass of the particle, and stated that the lattice operator would have non-zero overlap not only with the ground state of the particle with the same quantum numbers as the lattice operator, but also with higher mass excited states. Thus, with the Kahler-Dirac definition of particle operators, we choose to fit the data to a function of the form:

$$f(t) = Ae^{-m_1 t} + Be^{-m_2 t} \qquad (5.2)$$

where t is the time coordinate in lattice units, and A, B, m_1 and m_2 are chosen so as to minimise:

$$\frac{[\Delta(t) - f(t)]^2}{[\Delta(t) + f(t)]^2} \qquad (5.3)$$

where $\Delta(t)$ is the time slice propagator. We note that because of the boundary conditions, we should really fit to hyperbolic cosines, rather than exponentials, but because we are on such a large lattice the contribution from backward propagation across the lattice is negligible near the origin, where we must needs fit because of the small correlation lengths of even the lightest states.

When we consider the local definition of particle operators, which we know mix two of the physical states, we fit to a function of the form:

$$f(t) = Ae^{-m_1 t} + (-1)^t Be^{-m_2 t} \qquad (5.4)$$

where m_1 and m_2 now represent the masses of two different physical states, rather than of the ground state and the first radial excitation as in (5.2). No attempt is made to fit to any radial excitation here: the quality of the data makes even a four parameter fit like (5.4) unreliable.

If we consider the correlation lengths of the physical particle states in the two species Schwinger model, we see that we are going to encounter severe difficulties in extracting masses for any but the lightest state. The mass of the 1^+ state in lattice units at β=3.0 is about 0.4, and hence we see that the correlation length is little over two lattice spacings. When we consider the Kahler-Dirac form of the operators, we have to work on a lattice whose spacing is twice that of the original, where the correlation length of the 1^+ state is only about one lattice spacing, and hence we may expect the time slice propagator to disappear into noise very rapidly. This would perhaps not be so bad if the lattice operator produced only a 1^+ state, with no contamination from other states. However, this does not appear to be so: at large times, the time slice propagator for every operator we considered behaved remarkably like the pion, although it should be noted that at these large times, the signal is often below the level of the statistical noise. These observations are supported by the results of the fitting routine: fitting the 1^+ operator data near the origin gives a mass significantly greater than that of the pion, and compatible with the expected 1^+ mass. However,

as we fit to more and more points, moving us further from the origin, the mass we extract begins to fall to about the value expected for the pion. Because we have so few points from which we can sensibly extract a mass for the heavy states, then, the calculated errors are considerable. We tried to improve the data by averaging the data on both sides of the origin, and by summing separately on both directions to produce the time slice propagator (as we have a free choice of which direction to choose as time on a Euclidean lattice). For every particle state, we fitted the data over 2,3,4,6 and 10 timeslices (throwing away the origin), and averaged in each case over 24 gauge configurations. The 24 configurations were subdivided into bins of 12 and of 6 configurations, and for each bin a separate particle mass was calculated, allowing us to estimate the statistical error arising from the gauge field average. The calculation was repeated for periodic and antiperiodic boundary conditions.

In figure 5.4 we show examples of the timeslice propagators, averaged over the 24 gauge configurations, and on the same scale we plot the standard deviation of the gauge average. The statistical errors are considerably worsened in the case of operators that are one or two link and hence must be multiplied by gauge fields. This may be seen clearly in figure 5.5, which shows the $(1,0)^-$ (the pion) operator defined with γ_2 diagonal (a one link operator, 5.4c) and with γ_5 diagonal (when the operator is local in the sense that it requires no gauge field multiplications to make it gauge invariant). The 0^+ operator, which, like the 'local' pion contains no gauge link variables, still suffers badly from statistical errors. This is because the operator is produced by cancellations between quark propagators, as we see from (3.40):

$$O^+(y_j) = \sum_{HK} \overline{\chi}_H(y_j) C^{0^+}_{HK} \chi_K(y_j) = \sum_H \overline{\chi}_H(y_j) \chi_H(y_j) \qquad (5.5)$$

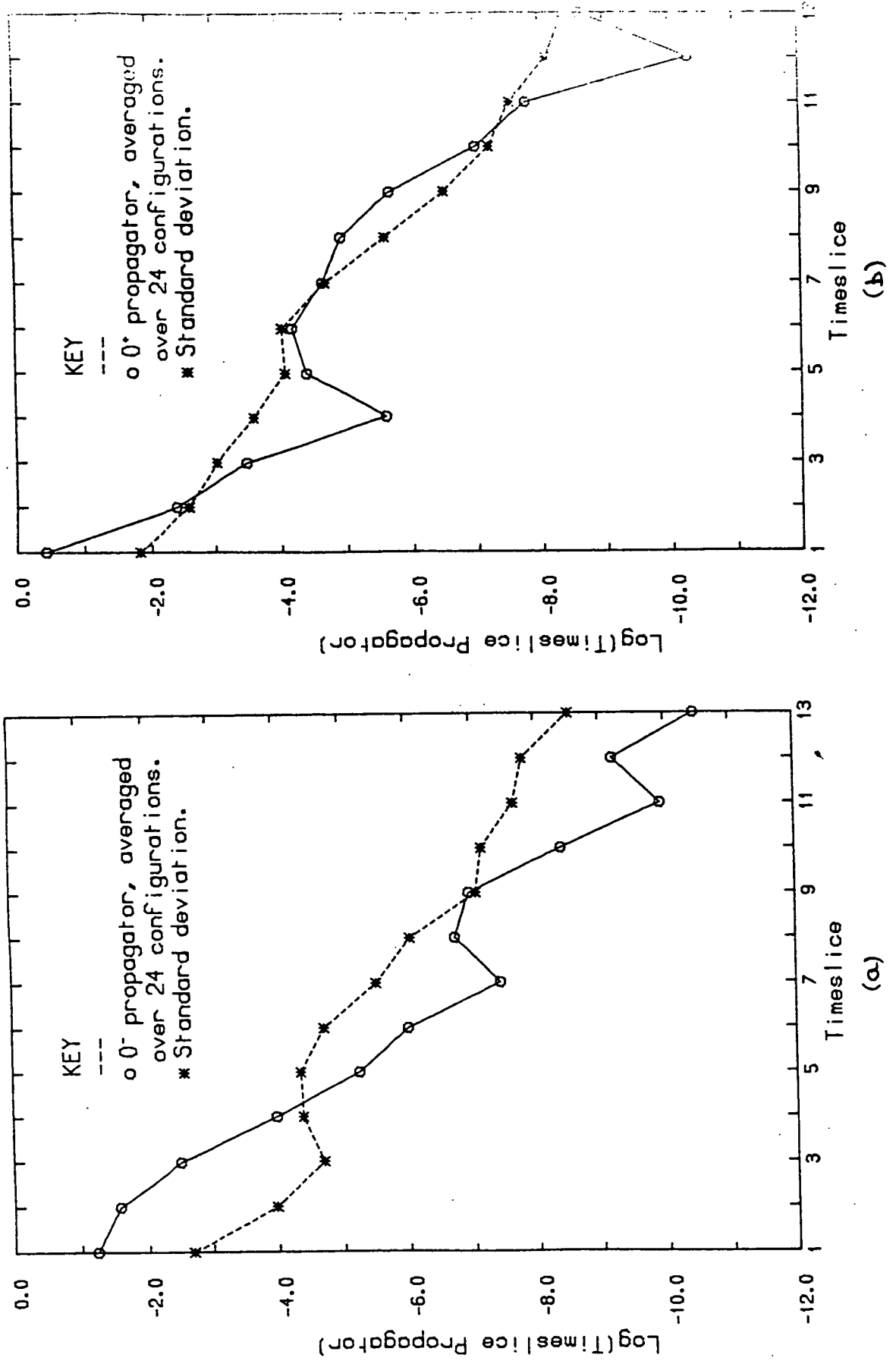

Fig 5.4

Timeslice propagators for extended Kahler-Dirac mesonic operators at $m_u = 0.05$. Quenched case.

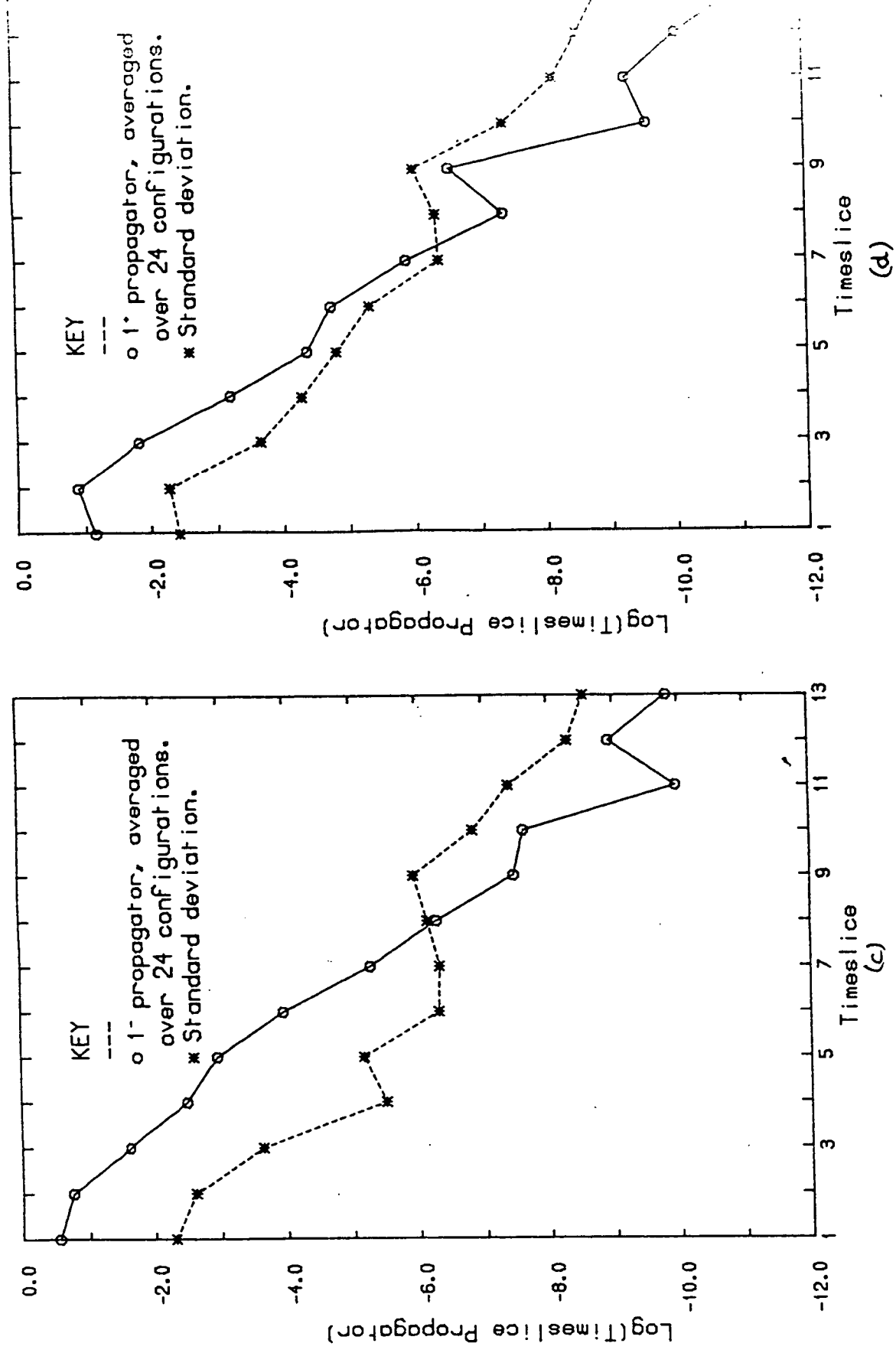

Fig 5.4

Timeslice propagators for extended Kahler-Dirac mesonic operators at $m_u = 0.05$. Quenched case.

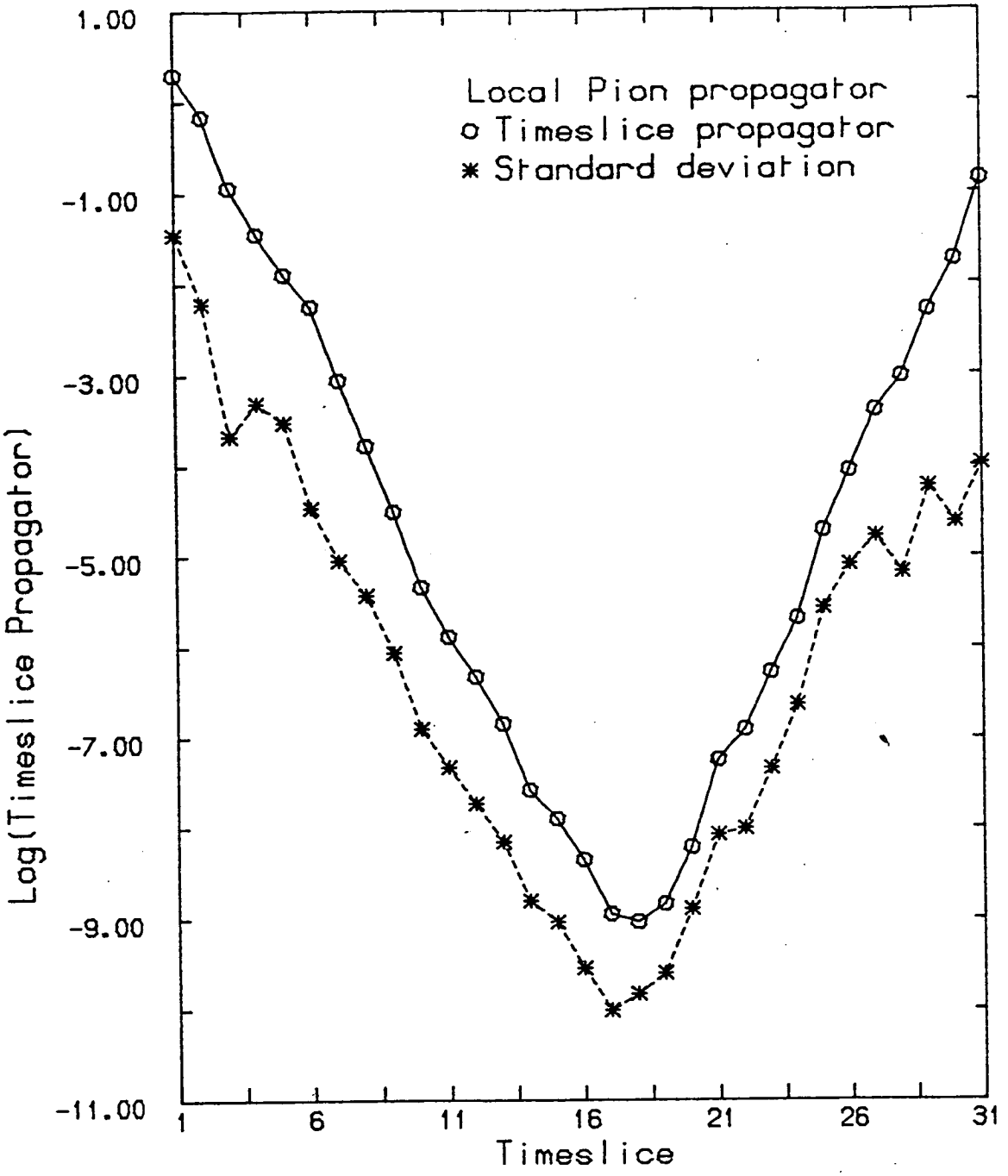

Fig 5.5

Timeslice propagator for the local Kahler-Dirac pion at m=0.05. Quenched case.

so that the propagator is given by:

$$\langle \bar{O}^{+}(y)\, O^{+}(y) \rangle = \sum_{HK} \langle \bar{\chi}_H(0)\chi_K(y)\rangle \langle \bar{\chi}_K(y)\chi_H(0)\rangle$$

+ annihilation terms

$$= \sum_{HK} G_{KH}(y,0)\, G_{HK}(0,y) \qquad (5.6)$$

+ annihilation terms

$$= \sum_{HK} (-1)^{e_{H_1}+e_{H_2}+e_{K_1}+e_{K_2}} \left| G_{HK}(y,0) \right|^2$$

+ annihilation terms

The 'local' pion is given by:

$$\langle \bar{\pi}(y)\, \pi(0) \rangle = \sum_{HK} \left| G_{HK}(y,0) \right|^2 \qquad (5.7)$$

and hence is produced by a sum of positive terms, and as such is not subject to such large statistical errors. Similarly, we can show that in terms of the quark Green functions defined from the origin, the $(1,0)^+$ state is also produced by cancellations, whereas the one link $(1,0)^-$ operator is produced by a sum of positive terms. In fact, this result is true more generally: the scalar states are all produced by cancellations, and are hence subject to large statistical fluctuations whereas the pseudoscalar states are produced from sums of positive terms, and are much less affected by these fluctuations.

The mass calculations were repeated at β=8.0 and 0.25. As we expect, at β=8.0, where correlation lengths are longer, the statistical noise does not become larger than the signal as soon as at β=3.0, although for β=0.25, the signal from the 1^+ state does not rise above the noise, except at the origin.

Consider first the Kahler-Dirac extended form of the mesonic operators. Using this definition, we calculated masses for the 0^+ and 0^- states, and for the $(1,0)^+$ and $(1,0)^-$ states, and their isotriplet partners, the $(1,\pm 1)^{\pm}$ states. As we made no attempt to include the effects of the annihilation terms, the masses we extract for the 0^+ and 0^- states should correspond with the masses of the 1^+ and 1^- states respectively, as we pointed out in chapter 3. We found that the local definition of the pion (γ_5 diagonal) produced the clearest signal, and the mass extracted did not alter significantly from bin to bin, nor on a change in the definition of the time direction. In fact, the signal from the local Kahler-Dirac pion is so clean that the fitting routine fails to extract a second mass, representing an excited state. The routine returns the same mass twice. This mass must be supposed to be the ground state mass rather than some effective mass resulting from contamination from excited states as it does not alter with the number of timeslices fitted, nor does it change when points near the origin are discarded in the fit. However, in all other cases, statistical fluctuations coupled to the fact that we have so few points to fit, result in masses which vary from bin to bin and also with definition of the time direction. The results are really only reliable as an order of magnitude estimate. In figure 5.6 we plot particle masses (divided by g) as a function of the dimensionless parameter, (m/g). Errors are estimated by comparing the gauge field configuration bins, and altering the definition of the time direction.

Despite the large errors, we can draw some tentative conclusions from our results: the 0^+ and 0^- states do indeed behave like the 1^+ and 1^- minus states respectively, the 0^+ remaining heavy in the limit of vanishing quark mass, and the 0^- mass going to zero. This difference is due to the absence of the annihilation terms in the numerical results.

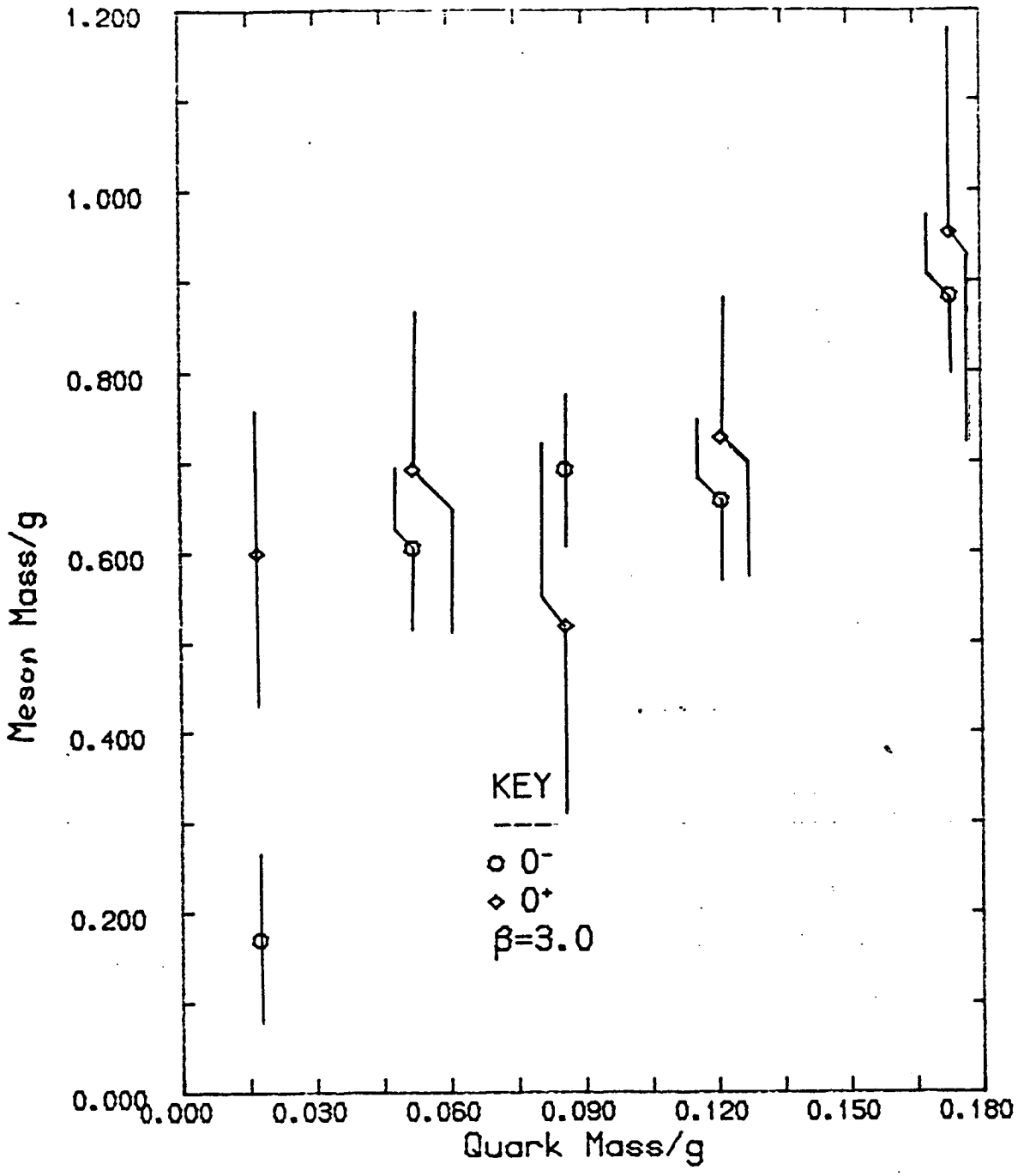

Fig 5.6(a)

Particle masses for Kahler-Dirac particles in the quenched approximation.

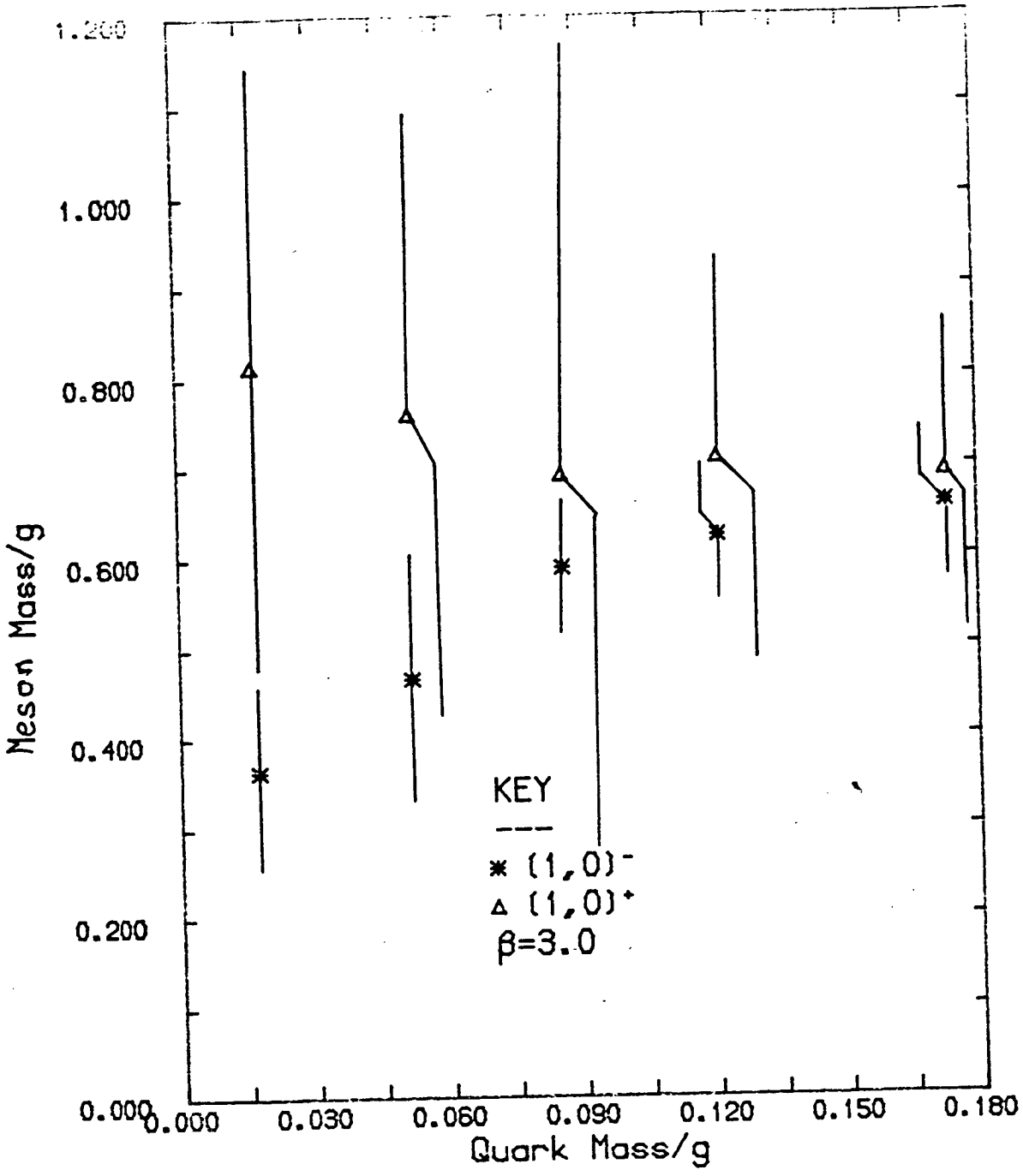

Fig 5.6 (b)

Particle masses for Kahler-Dirac particles in the quenched approximation.

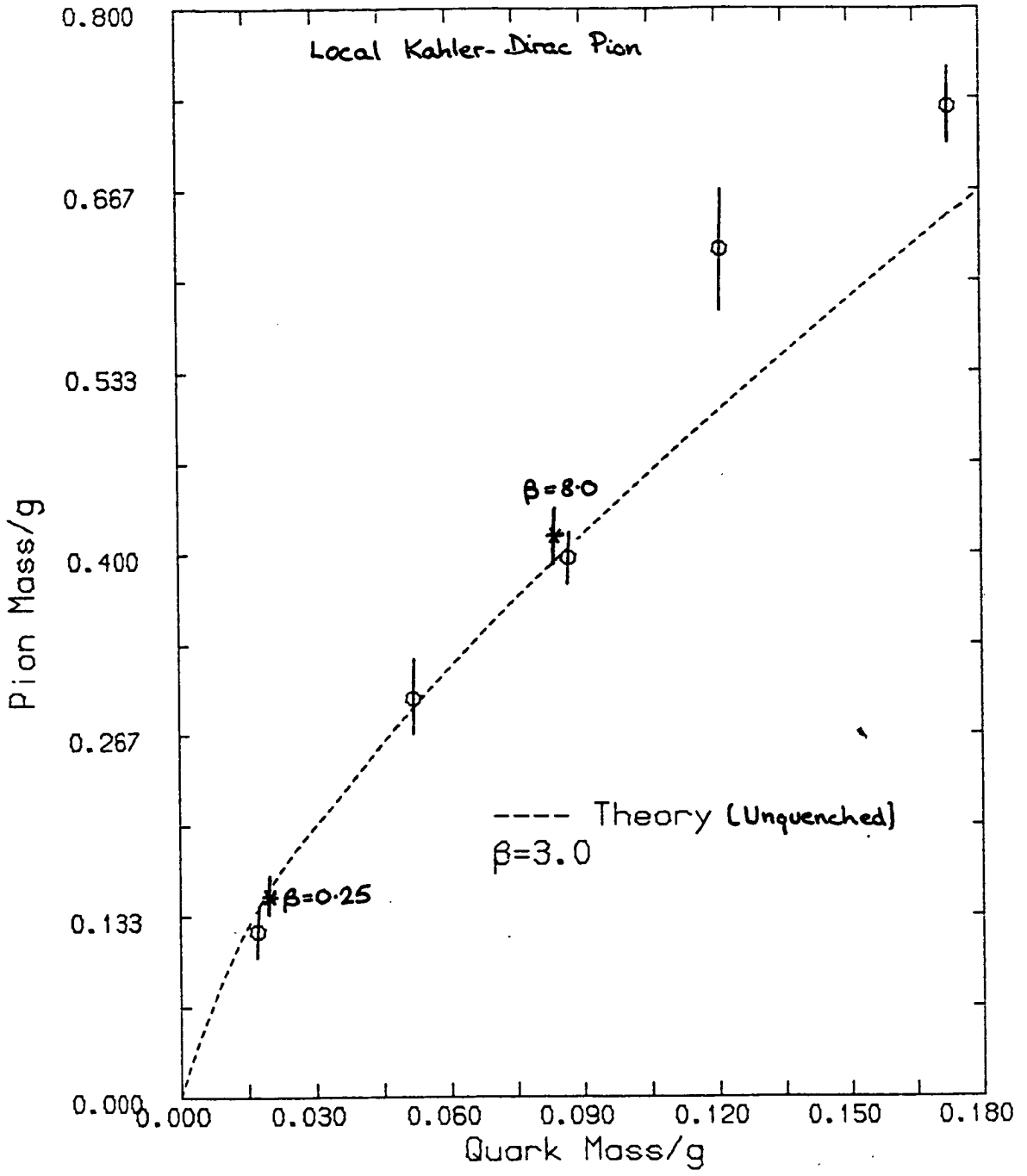

Fig 5.6 (c)

Particle masses for Kahler-Dirac particles in the quenched approximation.

The $(1,0)^+$ operator remains heavy as the quark mass goes to zero, as we expect, and the states with $I_3 \neq 0$ are degenerate with the I=1, I_3=0 states.

We have also extracted masses from the local definitions of the particle operators. Here again, we find we can only obtain a reliable estimate of the pion mass. The second mass to which we fit (which should be the mass of the 1^+ state) has such a large error associated with it as to be meaningless. We also note that unlike the four-dimensional case, where the local operator of the form $|G|^2$ has an overlap only with the physical pion state, the pion mass we extract from the local definition in two dimensions is not as clean as the local Kahler-Dirac definition, and has a larger error associated with it. In fitting the local operators, as we cannot allow for contributions from radial excitations near the origin, we have investigated the effect of discarding points near the origin, in an attempt to eliminate these excitations.

Note that although we are here investigating the quenched model, we do not see any marked departure from the expected analytical behaviour of the unquenched model. The local Kahler-Dirac definition of the pion, where departure from unquenched behaviour might be expected to be most clearly exhibited, seems to behave exactly as the unquenched pion. This is true at all the values of the coupling that we investigated.

Finally, note that the above calculations were repeated with both periodic and antiperiodic boundary conditions. The results in the two cases were identical. The masses extracted for the local Kahler-Dirac pion lie on top of each other when plotted against fermion mass. This is of particular importance in a study of the unquenched model, as we shall see.

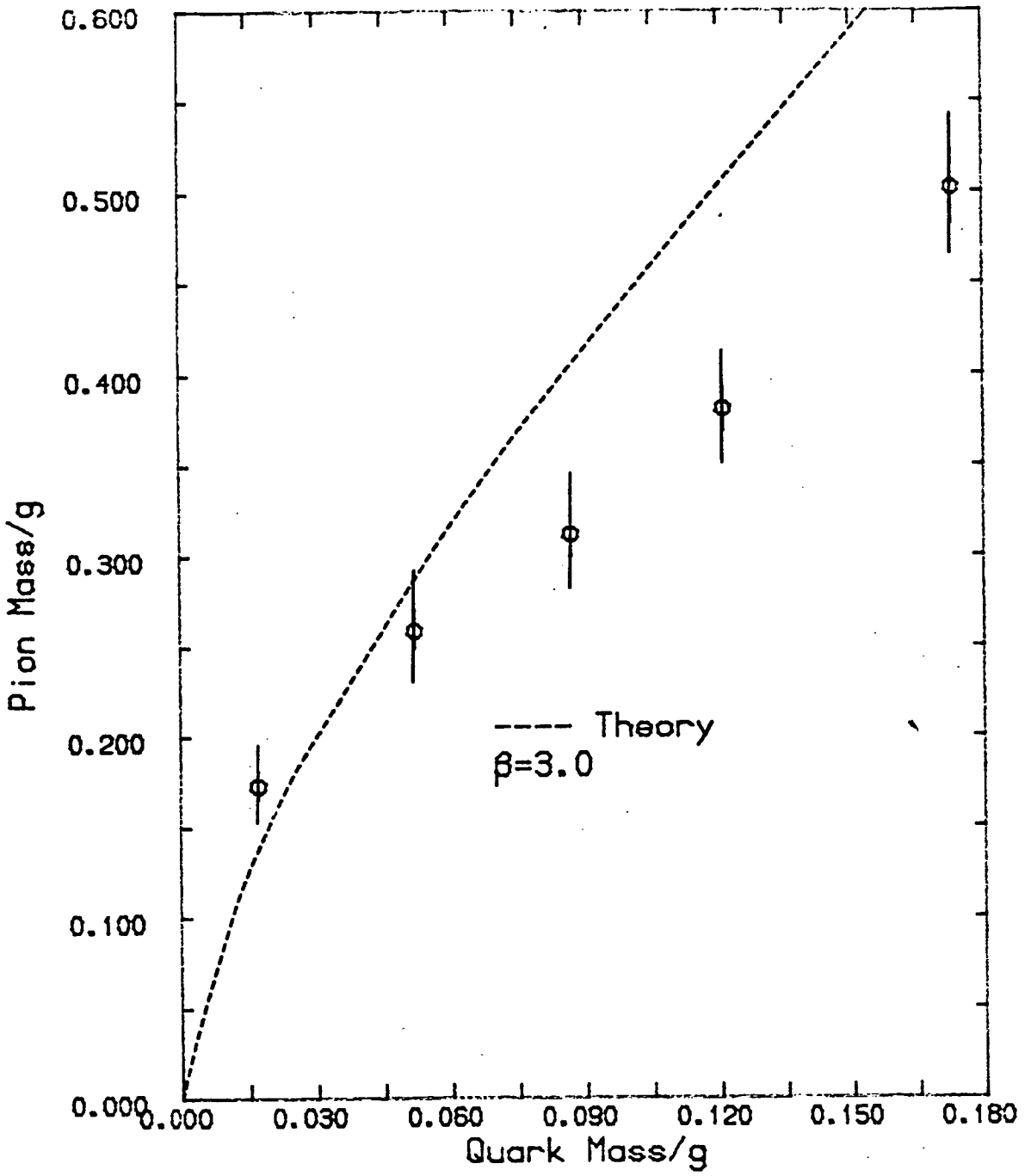

Fig 5.7

Pion mass extracted from the local definition of mesonic operators in the quenched approximation.

5.2 The Unquenched Model.

To investigate the effect of dynamical fermions, we need to generate gauge configurations using the effective action (4.27), and using the pseudofermion technique to calculate elements of the quark Green function, as described in chapter four. It is now necessary to generate a different set of configurations at each value of the quark mass. In all, at least 24 configurations were generated at β=3.0 for 7 values of the quark mass having discarded at least 4 configurations for equilibration. Initially, 50 pseudofermion sweeps of the lattice were carried out between each update of the gauge fields. An update angle of $0.1 \times 2\pi$ was used, a compromise between the need to linearise the action as in (4.27), and thus to mimimise $(\delta U)^2$ errors, and the need to generate statistically independent gauge field configurations in a reasonable amount of computer time. 100 sweeps through the lattice were performed on the gauge field between configurations that were actually used. The procedure was repeated for both periodic and antiperiodic fermionic boundary conditions. As a by-product of generating the gauge field configurations, the pseudofermionic configurations give us the value of $\langle\bar{\psi}\psi\rangle$ within the gauge field configurations. As configurations were generated, a calculation of $\langle\bar{\psi}\psi\rangle$ was performed for each gauge field update. We found that from a cold start, the value of $\langle\bar{\psi}\psi\rangle$ slowly increased for about the first 400 gauge field updates (=20000 pseudofermionic updates), before settling down to some value that would then fluctuate by at most 2 or 3% on subsequent gauge field updates. As the gauge fieds were updated only once for every 50 pseudofermionic updates, and changed by only a small amount, where the pseudofermions were updated with a heat bath algorithm, it seemed reasonable to assume that the pseudofermions had thus come into equilibrium with the

gauge fields. To check this, after generating 24 configurations, the last pseudofermionic configuration was saved, and holding the gauge field fixed, the pseudofermions were updated a further 5000 times, and a new value of $\langle\bar{\psi}\psi\rangle$ was then calculated over a further 5000 sweeps. Surprisingly, we found that at small quark mass values, the value of $\langle\bar{\psi}\psi\rangle$ thus calculated was different from that returned during the generation of the configurations. In fact with periodic boundary conditions on the pseudofermions, the two values agree down to about $m=m_u=m_d=0.05$, and disagree by only about 10% at m=0.04. At m=0.03, the disagreement is about 20% and at m=0.01, about 60%! In all cases, the second value, generated by the long pseudofermion run on the final gauge field configuration, was higher than that produced during the generation, both values, though, being below that produced in the quenched case. Hence, it seems that with only 50 pseudofermionic sweeps between gauge field updates at the small quark mass values, we are producing configurations which are partially quenched. The true value of $\langle\bar{\psi}\psi\rangle$ might be expected to lie somewhere between our two numerical values. To try and obtain good estimates for $\langle\bar{\psi}\psi\rangle$ in the unquenched theory, the number of pseudofermionic sweeps performed between gauge field updates was increased, and several hundred gauge field updates performed, until the pseudofermions had once again settled down to some constant value. Very long pseudofermionic runs were then performed on the final gauge field configuration, and the two values of $\langle\bar{\psi}\psi\rangle$ thus obtained were compared. The number of pseudofermionic sweeps was then increased again, and the whole procedure repeated, until the two values of $\langle\bar{\psi}\psi\rangle$ obtained agreed with each other.

The results for the unquenched theory with periodic boundary conditions are summarised in figures 5.8 to 5.10. The first of these shows the value of $\langle\bar{\psi}\psi\rangle$ obtained with

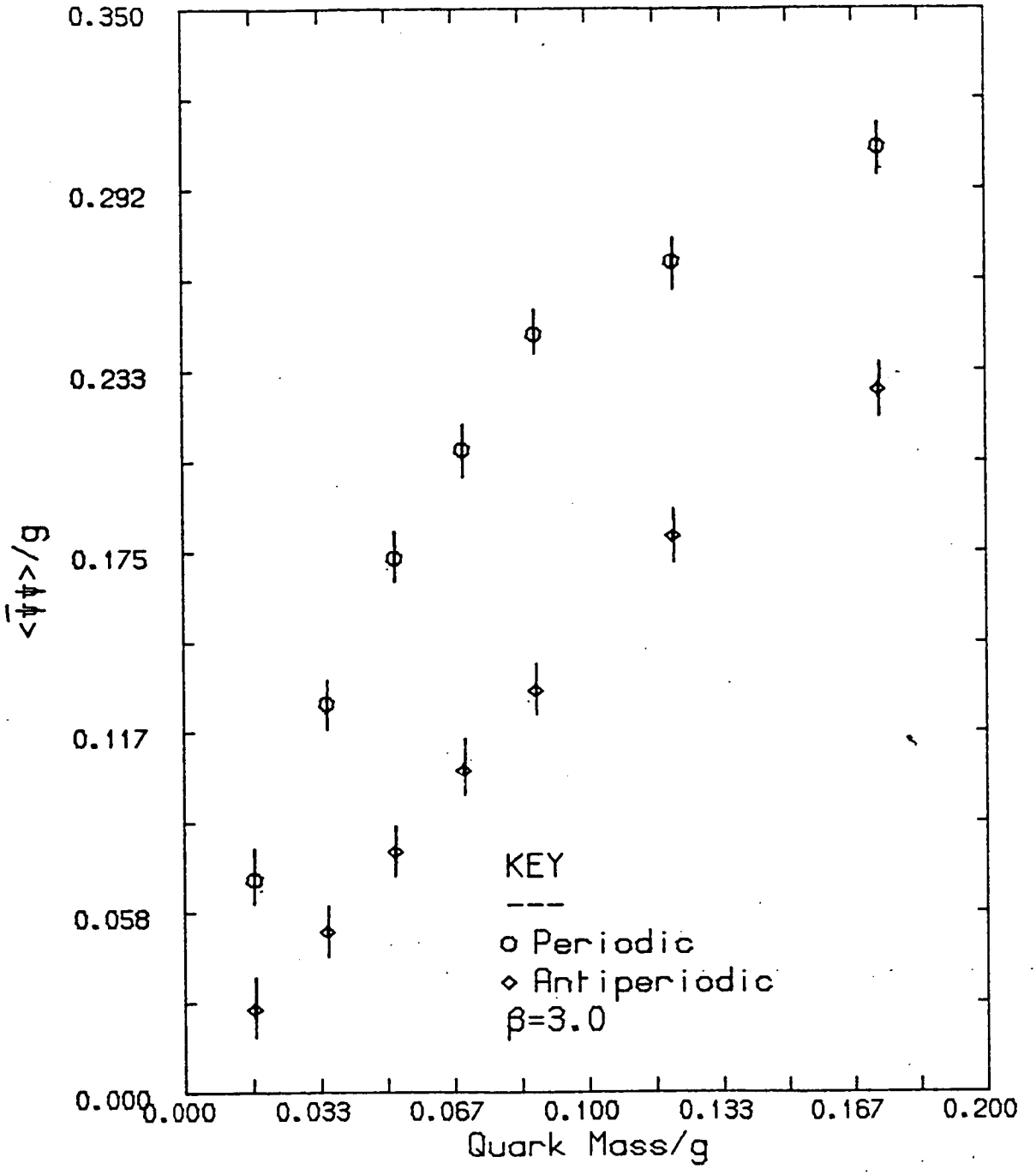

Fig 5.8

Fermionic condensate in the unquenched two species model. 50 pseudofermionic sweeps per gauge field update, showing the effects of boundary conditions.

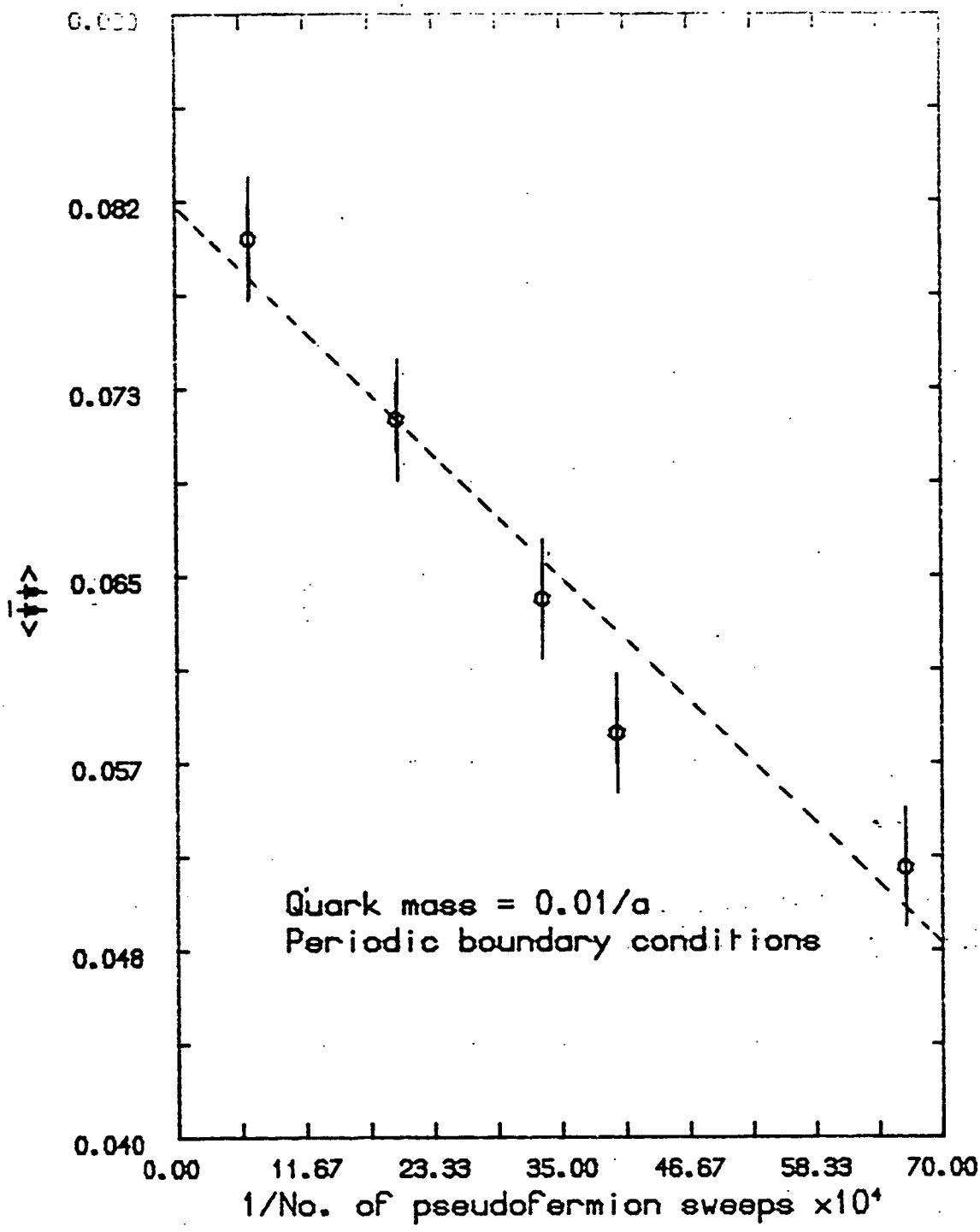

Fig 5.9

Convergence of the pseudofermion heat bath algorithm at m=0.01. Periodic boundary conditions.

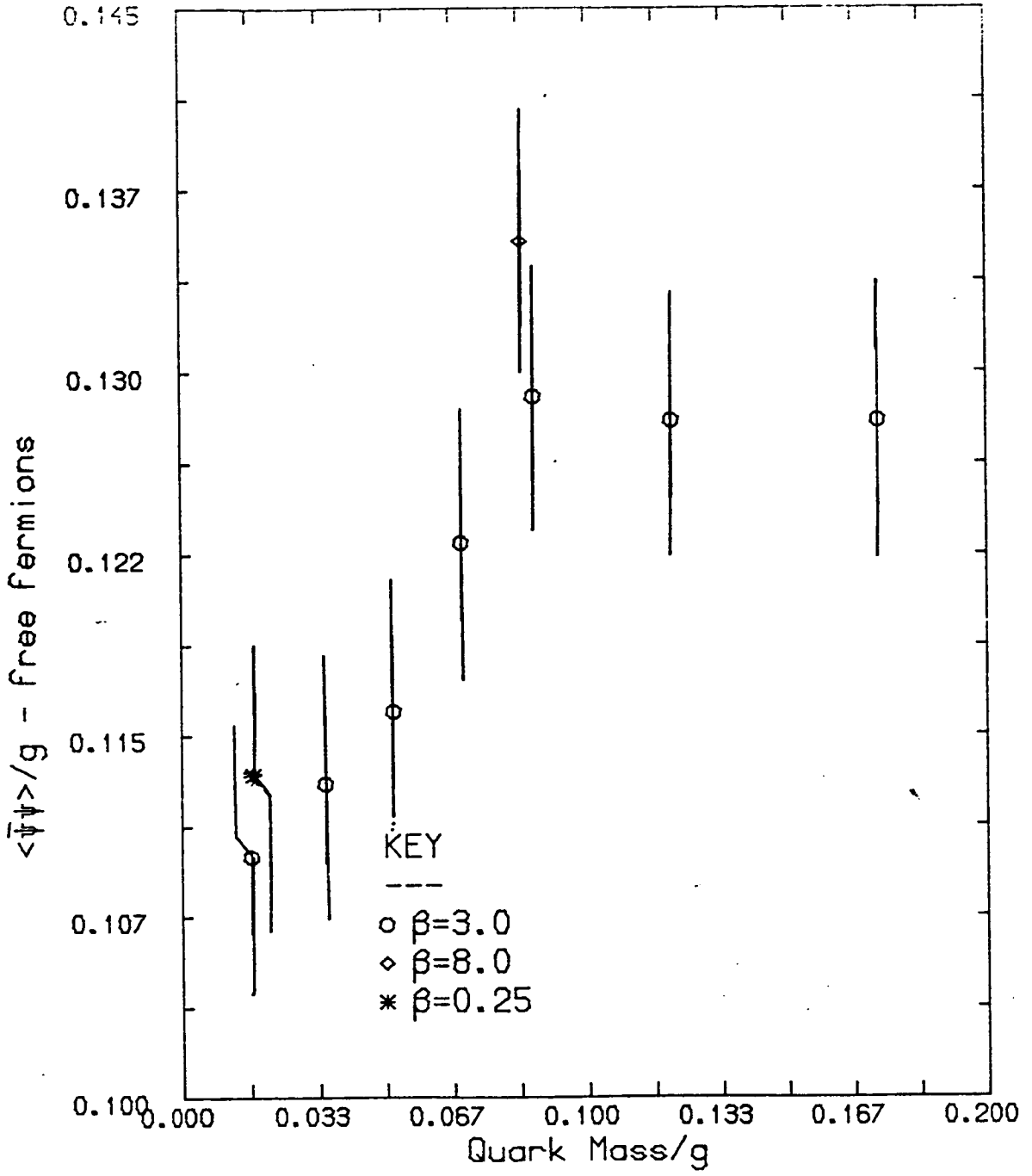

Fig 5.10

Fermionic condensate in the unquenched two species model, equilibrated values after free fermion subtraction.

50 pseudofermionic sweeps between gauge field updates. In the second we show the effects of increasing the number of pseudofermionic sweeps, at the lightest quark mass, m=0.01. By plotting $\langle\bar{\psi}\psi\rangle$ against the reciprocal of the number of sweeps, we can sensibly extrapolate to a value that might be obtained in the limit of an infinite number of pseudofermionic sweeps between gauge field updates. In the last figure, we plot $\langle\bar{\psi}\psi\rangle$ as a function of quark mass, where $\langle\bar{\psi}\psi\rangle$ has been calculated from extrapolations like the above. The free fermion results have been subtracted out from this last figure.

If we impose antiperiodic boundary conditions on the pseudofermions, the situation is much worse. In figure 5.8 we plot the values of $\langle\bar{\psi}\psi\rangle$ obtained with 50 pseudofermionic updates between gauge field updates. We see that $\langle\bar{\psi}\psi\rangle$ is much lower than when we impose periodic boundary conditions. Our experience with the quenched model leads us to expect that $\langle\bar{\psi}\psi\rangle$ calculated with periodic and antiperiodic boundary conditions should not differ by more than a few percent at even the lowest quark mass values, and we thus conclude that the antiperiodic case is taking much longer to equilibrate. Indeed, performing long pseudofermionic runs on the final gauge field configuration produces results far more like the quenched case than when using periodic boundary conditions. Again we tried increasing the number of pseudofermionic sweeps between each gauge field update, and found $\langle\bar{\psi}\psi\rangle$ increasing. In figure 5.11 we show how $\langle\bar{\psi}\psi\rangle$ varies with the number of pseudofermionic sweeps between gauge field updates at the heaviest quark mass, m=0.10, with antiperiodic boundary conditions on the pseudofermions, together with the periodic results for comparison. We do at least find that with a very large number of pseudofermionic sweeps between gauge field updates, periodic and antiperiodic values are in agreement. Quite why imposing antiperiodic boundary

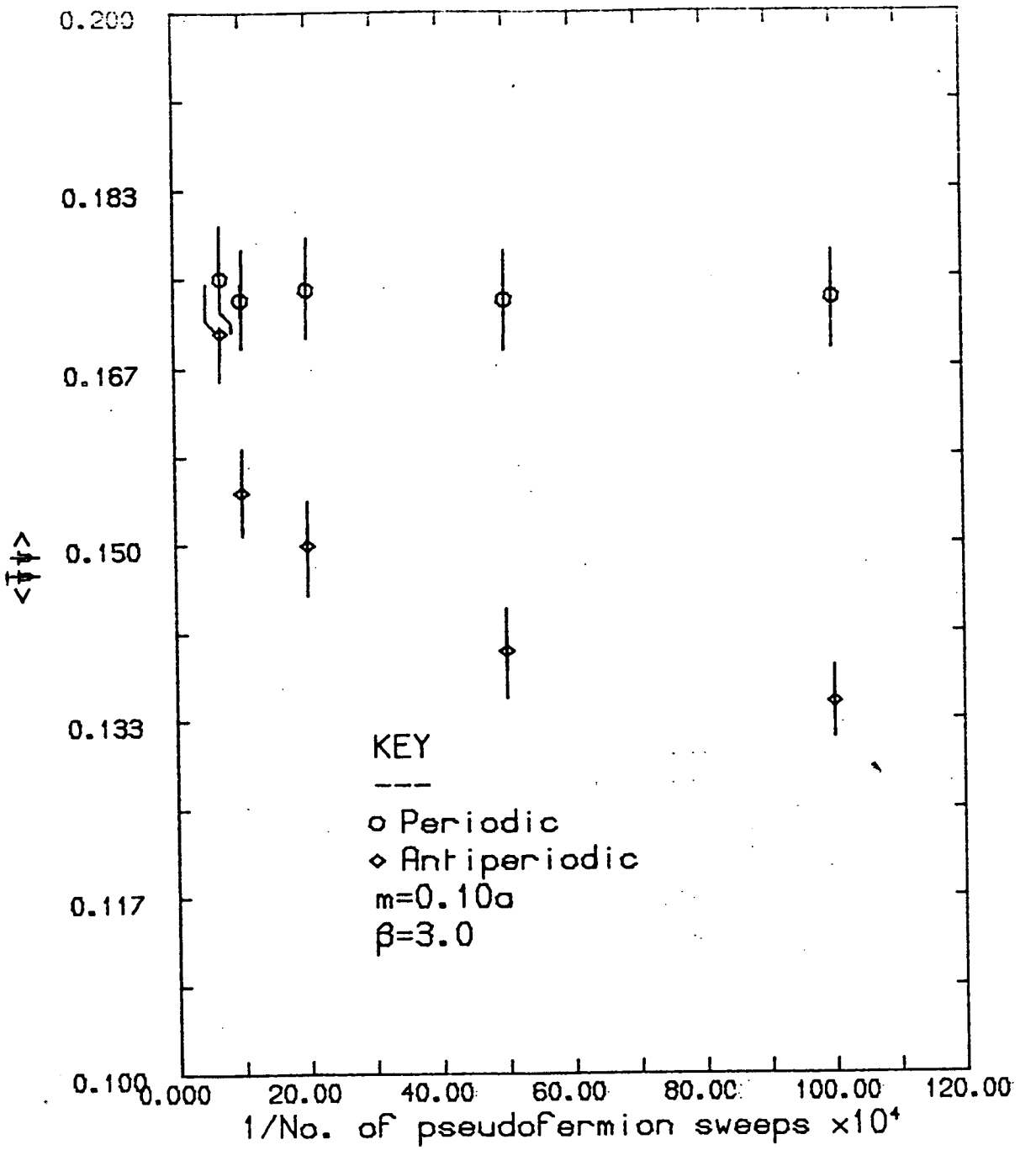

Fig 5.11

Convergence of the pseudofermion heat bath algorithm at m=0.10, with antiperiodic boundary conditions.

conditions should slow equilibration down so much is not clear, but if true, calls into question the usefullness of pseudofermions for generating unquenched configurations in 4 dimensions, where one is usually forced to work on quite small lattices, and thus wants to use antiperiodic boundary conditions in order to eliminate finite size effects.

The results of calculations in the quenched theory, where $\langle\bar{\psi}\psi\rangle$ varies only slightly between periodic and antiperiodic cases, and where the pion mass is identical, within errors in the two cases, give us confidence in proceeding with the calculations in the unquenched case using periodic boundary conditions. We emphasize that the boundaries are at least 30 correlation lengths apart in our simulation, so that the particles should not see them. Hence, particle masses masses are calculated in this way, although we also analysed the antiperiodic configurations we generated for comparison.

Figure 5.10, giving the value of $\langle\bar{\psi}\psi\rangle$ against quark mass, for periodic boundary conditions does show a difference from the quenched case. We see no divergence of $\langle\bar{\psi}\psi\rangle$, but instead see a small dynamical breaking of chiral symmetry.

Particle masses were calculated exactly as in the quenched case, and with very similar results. Nearly all the comments made for the quenched case are equally valid here. The 0^+ and 0^- operators seem to behave like the 1^+ and 1^- operators respectively, when the annihilation terms are neglected, although once again the error bars on the masses are considerable, and the results not so clear cut as in the quenched case. The local Kahler-Dirac pion is once again the clearest operator, and again the fitting routine fails to fit to any excited state, returning only a single mass. The local operators once again only give a reliable estimate of the pion mass, and again the mass extracted is not as free

from error as a similar result in 4 dimensions would be, due to the mixing of states other than the pion with the local operators. Results are shown in figure 5.12. Our results are in reasonable agreement with theory, in particular, the pion mass is in excellent agreement. Note that the pion mass we extract in the unquenched case is in better agreement with theory than in the quenched case. In both cases, though, we seem to be seeing the expected unquenched result. However, if the quenched two species model is indeed like the quenched one species model (as we argued earlier), then we would expect to see the pion mass going to zero in both quenched and unquenched cases.

In the unquenched case, an attempt was made to calculate the contribution to the 0^- and 0^+ states from annihilation terms, using the pseudofermion technique. Consider the 0^+ operator. We know that in terms of the fields $\bar{\chi}$ and χ we have:

$$O^+(y) = \sum_H \bar{\chi}_H(y)\chi_H(y) \tag{5.8}$$

and hence the propagator is given by:

$$\begin{aligned}
\langle \bar{O}^+(\underline{o})\, O^+(\underline{y})\rangle &= \Big\langle \sum_H \chi_H(\underline{o})\bar{\chi}_H(\underline{o}) \sum_K \bar{\chi}_K(\underline{y})\chi_K(\underline{y})\Big\rangle \\
&= \sum_{HK} \langle \bar{\chi}_H(\underline{o})\chi_K(\underline{y})\rangle\langle \bar{\chi}_K(\underline{y})\chi_H(\underline{o})\rangle \\
&\quad - \sum_{HK} \langle \bar{\chi}_H(\underline{o})\chi_H(\underline{o})\rangle\langle \bar{\chi}_K(\underline{y})\chi_K(\underline{y})\rangle \\
&= \sum_{HK} \{G_{HK}(\underline{o},\underline{y})\, G_{KH}(\underline{y},\underline{o}) \\
&\qquad - G_{HH}(\underline{o},\underline{o})\, G_{KK}(\underline{y},\underline{y})\} \qquad (5.9) \\
&= \sum_{HK} \{G(\underline{e}_H, 2\underline{n}+\underline{e}_K)\, G(2\underline{n}+\underline{e}_K, \underline{e}_H) \\
&\qquad - G(\underline{e}_H,\underline{e}_H)\, G(2\underline{n}+\underline{e}_H, 2\underline{n}+\underline{e}_K)\}
\end{aligned}$$

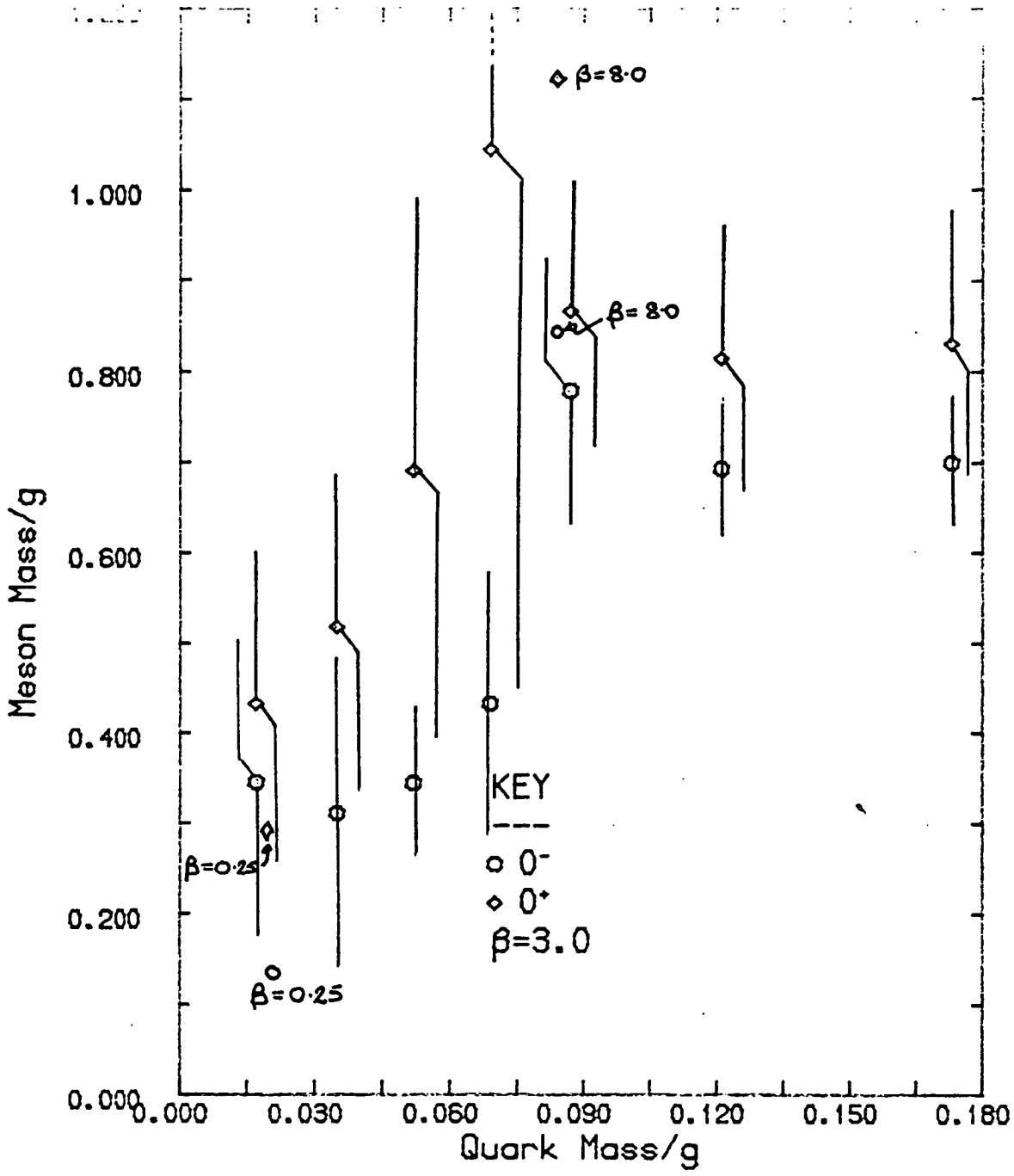

Fig 5.12 (a)

Particle masses for Kahler-Dirac and local particles in the unquenched model.

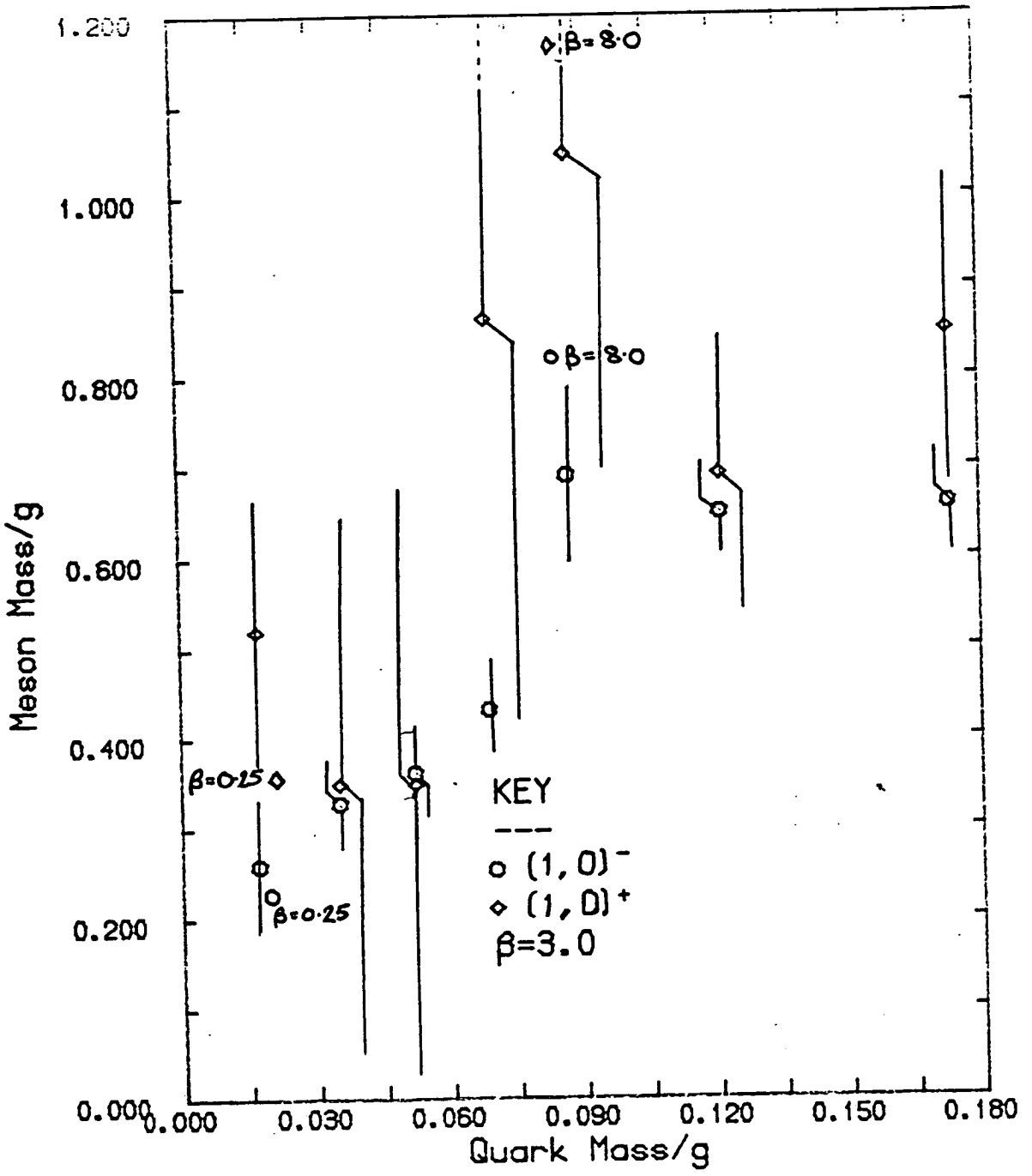

Fig 5.12(b)

Particle masses for Kahler-Dirac and local particles in the unquenched model.

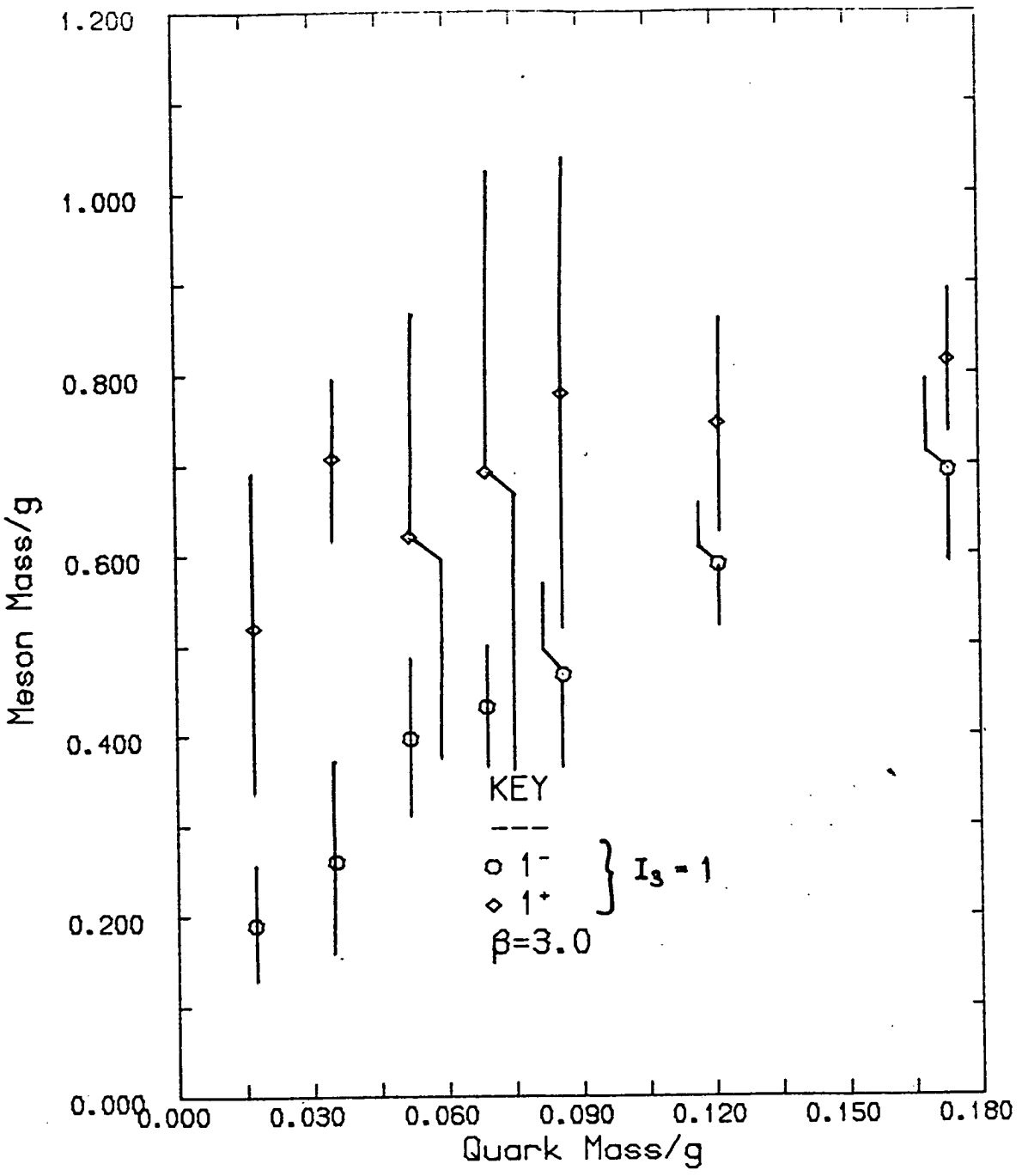

Fig 5.12 (c)

Particle masses for Kahler-Dirac and local particles in the unquenched model.

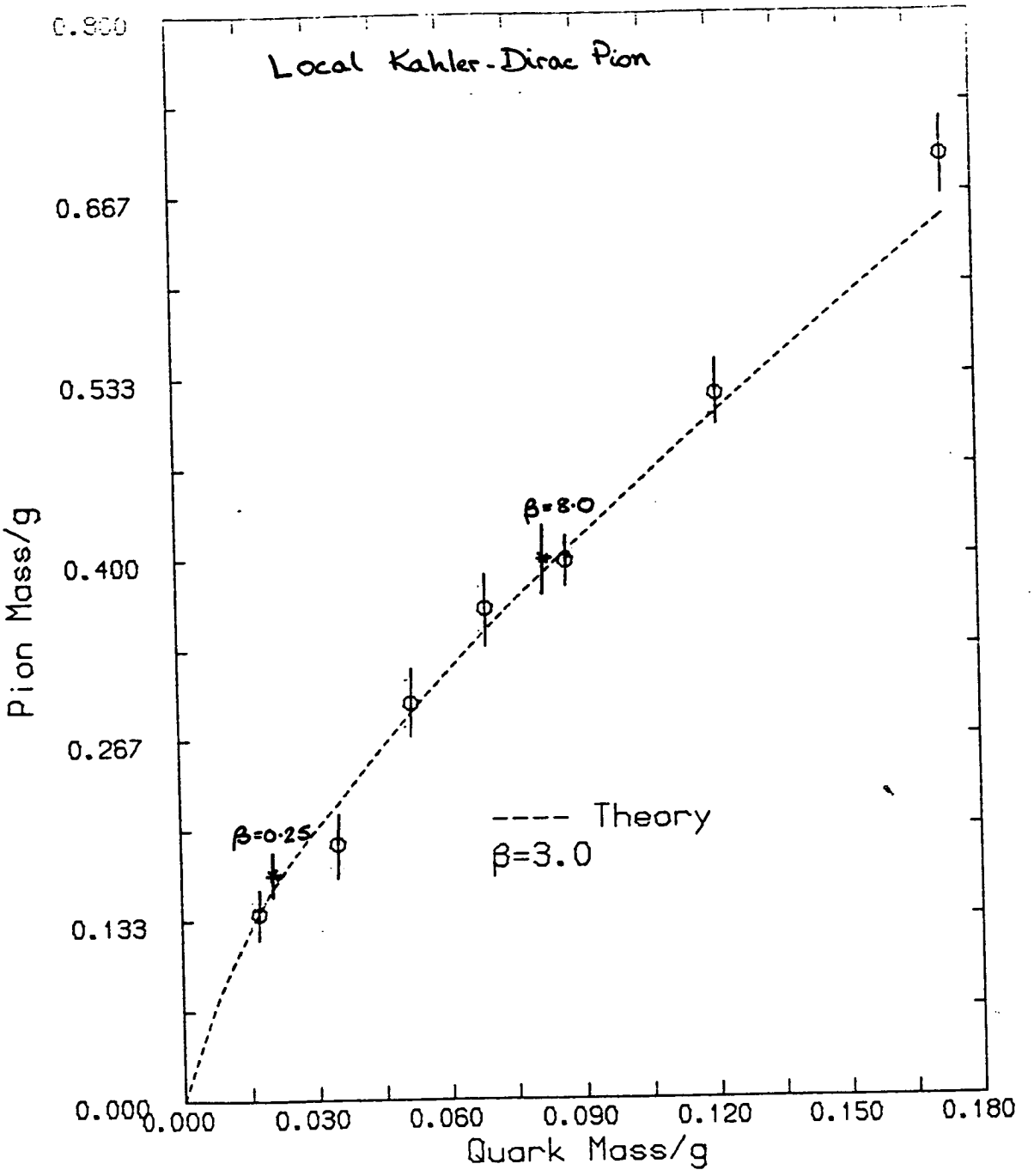

Fig 5.12

Particle masses for Kahler-Dirac and local particles in the unquenched model.

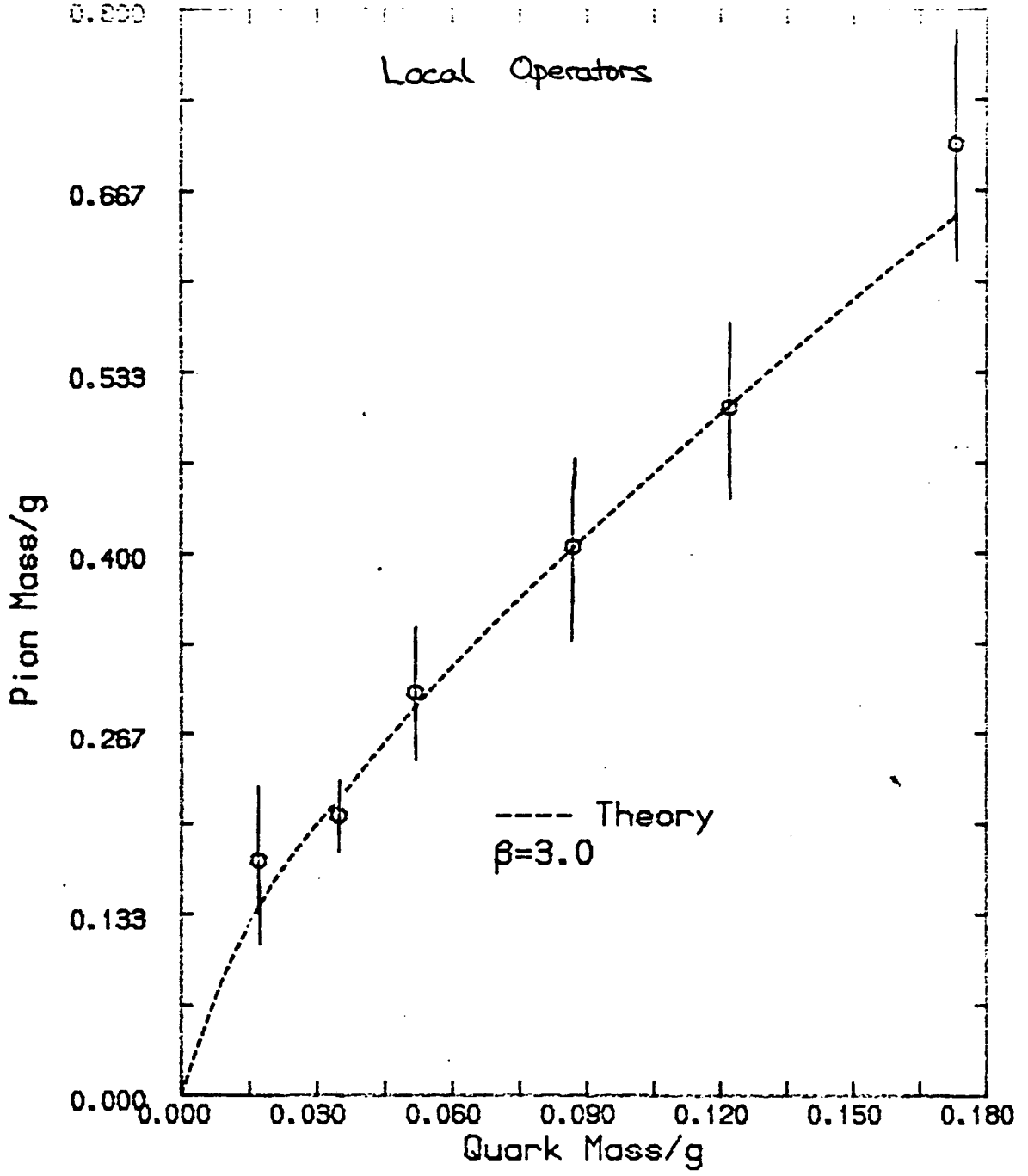

Fig 5.12

Particle masses for Kahler-Dirac and local particles in the unquenched model.

in the notation of chapter three. It is the second term that causes problems, as it cannot be calculated using the conjugate gradient technique in any reasonable amount of time. However, we may use pseudofermions by observing that:

$$\begin{aligned} G(\underline{n},\underline{m})\big|_{\{U\}} &= \langle \bar{\chi}(\underline{m})\chi(\underline{n})\rangle\big|_{\{U\}} \\ &= \langle [(\not{D}+m)\varphi]^{*}(\underline{m})\,\varphi(\underline{n})\rangle\big|_{\{U\}} \\ &\simeq \frac{1}{N_{PF}} \sum_{\{\varphi^{*},\varphi\}} [(\not{D}+m)\varphi]^{*}(\underline{m})\,\varphi(\underline{n})\big|_{\{U\}} \end{aligned} \qquad (5.10)$$

where φ represents the pseudofermionic field, $(\not{D}+m)$ is the lattice Dirac operator, and the sum is over pseudofermion configurations in a fixed gauge field configuration. Finally, of course, we have to average over gauge field configurations. We calculated the annihilation terms for the 0^{+} state and the 0^{-} state at three values of the quark mass - 0.01, 0.05, 0.10 - at β=3.0. In order to make the signal stand out from the statistical noise as clearly as possible, we averaged over all possible origins on the lattice. That is, rather than calculate:

$$\sum_{HK} G(\underline{e}_H,\underline{e}_H)\,G(2\underline{n}+\underline{e}_K,2\underline{n}+\underline{e}_K) \qquad (5.11)$$

we calculated:

$$\frac{1}{32^2}\sum_{\underline{m}}\sum_{HK} G(2\underline{m}+\underline{e}_K,2\underline{m}+\underline{e}_H)\,G(2\underline{m}+2\underline{n}+\underline{e}_K,2\underline{m}+2\underline{n}+\underline{e}_K) \qquad (5.12)$$

where 32^2 is the number of possible origins on a 64x64 lattice, when using the Kahler-Dirac definition of the

mesonic operators. For a given gauge configuration, about 5000 pseudofermion sweeps were performed to allow the pseudofermions to come into equilibrium with the the gauge fields. Pseudofermionic averages were then calculated over a further 5000 sweeps. This procedure was carried out for all 24 gauge configurations at each mass value. Finally, the value of the square of the operator was subtracted out, as this clearly does not contribute to the propagation of the physical state. The annihilation terms were then combined with the conjugate gradient results, and new fits to the data performed. The results were unfortunately disappointing. The errors on the masses extracted from the time slice propagators are sufficiently large as to obscure any effect the annihilation terms might have on the masses. The time slice propagators do show some evidence of a signal but this disappears into the noise after only one or two lattice spacings, and it is not then surprising that errors are very large. In figure 5.13 we show the masses of these two states at the three quark masses where the annihilation terms have been included.

As in the quenched case, we repeat all our calculations at β=0.25 and 8.0. Here, as in the quenched case, we find good agreement with calculations performed at β=3.0. At both these new values of the coupling, we generated 16 configurations at a single quark mass: at β=0.25, we set m=0.035, and at β=8.0, m=0.030. These values correspond to masses of about 0.010, and 0.049 repectively, at β=3.0, and are sufficiently large to eliminate finite size effects. In both cases, 300 pseudofermion sweeps were performed between gauge field updates. Again, we see no difference between the quenched and unquenched results.

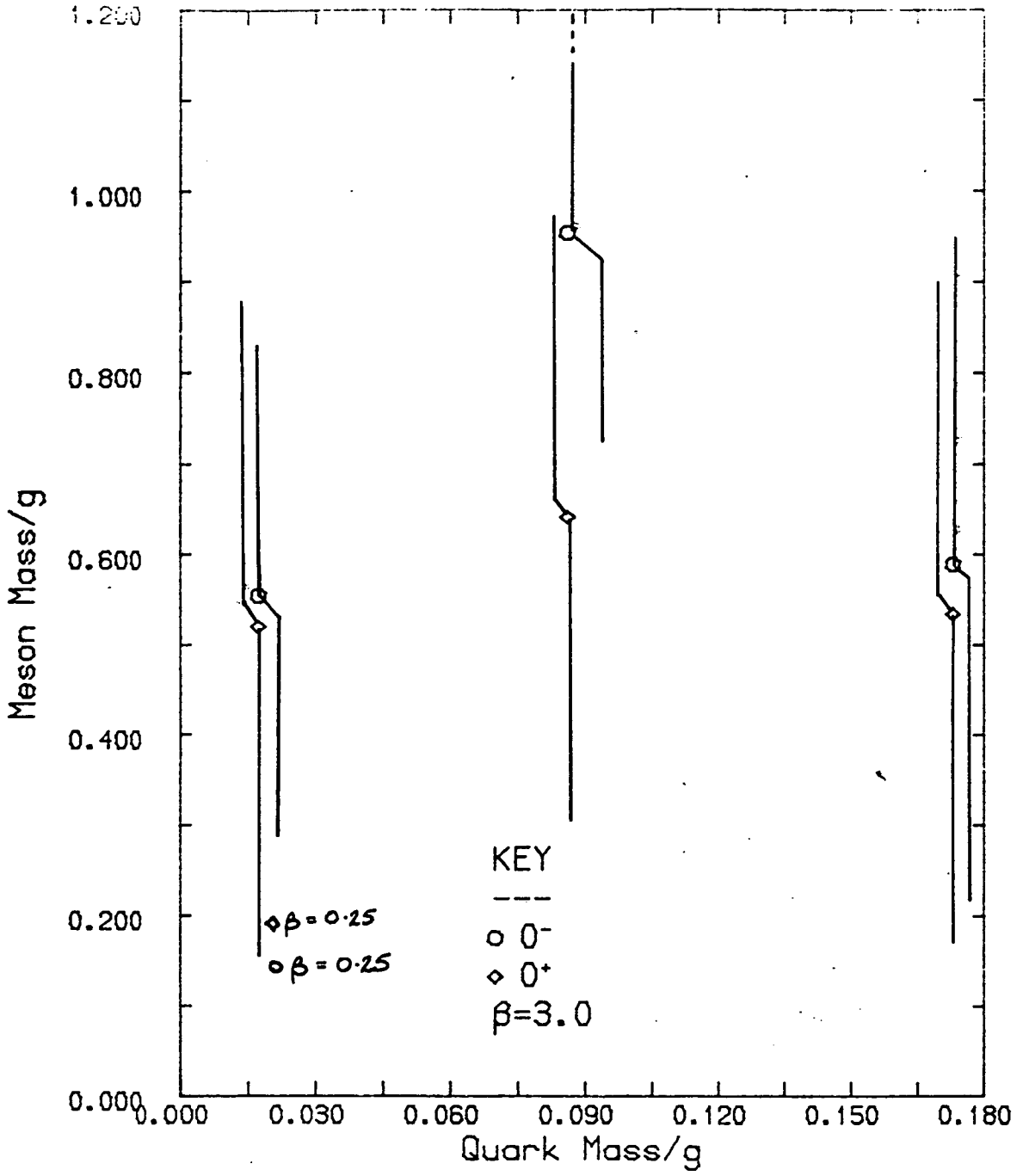

Fig 5.13

Particle masses extracted from the 0^- and 0^+ operators, with annihilation terms included. Unquenched case.

5.3 Conclusions.

The results we have obtained in this investigation of the two species Schwinger model are somewhat disappointing. We have been unable to obtain unambiguous values for any of the meson masses, except for the pion, due to large statistical fluctuations in the mesonic time slice propagators when these are defined according to the Kahler-Dirac prescription. These statistical fluctuations are due to the introduction of gauge fields into the mesonic operators, making them gauge invariant. In two dimensions, at least for the quenched theory, it would be possible to increase the number of gauge field configurations averaged over, and thus reduce the statistical error. For the unquenched theory, where the time required to generate good configurations increases dramatically, averaging over large numbers of configurations becomes prohibitively expensive in computer time. This is especially true in four dimensions, where one wishes to work with non-Abelian groups, and where one is forced to work on small lattices, and therefore should use antiperiodic boundary conditions.

However, the fact that the Kahler-Dirac definition of the pion that is local in the sense that it needs no gauge field multiplications to make it gauge invariant produces such a clear signal, in excellent agreement with the theoretical prediction, encourages us in the belief that this definition of mesonic operators is indeed the correct one, especially when one compares it with the rather poorer results obtained from local operators.

We have succeeded in showing some difference between the quenched and unquenched models. Our calculations indicate that $\langle\bar{\psi}\psi\rangle$ diverges for the quenched theory, whilst there is a small chiral symmetry breaking in the unquenched

theory (although difficulties with equilibration make these last results unreliable). However no such striking difference is seen in the particle masses, not even in the case of the local Kahler-Dirac pion. This is at first sight surprising. However, our analytical results for the one species model (chapter 2) show that whilst $\langle\bar{\psi}\psi\rangle$ diverges in the quenched case, and there is a dynamical breaking of chiral symmetry in the unquenched, the pion behaves qualitatively similarly at large quark masses, and only at very small quark masses are the two models significantly different. In the two species model, a similar phenomenon may occur, and as we do not know how large an effect we are looking for, it may be that that a small difference is hidden in the error bars. If so, this difference can only be of the order of 10%. Alternatively, it may be that poor equilibration of the unquenched configurations has reduced real differences in the particle masses. This was investigated by calculating particle masses in configurations with a greater number of pseudofermionic sweeps between gauge field updates. No noticeable change was seen in the pion mass.

CHAPTER SIX

NUMERICAL SIMULATION OF TWO DIMENSIONAL QED WITH ONE FLAVOUR

In this final chapter, we present the results of our numerical simulation of the one species model. This is simulated using the one link mass term to lift the flavour degeneracy as described in chapter three. The mass of the d quark is set to unity in reciprocal lattice spacings. Much of what has already been said for the two species model in chapter five, regarding methods and sources of error, is equally valid here.

6.1 The Quenched Approximation.

Measurements of the fermionic condensate, $\langle\bar{\psi}\psi\rangle$, are made as for the quenched two species model (section 5.1). As we are dealing with fermions of unequal masses, we measure $\langle\bar{u}u\rangle$ and $\langle\bar{d}d\rangle$ separately. We use the same configurations as for the two species quenched model: as these were generated without including the effects of internal fermion loops, they may be used at any values of the quark masses.

As in the two species model, we calculate $\langle\bar{u}u\rangle$ and $\langle\bar{d}d\rangle$ using the pseudofermion technique, allowing 5000 pseudofermionic sweeps for equilibration, and a further 5000 sweeps for the average. At β=3.0, we average over a few configurations, again as in the two species case. We repeated the calculation for both periodic and antiperiodic boundary conditions, and at 7 values of the quark mass. The results are shown in figure 6.1 together with the analytical results derived in chapter two. Free fermion results have

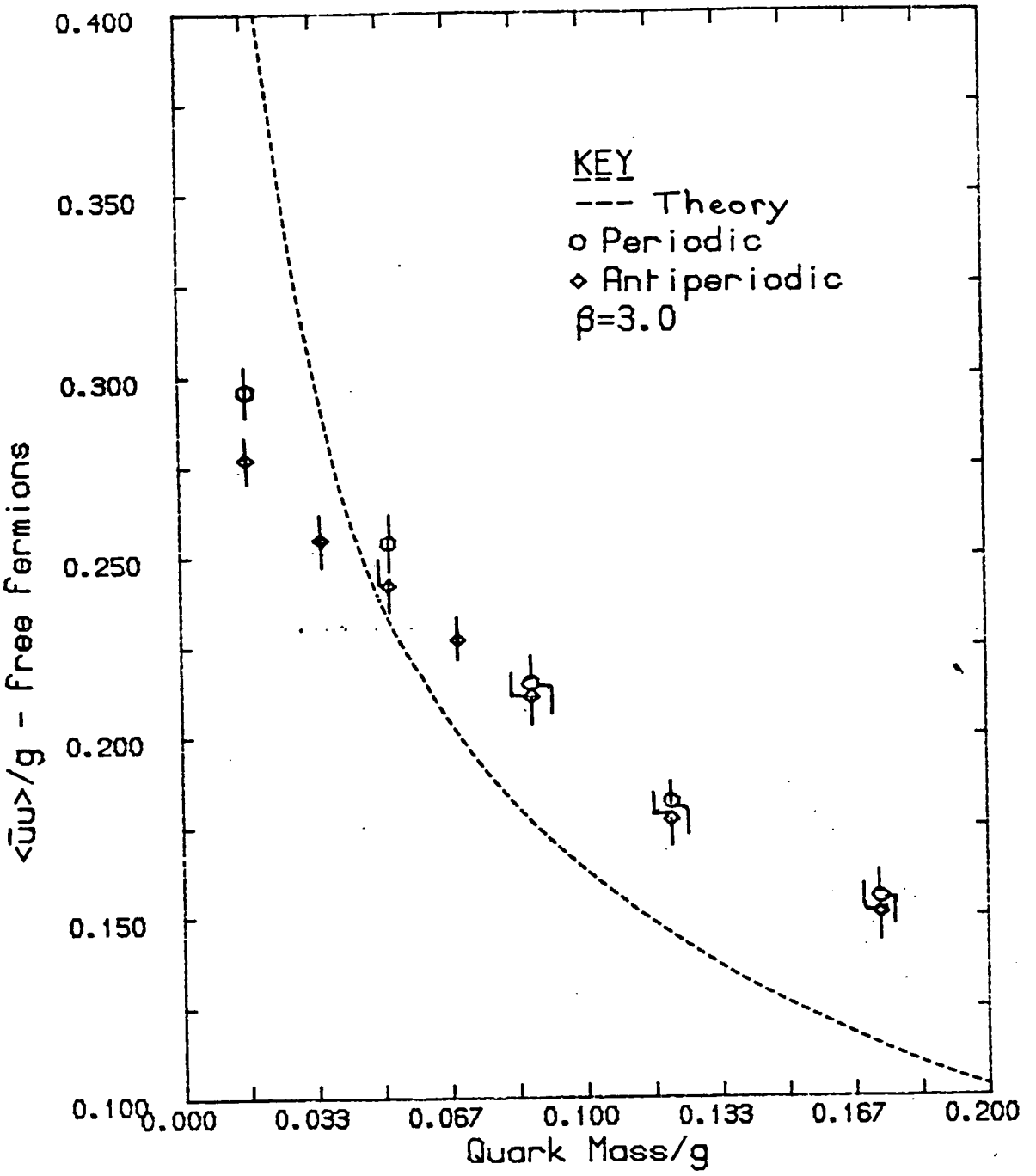

Fig 6.1

Fermionic condensate in the quenched one species model, showing the effects of boundary conditions.

been subtracted out. We find quite good agreement, observing a divergence in the value of $\langle\bar{u}u\rangle$ in the limit of vanishing quark mass. The value of $\langle\bar{d}d\rangle$ remains constant, within errors, as the u quark mass varies, encouraging us in the belief that the d quark is indeed decoupled from the model. We find that the boundary conditions are not important, periodic and antiperiodic cases differing by only a few percent at even the lightest quark mass values.

Again, as in the two species model, to check that we are near the continuum limit, we wish to repeat our calculations at a smaller value of the coupling, β. In the one species model, all the particle masses are quite large, so that we have not done calculations at β=0.25, as at this value of the coupling, the correlation lengths of the physical particle states are less than one lattice spacing. However, we have repeated all the calculations at β=8.0, using 16 quenched configurations. The generation of these configurations is described in chapter five. We find good agreement with the result at β=3.0, at four values of the quark mass. The results at β=8.0 are shown in figure 6.2, for periodic boundary conditions.

It is far more difficult in the one species model to extract particle masses than in the two species model. Because we have chosen to use a one link mass term to break the flavour degeneracy rather than the two link term also discussed in chapter three, there are no Kahler-Dirac operators that do not require gauge field multiplications to make them gauge invariant, except the 0^+ operator (although isospin has no meaning in the one species model, we continue to use the notation established in chapter three for clarity. We expect that in the one species model the operators corresponding to different isospin states in the two species model should be degenerate. Only those states with I_3=0 in the two species model, and which do not

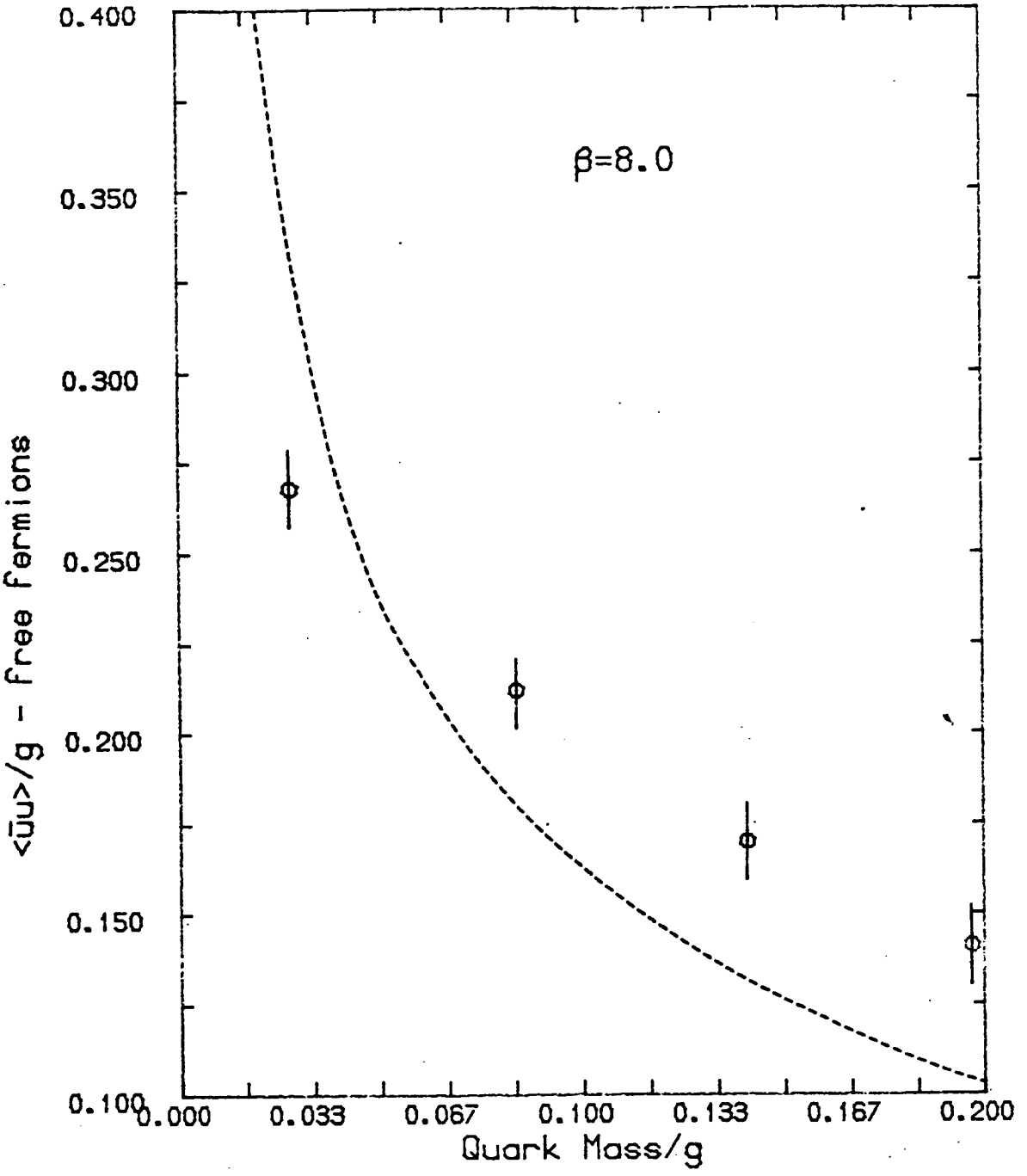

Fig 6.2

Fermionic condensate in the quenched one species model at β=8.0.

therefore contain terms like $\bar{u}d$, retain any meaning). There is no version of the local Kahler-Dirac pion in the one species model, when using the one link mass term, and hence we might expect to find large statistical errors on the masses we extract.

A second difficulty lies in the fact that as there is no isospin symmetry in the one species model, annihilation terms contribute to all the states. As we have already seen in the two species model, the calculation of these terms does not yield good results, and is very time consuming. In the quenched case, then, we have chosen to calculate particle masses without these troublesome terms. If we extract any results from this procedure it will be because the lightest mass state might be expected to contaminate almost any operator. At one mass value, and at one value of the coupling, we do calculate the annihilation terms in the quenched theory, to see if there is any significant difference when these terms are included.

The presence of the heavy d quark does seem to have a beneficial effect on the convergence of the conjugate gradient algorithm. In the one species model, this is significantly faster than in the two species model. For example, to reduce the error function (4.45) to a value of at most 10^{-70} required about 2500 conjugate gradient steps at a quark mass of 0.01 in the two species model, whereas in the one species model, only about 1500 conjugate gradient steps were required to achieve the same accuracy.

In fact, we found that the results extracted by neglecting the annihilation terms were in good agreement with the expected analytical results. The error bars on the masses, however, are large, due to the statistical fluctuations introduced with the gauge field multiplications. These are sufficiently large so as to obscure any difference

between the quenched and unquenched cases. In figures 6.3 we present examples of the time slice propagators of the the four states: 0^-, 0^+, 1^-, 1^+. In figure 6.4 we present the masses, divided by the coupling g, against the quark mass parameter, (m/g). Included in figure 6.4 is the point produced with the annihilation terms included at β=8.0.

At this stage, we make mention of a time saving procedure we have used in the calculation of time slice propagators. In general, given some mesonic operator, $|M\rangle$, we are interested in the matrix element of the Hamiltonian, $\langle M|e^{-Ht}|M\rangle$. As in chapter one, we have:

$$\begin{aligned}\langle M|e^{-Ht}|M\rangle &= \sum_{n\neq 0}\langle M|e^{-Ht}|n\rangle\langle n|M\rangle \\ &= \sum_{n\neq 0}|\langle M|n\rangle|^2 e^{-E_n t}\end{aligned} \tag{6.1}$$

At large values of t, only the lightest state remains, and:

$$\langle M|e^{-Ht}|M\rangle \simeq \langle M|n_0\rangle\langle n_0|M\rangle e^{-E_{n_0}t} \tag{6.2}$$

This is all as we had before. But now note that we do not need to use the full operator at $\underline{o}$: all we require at the origin is any operator that has a non-zero overlap with the state we wish to measure. For example, consider the 0^+ operator:

$$O^+(y) = \sum_H \bar{\chi}_H(y)\chi_H(y) \tag{6.3}$$

The full mesonic propagator is given by:

$$\begin{aligned}\langle \bar{O}^+(\underline{o})\,O^+(y)\rangle &= \sum_{HK}\langle \chi_H(\underline{o})\bar{\chi}_H(\underline{o})\bar{\chi}_K(y)\chi_K(y)\rangle \\ &= \sum_{HK} G_{HK}(\underline{o},y)\,G_{KH}(y,\underline{o}) + \text{annihilation terms}\end{aligned}$$

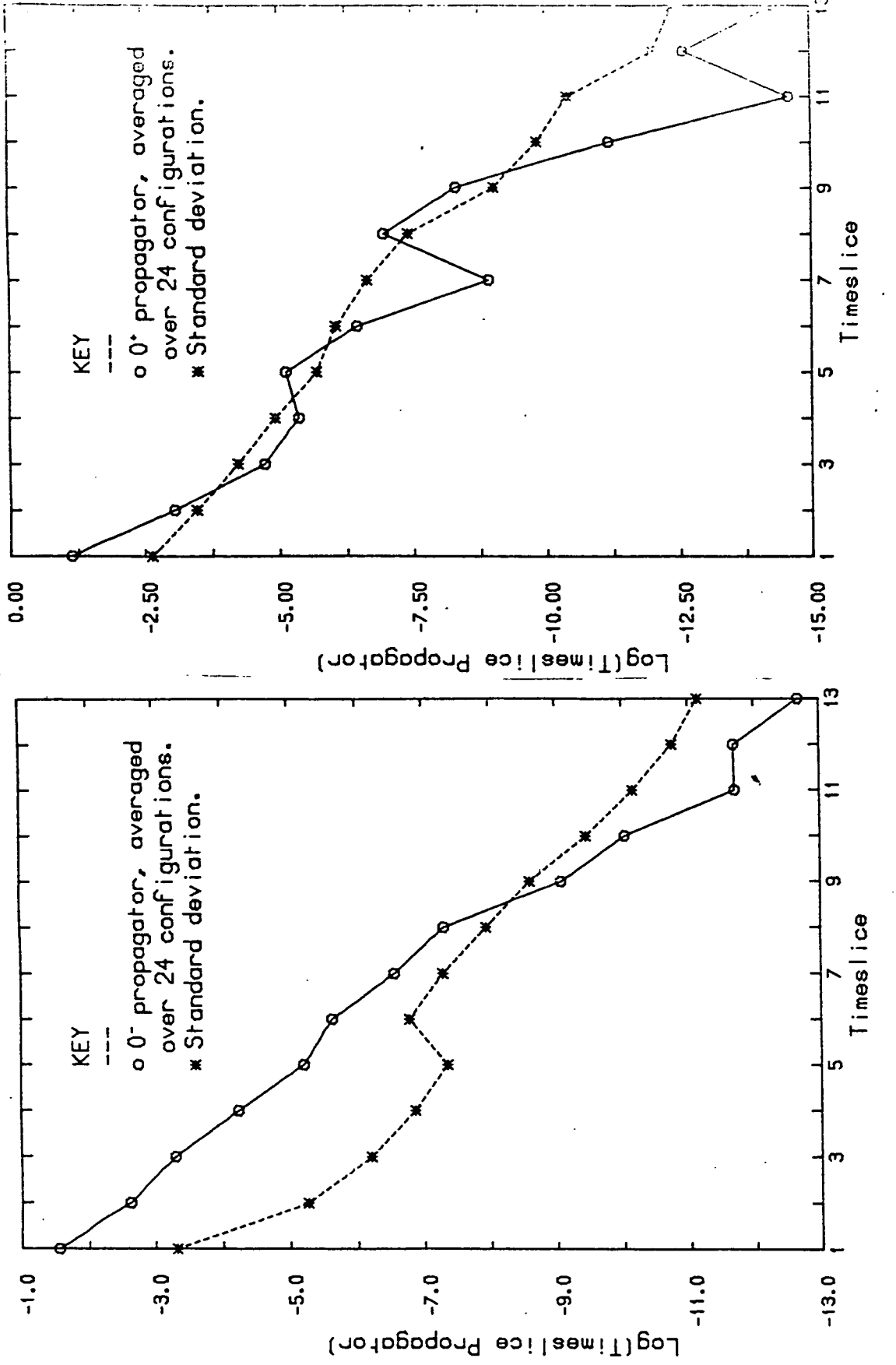

Fig 6.3(a)

Timeslice propagators for extended Kahler-Dirac mesonic operators at m_u=0.05. Quenched case.

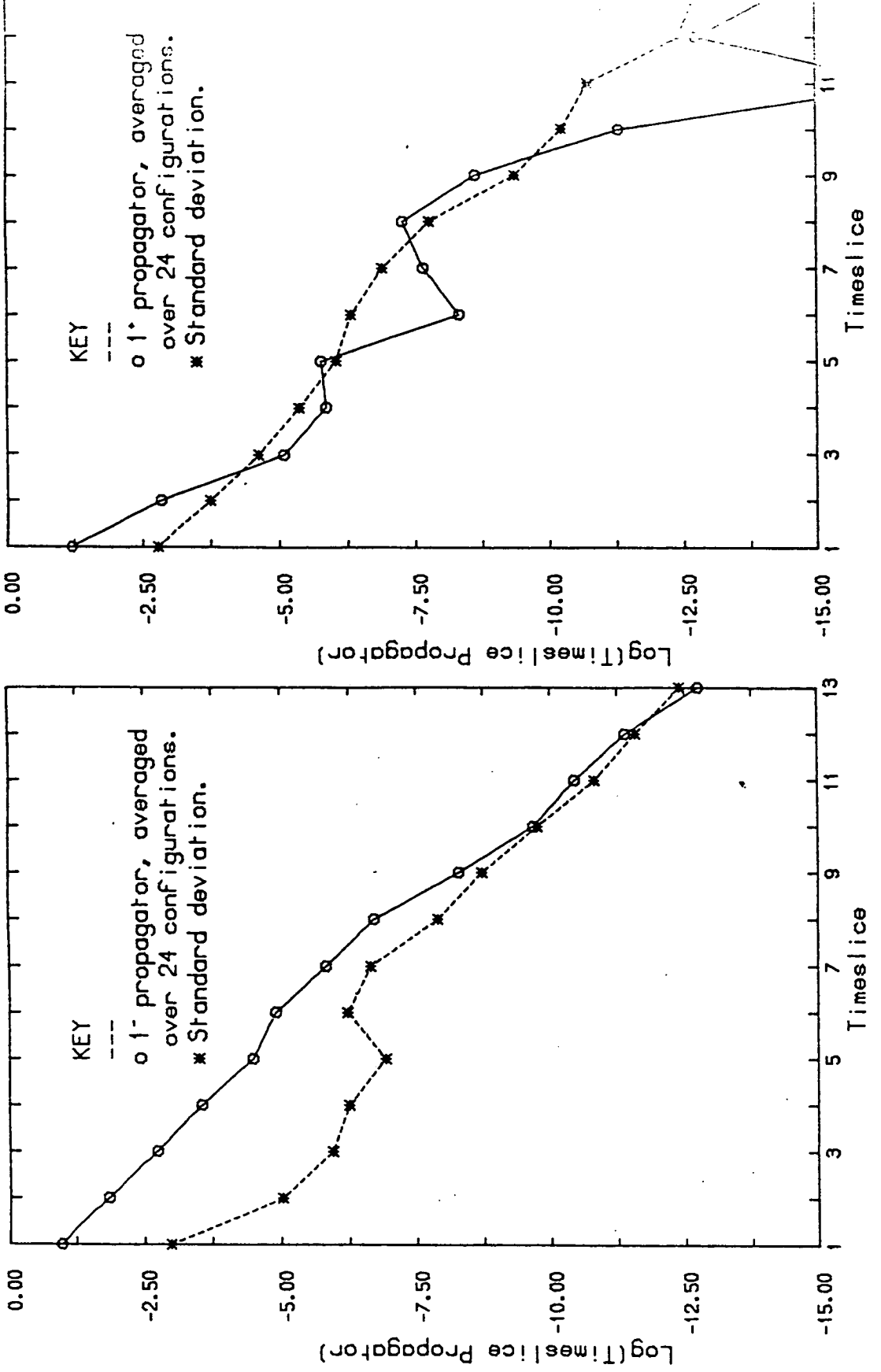

Fig 6.3 (b)

Timeslice propagators for extended Kahler-Dirac mesonic operators at m_u=0.05. Quenched case.

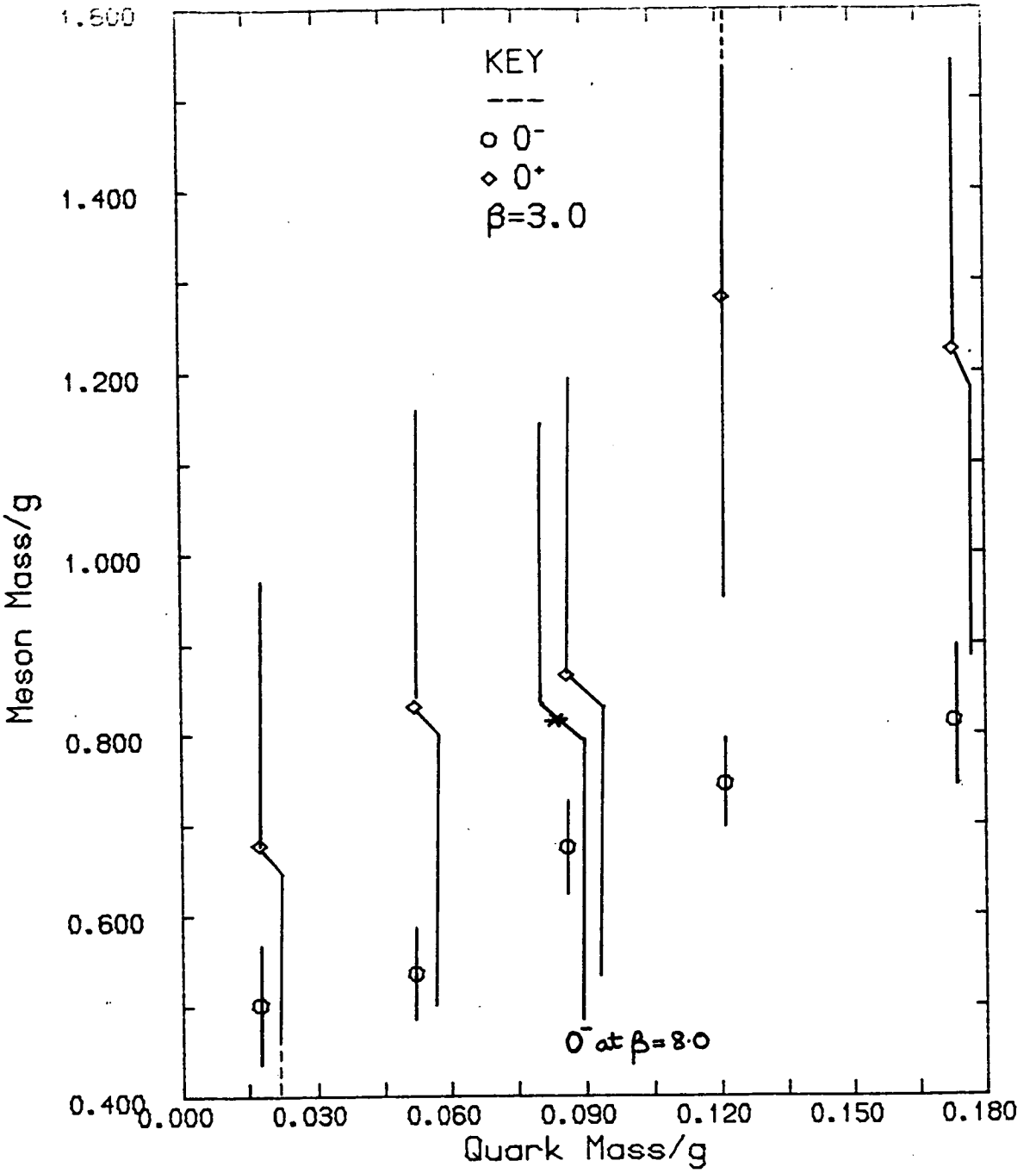

Fig 6.4 (a)

Particle masses for Kahler-Dirac particles in the quenched approximation.

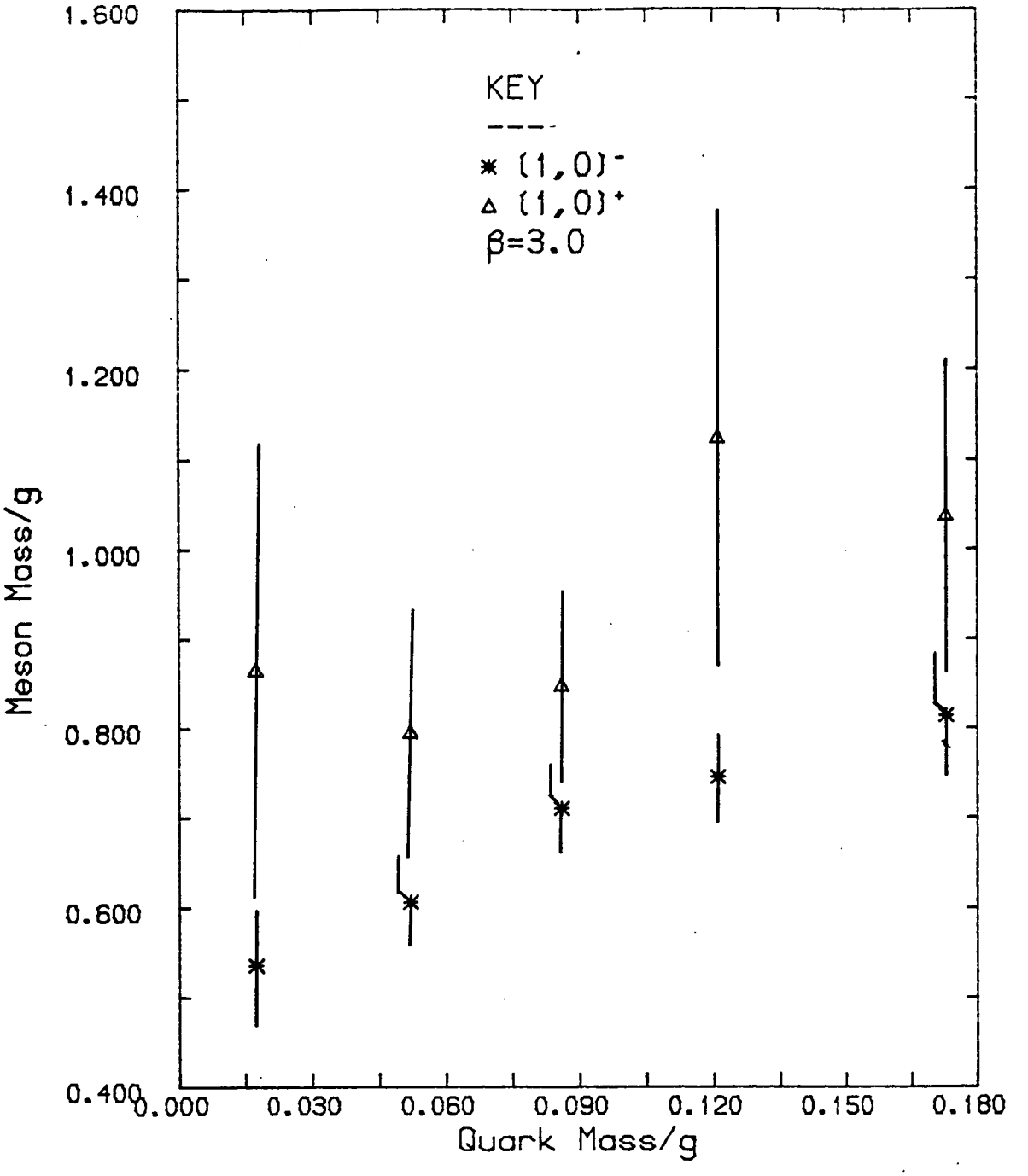

Fig 6.4 (b)

Particle masses for Kahler-Dirac particles in the quenched approximation.

$$\langle \bar{O}^{+}(\underline{0})\, O^{+}(\underline{y}) \rangle = \sum_{HK} G(\underline{e}_H, 2\underline{s}+\underline{e}_K) G(2\underline{s}+\underline{e}_K, \underline{e}_H) + \text{annihilation terms} \tag{6.4}$$

and hence, we have to calculate four quark propagators from the Kahler-Dirac origin, out to the site $\underline{y}$, and four back from $\underline{y}$ to $\underline{0}$. This is no problem in the two species case, where the simple relationship between the quark Green function and its transpose means that we only need to calculate the propagators in one direction. However, there is no such simple relationship between the quark Green function and its transpose when using the one link mass term, and both have to be calculated separately. Hence, rather than use (6.4), we use only part of the operator at the origin, say $\bar{\chi}_\varphi(\underline{0})\chi_\varphi(\underline{0})$, which has a non-zero overlap with the mesonic operator. Then we calculate:

$$\langle \bar{\chi}_\varphi(\underline{0})\chi_\varphi(\underline{0})\; O^{+}(\underline{y}) \rangle = \sum_{H} G_{H\varphi}(\underline{y},\underline{0})\, G_{\varphi H}(\underline{0},\underline{y}) + \text{annihilation terms} \tag{6.5}$$

Hence, we only need to calculate one quark propagator from the origin to the site $\underline{y}$ and four propagators back from $\underline{y}$ to $\underline{0}$. We have checked the validity of this procedure in the two species model, where it is easy to do, and find no difference in the quality of the results from using full operators rather than the reduced form, and the local Kahler-Dirac pion remains clean when the reduced form is used. The reduced form of the operator at the origin corresponds to creating at the origin a whole set of physical states that have a non-zero overlap with the reduced operator (for example, $\bar{\chi}_\varphi\chi_\varphi(\underline{0})$ will create both the 0^+ state and the local pion in the two species model), but this should not matter so long as we measure only single states at the site $\underline{y}$ (together of course with its radial

excitations).

So far, we have discussed only the Kahler-Dirac definition of the particle operators. It is also possible to define local operators as for the two species model, that mix two of the physical states. Note though that if we use the local operators we are necessarily neglecting the annihilation terms. In fact, defining time in the one direction, as in chapter three, only one of the local operators mixes with the physical states. This is the operator $G(\underline{0},\underline{y})G^{T}(\underline{0},\underline{y})$, corresponding to $(-1)^{e_{\mu_1}+e_{\mu_2}+e_{\kappa_1}+e_{\kappa_2}}|G(\underline{0},\underline{y})|^2$ in the two species model. As in the two species model, we find we can sensibly extract only the pion mass from the time slice propagators, the second mass returned by the fitting routine being so variable as to be meaningless. The results for the pion are plotted in figure 6.5, a point at β=8.0 being included. We see that the local operators yield masses that do not agree well with analytical results, and with errors that make the results almost meaningless. In this case, then, it is the non-local Kahler-Dirac operators that produce the better results.

6.2 The Unquenched Model

To investigate the unquenched one species model, we need to generate new configurations at each value of the u quark mass. This was done as described in chapter five for the two species model, the d quark mass being held constant at unity as the u quark mass was varied. 24 configurations at each of 7 quark masses were generated, with, initially, 50 pseudofermionic sweeps between gauge field updates. An update angle on the gauge fields of $0.1\times2\pi$ was used, with 100 gauge field updates being performed between the configurations used in the mass calculations.

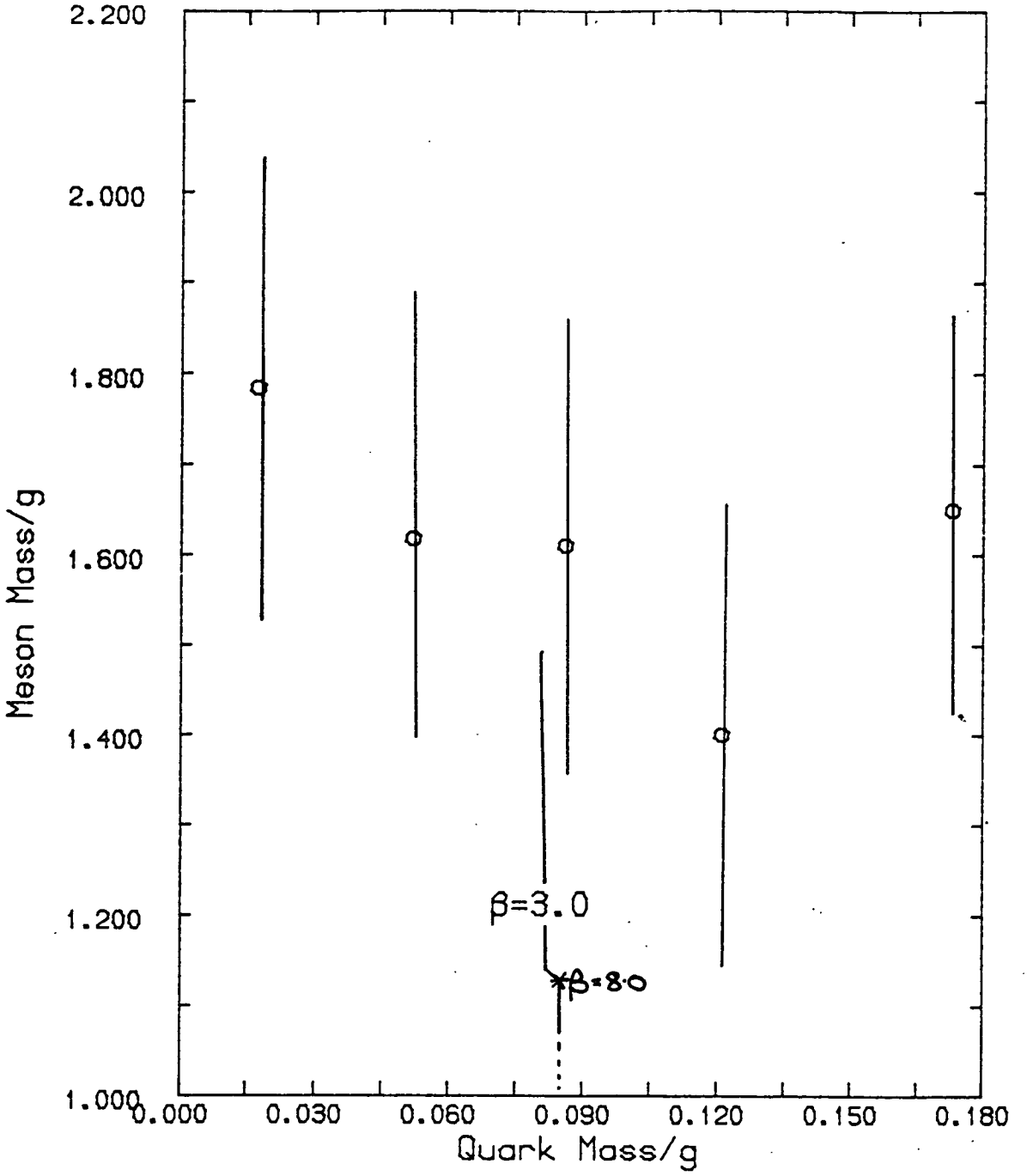

Fig 6.5

Pseudoscalar mass extracted from the local definition of mesonic operators in the quenched approximation.

The first four gauge configurations generated at each mass value were discarded to allow for equilibration. This process was repeated for both periodic and antiperiodic pseudofermionic boundary conditions.

Whilst the gauge field configurations were being generated, we used the pseudofermionic configurations to calculate values of $\langle\bar{u}u\rangle$ and $\langle\bar{d}d\rangle$, as in the two species case. Consider first the results obtained using periodic boundary conditions.

Encouragingly, the value of $\langle\bar{d}d\rangle$ returned remained constant as the u quark mass was varied, and in fact is the same as that produced in the quenched case and in the free case. We also found that on generating unquenched configurations at β=8.0, the value of $\langle\bar{d}d\rangle$ returned was again the same. Thus, the d quark does indeed appear to be decoupled from the model. The value of $\langle\bar{u}u\rangle$ returned is significantly different from the quenched case, but we must check that the configurations are properly equilibrated. We did this by performing long pseudofermionic runs on the last gauge configuration of several thousand updates, holding the gauge fields fixed, as in the two species model. If the configurations are well equilibrated unquenched configurations, then the value of $\langle\bar{u}u\rangle$ returned in this long run should be the same as that calculated during the generation of the configurations. We found that the situation in the one species model is much better than in the two species case. As we mentioned in section 6.1 when discussing the convergence of the conjugate gradient algorithm, the presence of the heavy d quark seems to improve the equilibration of the pseudofermion technique. Certainly, performing long runs on the last gauge configuration produces a value of $\langle\bar{u}u\rangle$ that differs from that generated during the production of the gauge field configurations by only about 10% at even the smallest quark

mass values. In figure 6.6, we present the values of $\langle\bar{u}u\rangle$ in the unquenched model, together with the analytical result derived in chapter two. Free fermions have been subtracted out. We find quite good agreement with analytical result (note the scale on figure 6.6). At some of the mass values we investigated, we increased the number of pseudofermion sweeps between gauge field configurations, and calculated new values of $\langle\bar{u}u\rangle$. These new values do not differ from those generated with 50 pseudofermion sweeps between gauge field updates by more than a few percent at even the lowest quark masses.

When we consider the results produced with antiperiodic pseudofermionic boundary conditions, we find, as in the two species model, that the values of $\langle\bar{u}u\rangle$ are much lower than in the periodic case. Once again, if we increase the number of pseudofermionic sweeps between gauge field updates, this value slowly increases towards that produced in the periodic case. However, the number of pseudofermionc sweeps that would have to be performed to produce a value in accord with the periodic results (and with the analytical results) make the generation of unquenched configurations with antiperiodic pseudofermionic boundary conditions prohibitively expensive in terms of computer time. In figure 6.7, we show the values of $\langle\bar{u}u\rangle$ calculated with periodic and antiperiodic boundary conditions between gauge field updates. Free fermions have not been subtracted out here.

Particle masses were calculated as in the quenched case, in configurations generated with periodic boundary conditions on the pseudofermions. In the unquenched case, we also calculated the annihilation terms at 3 quark masses - 0.03, 0.05, 0.07. These were calculated as in the quenched case, and as in the two species model, by allowing the pseudofermions 5000 sweeps to come into equilibrium with the gauge fields, and then averaging over a further 5000

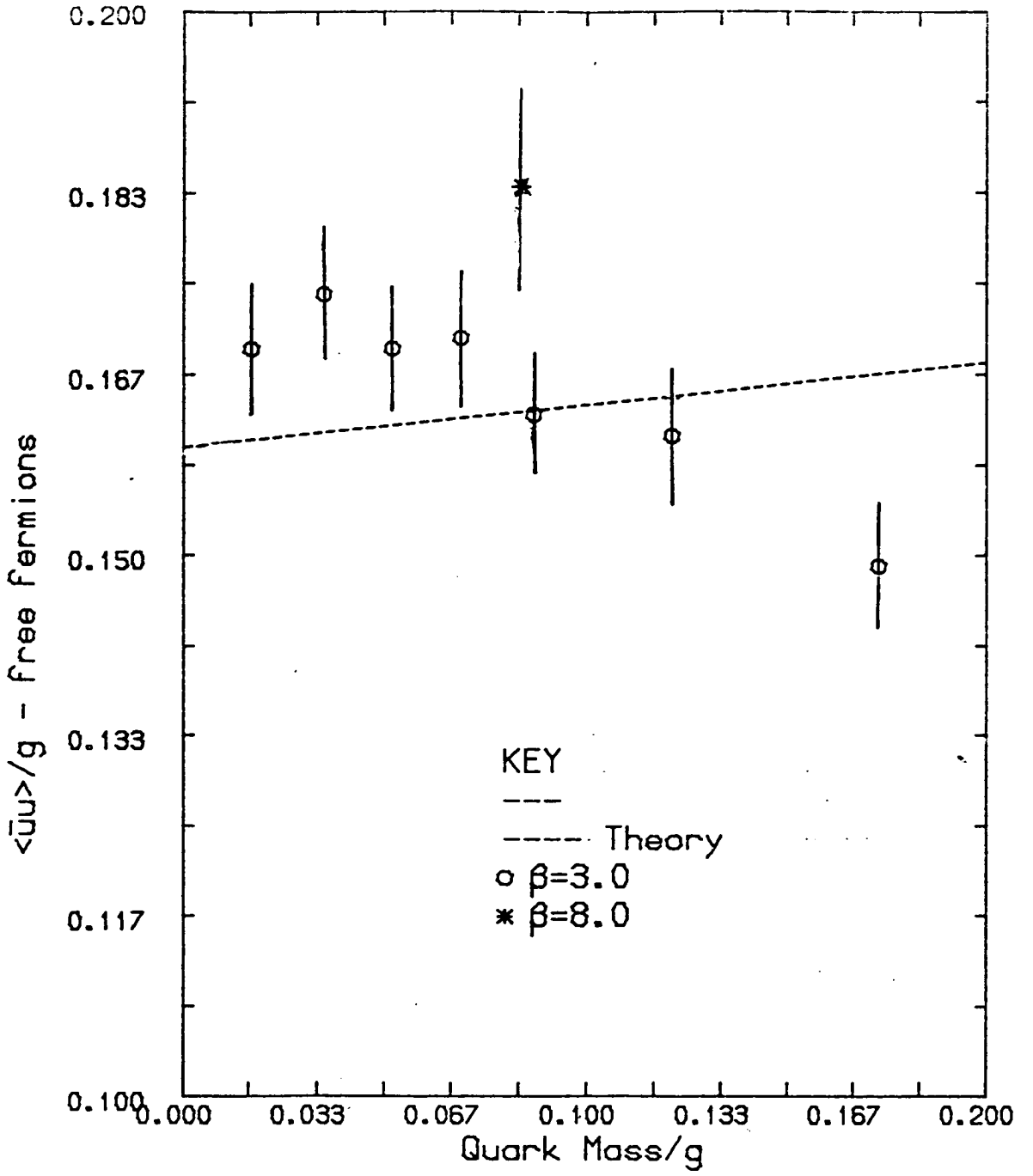

Fig 6.6

Fermionic condensate in the unquenched one species model.

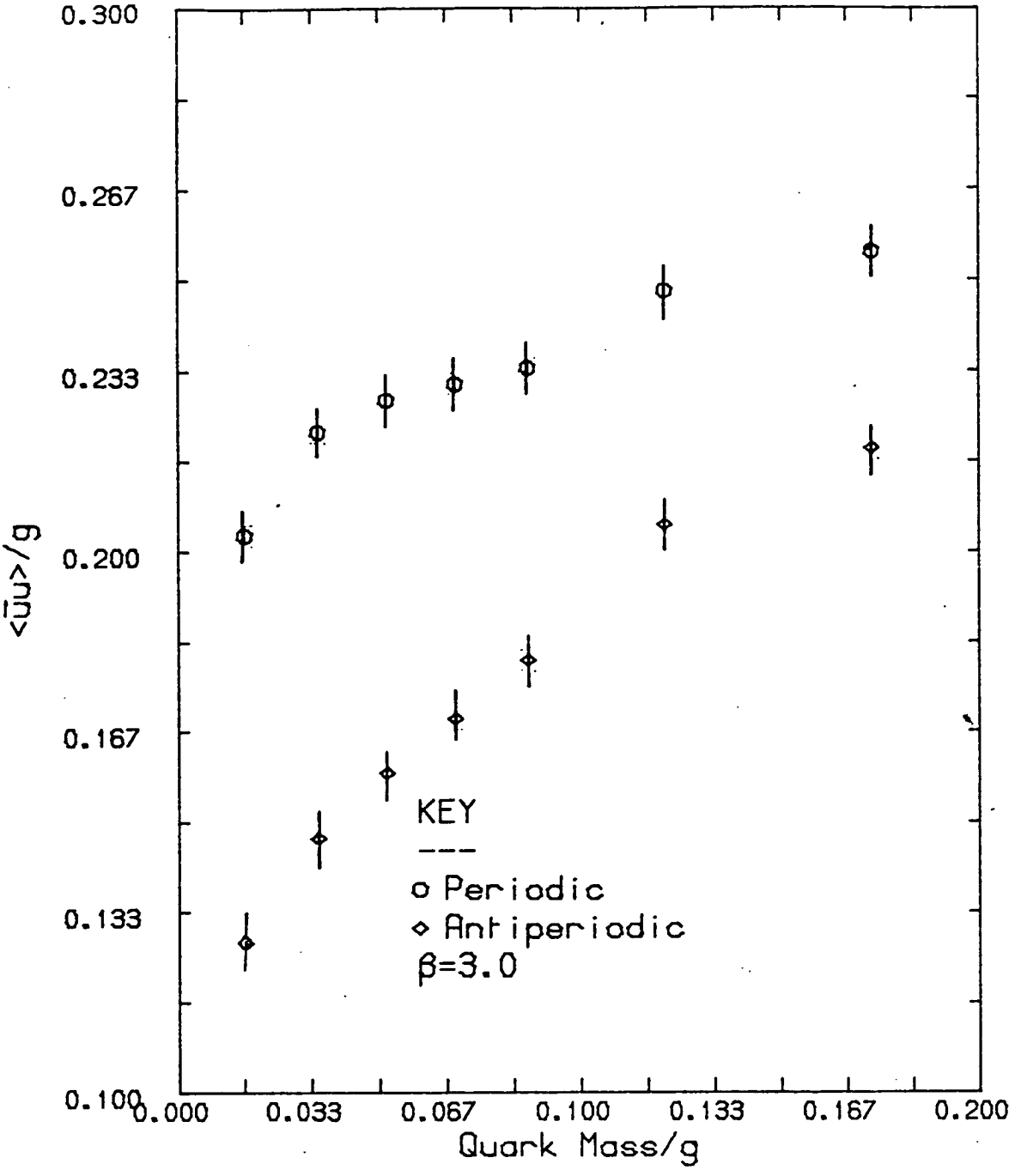

Fig 6.7

Fermionic condensate in the one species unquenched model, showing the effects of boundary conditions.

sweeps to produce the annihilation terms, finally averaging over the 24 unquenched configurations available at each value of the u quark mass. Again, we tried to improve statistics by averaging over all possible origins within a given configuration, as we described in chapter five.

In figure 6.8,we show the particle masses for the various mesonic operators, calculated without the inclusion of the annihilation terms. Once again, we see good agreement with the analytical results, for both the pseudoscalar (pion) state, and the scalar state, which is a sign that perhaps the annihilation terms are not as important to the one species model as we know them to be to the two species model. Note that the analytical results are obtained in perturbation theory, to first order in (m/g), and might therefore differ from the numerical results at large values of the quark mass. We again find large errors on the masses we extract, although we note that the errors are not as large as those on the one and two link mesonic operators in the two species model.

In figure 6.9 we show the particle masses at the three values of the quark mass at which we calculated the annihilation terms. The results are no improvement on those obtained by neglecting these terms. As in the two species model, the unquenched and quenched results for the mesonic masses are not significantly different.

As in the quenched case, we are also able to extract masses for the pseudoscalar state from the local operators. We have calculated this mass at 7 values of the quark mass, as for the Kahler-Dirac particle definition discussed above and at a mass of 0.03 at β=8.0. The results are shown in figure 6.10. As in the quenched case, they are poor.

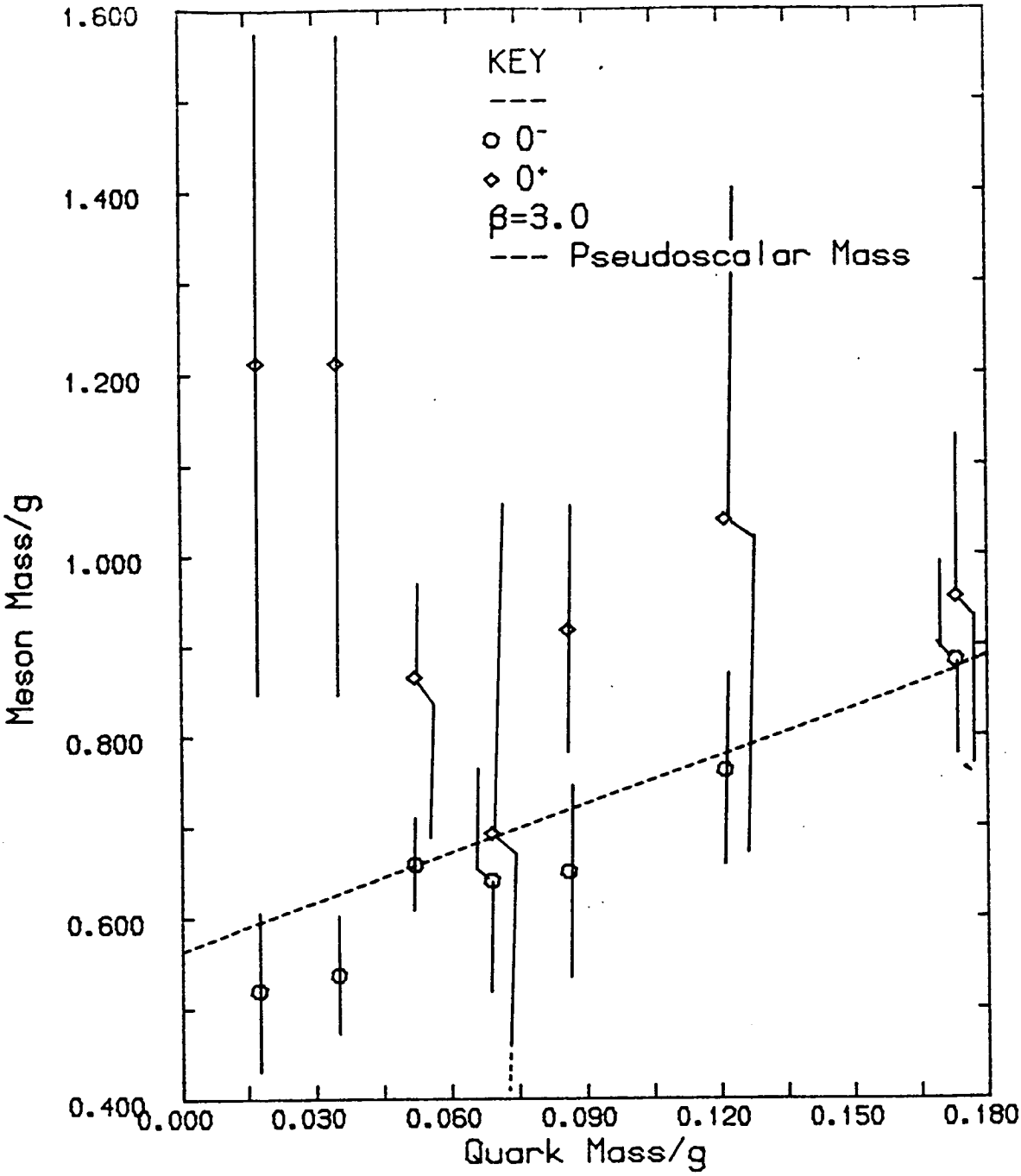

Fig 6.8(a)

Particle masses for Kahler-Dirac particles in the unquenched model.

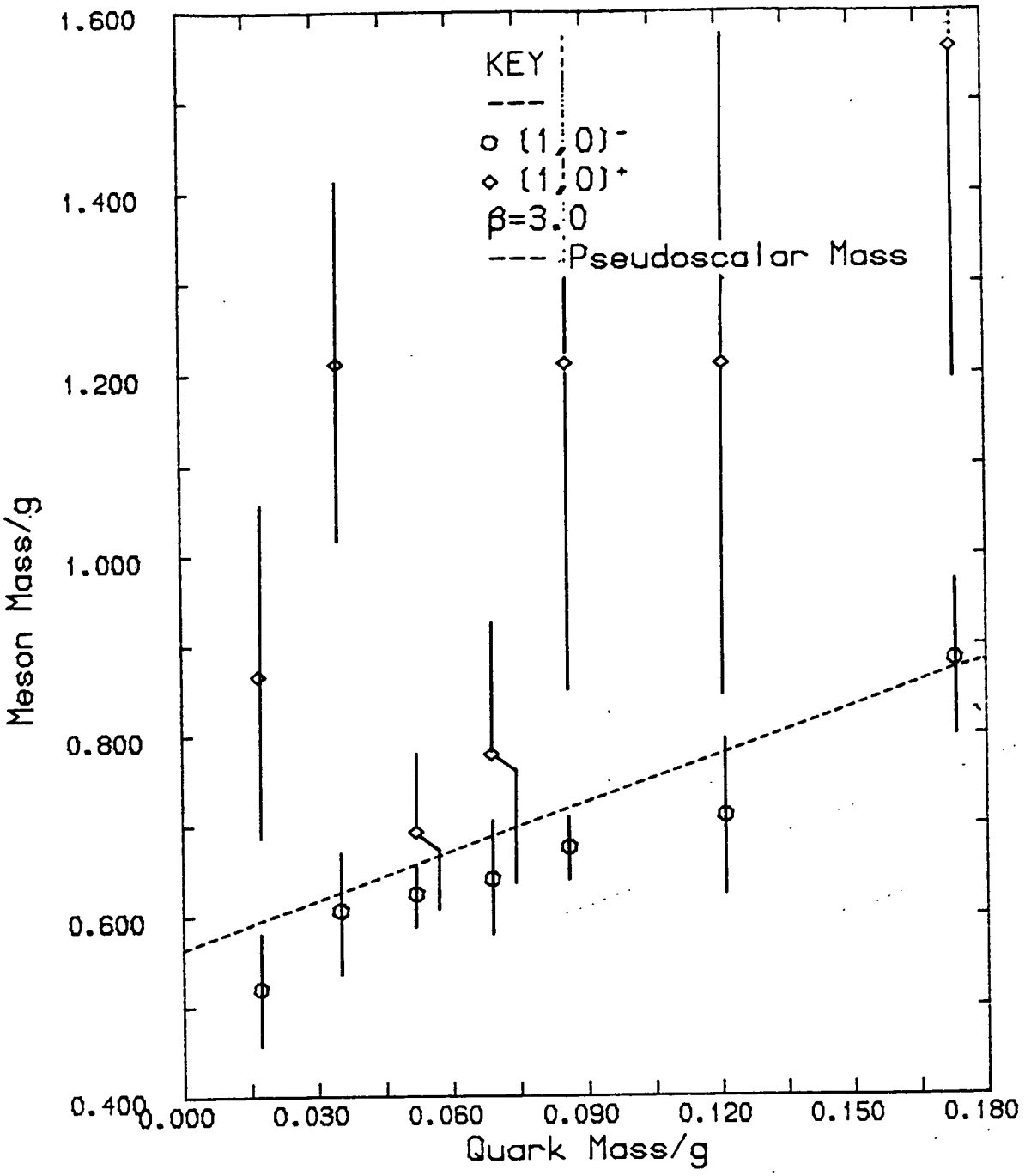

Fig 6.8(b)

Particle masses for Kahler-Dirac particles in the unquenched model.

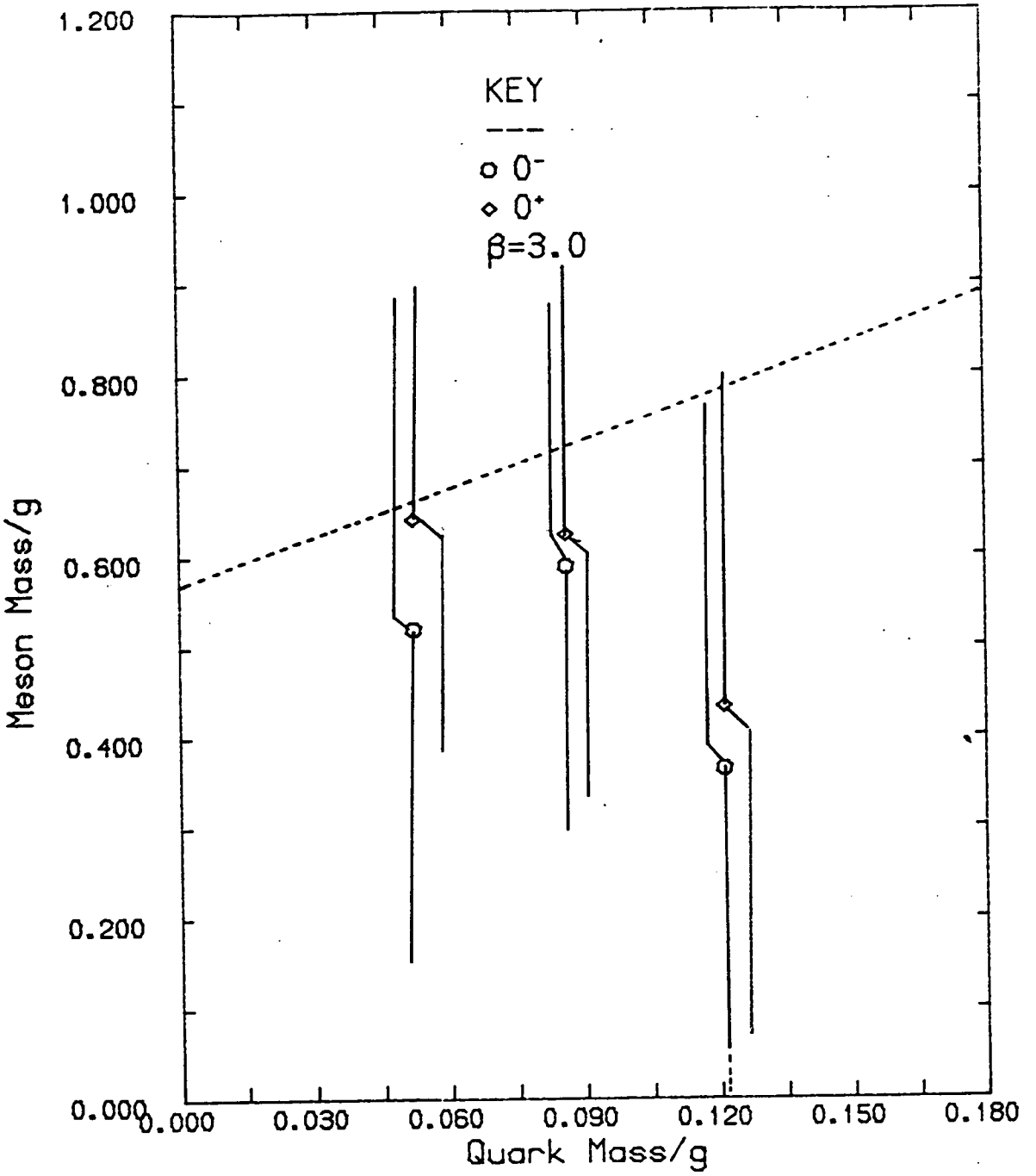

Fig 6.9

Particle masses extracted from the 0^- and 0^+ operators, with annihilation terms included. Unquenched case.

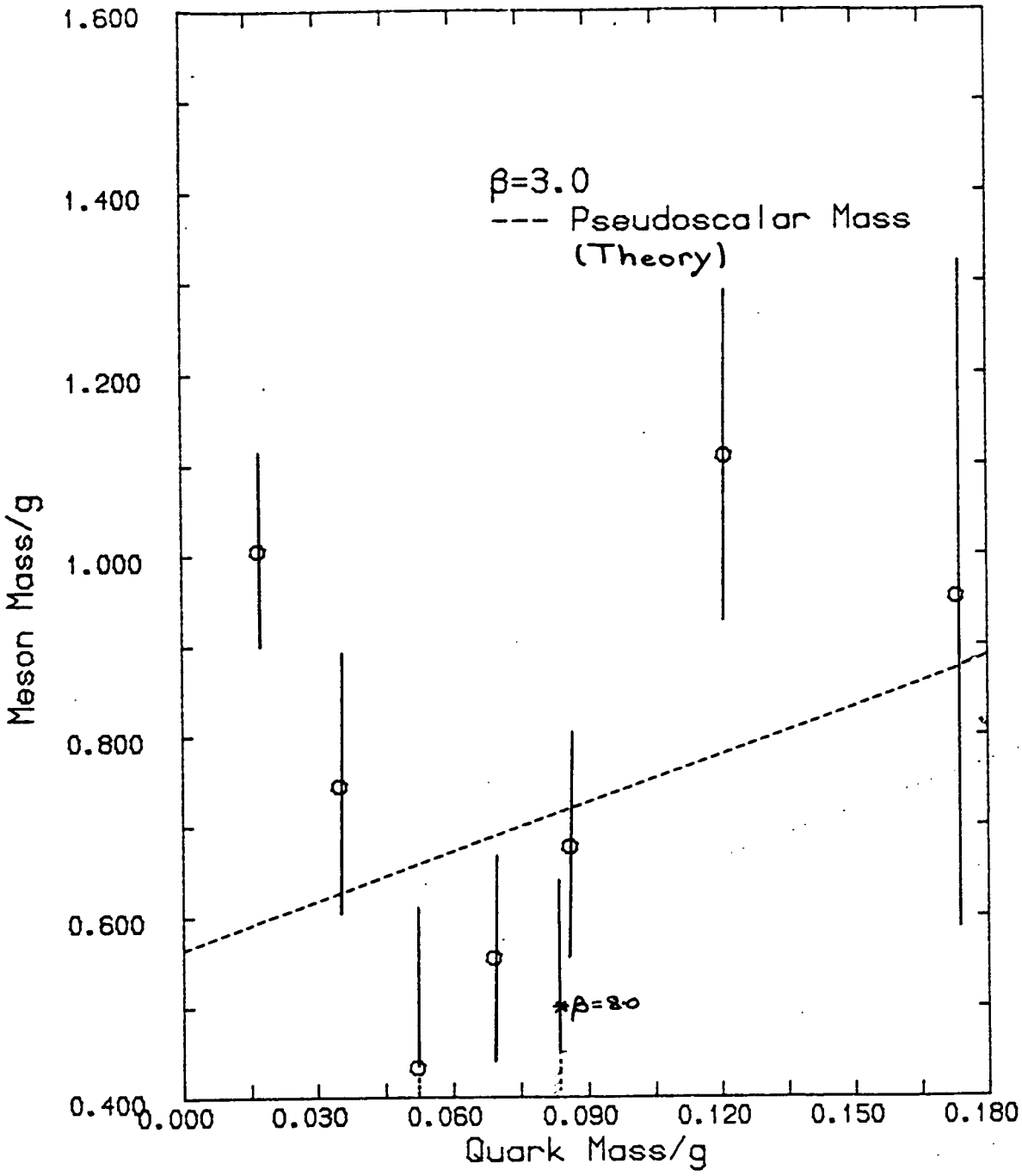

Fig 6.10

Particle masses extracted from the local definition of mesonic operators in the unquenched case.

6.3 Conclusions

The conclusions we can draw from our study of the one species model are much the same as for the two species model. The results for the mesonic masses, extracted from the non-local Kahler-Dirac definition of the mesonic operators are disappointing: once again, large statistical fluctuations together with a restricted number of time slices to which we may realistically fit result in large errors on the masses extracted. For the quenched theory, it would be practicable to increase the number of gauge configurations averaged over, and hence hopefully reduce this statistical error. However, as in the two species case, to increase the number of configurations significantly is prohibitively expensive in terms of computer time in the unquenched case.

We have unfortunately failed to see any significant difference between particle masses in the quenched and unquenched cases. However, the difference could well be hidden in the errors - analytical results suggest that it is small except at very small quark masses. It would be interesting to see what differences would be seen if one were to define γ_5 diagonal in the one species model. This would enable us to define a local Kahler-Dirac pion (local in the sense used in chapter five: no gauge field multiplications would be required to make it gauge invariant). Whilst it is true that it would still be necessary to include annihilation terms in the calculation of the mass of this state, our results suggest that these may not be so important. Making γ_5 diagonal would necessitate the use of a two link mass term to lift the flavour degeneracy. This is harder to programme, and would require

longer equilibration times (because each pseudofermionic sweep would require longer), but the clearer pion signal that would certainly be produced might enable us to observe the difference between the unquenched and quenched cases, and to assess the real importance of the annihilation terms to this model.

The local operators in this case do not produce good results at all. The errors associated with the extracted masses are larger than for the non-local Kahler-Dirac operators, and the values are far away from the analytical results. In the one species model, then, the Kahler-Dirac definition of particle operators is the better.

As in the two species model, we have succeeded in showing some difference between the quenched and unquenched cases in our calculation of $\langle\bar{u}u\rangle$: this quantity diverges for the quenched theory, in accordance with the analytical prediction of chapter two, and there is a finite breaking of chiral symmetry in the unquenched case, again in agreement with analytical predictions. Of course, this difference is much more marked than the difference predicted for the particle masses, and hence we need not be surprised that the latter cannot be resolved.

CONCLUSIONS

In this work, we have examined quantum electrodynamics in two dimensions, with both one and two flavours of massive fermions. We have attempted to simulate numerically both the fully interacting theory and its quenched counterpart, where internal fermionic loops have been neglected. The Kahler-Dirac prescription has been used in an effort to correctly identify the continuum flavours hidden in the Kogut-Susskind formulation of lattice fermions, and the resulting definition of mesonic operators has been compared with the easier local definition of these operators. The effects of boundary conditions on the results have been investigated. We have also made an attempt to calculate the annihilation terms contributing to a correct definition of particle propagators in both the one and two species models.

On the whole our results are somewhat disappointing and ambiguous. However, some interesting points have emerged. The local Kahler-Dirac definition of the pion in the two species model is extremely clear and gives unambiguous results at all values of the quark mass, in good agreement with theoretical predictions. In two dimensions, no local operator has an overlap solely with the pion, but they rather mix two physical states of different mass. In four dimensions there is a local operator that overlaps only with the pion. Hence, it is easier in two dimensions to assess the usefulness of the Kahler-Dirac definition of particle operators. The local Kahler-Dirac pion in two dimensions yields results that are much better than the results extracted from the local particle definition, and it thus

seems clear that the Kahler-Dirac definition is the one we must use to extract correct continuum results. This is especially true when we remember that some states - the 0- in two dimensions, for example - have no overlap with any local operators, and that we have been unable to extract masses for any particles other than the pion from the local operator definitions. However, the fact that most of the Kahler-Dirac operators require gauge field multiplications to make them gauge invariant means that statistical errors are large when averaging over only a small number of gauge field configurations. This is especially true in four dimensions, where it is not easy to increase the number of configurations, even in the quenched approximation.

It is difficult to assess how successful we have been in simulating the effects of dynamical fermions. Certainly, our results for $\langle\bar{\psi}\psi\rangle$ in both the one and two species models suggest that we are seeing the effects of internal fermion loops. When we consider particle masses, however, there is no clear difference between the quenched and unquenched cases. The fact that we need to average over many configurations to produce reliable masses prevents us from doing as exhaustive a job in checking equilibration as we have done for $\langle\bar{\psi}\psi\rangle$. However, if our unquenched configurations are really 'partially quenched', in the sense that the effects of internal fermionic loops have not fully been taken into account, we might expect to see results that differ from the unquenched analytical predictions, perhaps interpolating between expected quenched and unquenched cases. As it is, we fail to see any difference, even on varying the number of pseudofermionic sweeps performed between gauge field updates. In the two species model, we have a good operator, the local Kahler-Dirac pion, in which any difference might be expected to be displayed, but we see no difference. We do not know how big an

effect we are looking for, as we have no analytical results for the quenched two species model, but if we assume that it is basically the same as the quenched one species model, then the effect will be small. Such an effect could then be hidden within the errors. For the one species model, where we do have analytical results for both quenched and unquenched models, there is no operator whose signal is clear enough to reveal the difference.

The calculation of annihilation terms has also been disappointing. Whilst the pseudofermions equilibrate well after 5000 updates within a given gauge configuration, and produce a good average over a further 5000 updates, the signal that is left after subtracting out the disconnected piece suffers from large statistical errors. It is true that the signal is not expected to be clear for more than one or two lattice spacings, due to the small correlation lengths of the physical states, and our results do show a small signal over this distance. It seems, then, that the method could be useful, were the particle correlation lengths somewhat larger: the results are no worse than those produced using the conjugate gradient algorithm to calculate the other terms in the mesonic propagators. To produce operators with larger correlation lengths, though, is not easy. In the two flavour model, particle masses (for the lightest states) go like $g^{1/3}$, and hence a large decrease in g is required to produce a significant gain in signal. If we wish to see a difference between quenched and unquenched cases, we must work at small values of m_q, and hence if we decrease g we must also decrease m. Decreasing g slows down the Metropolis algorithm, whilst decreasing m slows down the pseudofermion algorithm.

The implementation of the one link mass term to break the flavour degeneracy of the Kogut-Susskind action seems to have been successful. Our results for the one species

model agree well with the theoretical predictions. The presence of the heavy d quark seems to speed up the convergence of the algorithms when compared with the two species model, and results suggest that this quark is indeed decoupled from the theory.

Finally, we note that in the quenched model, boundary conditions have not proved to be important. Particle correlation lengths are sufficiently small, and the lattice so large, that the physical states are insensitive to the finiteness of the system. However, in the unquenched case, we observed the puzzling slowing down of the pseudofermion algorithm when using antiperiodic boundary conditions. In view of the results for the quenched model, we felt confident in proceeding with calculations with periodic boundary conditions on the fermions. However, in four dimensions, where one is forced to use smaller lattices, finite size effects are more important, especially at small quark masses, and it is necessary to use the correct boundary conditions for fermions (Barbour et. al., 1983). Clearly, then, this phenomenon must be understood more fully.

APPENDIX

The work presented here has been numerical in nature, and the quality of the results depend largely on the computing power available. In this appendix, we outline some of the features of the ICL Distributed Array Processor (DAP) used in this work. We outline some of the architecture and software central to lattice gauge theory calculations (see also Hockney and Jesshope, 1981; Bowler, 1983).

The DAP combines computational power with a technology that is inexpensive in a machine with a wide performance range. Present versions use only relatively modest technology and only low levels of integration. Developments in very large scale integration offer the prospect of substantial improvements in computer times and in the size of lattice that might be contemplated in lattice gauge theory calculations.

Architecture

The DAP is designed to emulate a memory module for an ICL mainframe (called a host machine in this context). The DAP can provide store for the host in the conventional way when it is not operating as a parallel processor. The basic hardware of the DAP, indicated schematically in figure A.1, consists of a 64x64 array of processing elements (PE's) each having 4Kbits of store associated with it (giving a total of 2 Mbytes of store attached to the host). The array is

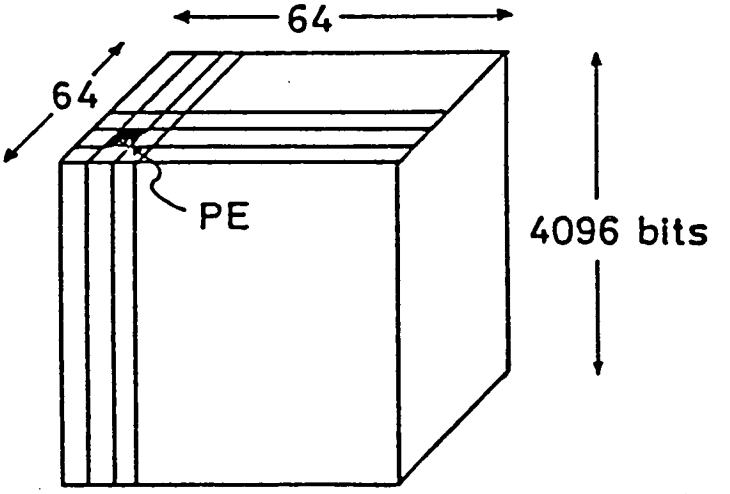

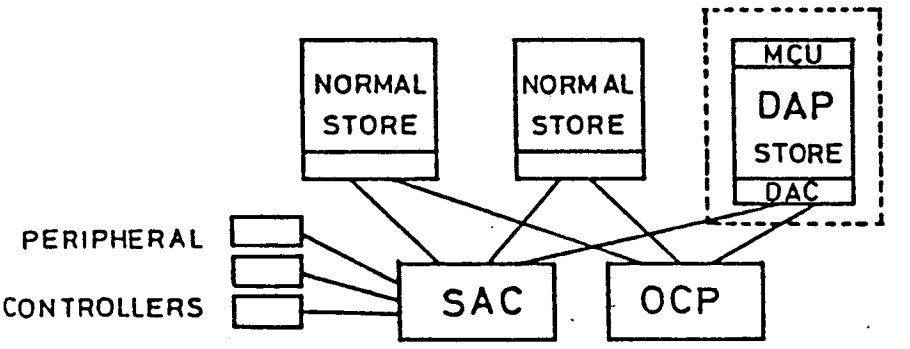

Fig. A.1

Schematic diagram of the DAP.

connected two dimensionally, with each PE having four neighbours to which it is connected. These are identified by points of the compass, N, S, W, E. The connections at the edge of the array depend on whether the machine is instructed to operate with PLANAR or CYCLIC geometry. PLANAR geometry defines a zero input at the edges, whereas CYCLIC geometry connects the edges of the DAP to form a 2-torus. In addition to the 4Kbit store, each PE contains three 1-bit registers (labelled A,Q, and C), two multiplexers and a 1-bit full adder, the most interesting of which is the A register. Certain instructions may be made conditional upon the setting of the A register in each processor. There is also a master control unit (MCU) which handles certain simple scalar functions such as control of DO loop variables in Fortran, and which also broadcasts instructions to the PE array.

Software Features

To take advantage of the DAP's parallel processing abilities, a language called DAP Fortran has been developed from ordinary Fortran. A DAP programme is run as a subroutine of a master Fortran programme run on the host machine. Communication between the DAP Fortran and Fortran routines is achieved through the use of shared COMMON blocks, loaded into the DAP store. Processing is initiated in the usual way with control being passed to a Fortran master programme which sets up the input routines and data, and might include some pre-processing to be performed by the host. Control is then passed to one of any number of DAP Fortran entry subroutines, which can in turn in turn call other DAP Fortran subroutines. Periodically, or on termination of the run, control is passed back to the host for Fortran post-processing and output.

The three basic types of variable in DAP Fortran are scalars, vectors and matrices. A scalar corresponds to an ordinary Fortran variable, whereas vectors have a range up to 64 in two dimensions. Variables and constants may be either of type REAL, of length 3 to 8 bytes, INTEGER, of length 1 to 8 bytes, or LOGICAL, and are declared in a manner similar to ordinary Fortran. For example, the code:

```
DIMENSION A(,),B(,),C(,)
C=A+B
```
(A.1)

means that at every PE the values of A and B are added and put into the the appropriate store for C, and this is done simultaneously at each of the 4096 PE's.

The two DAP Fortran features which give it considerable flexibility involve the ability to shift information between PE's and the use of logical matrices to provide local autonomy for the PE's by masking them out of a particular command. In order to bring information stored at one PE to another, there are a number of shift operations. For example:

```
DIMENSION A(,),B(,),C(,)
C=B+SHWC(A,3)
```
(A.2)

The effect of this statement at any PE is to assign to C the sum of the element of B stored at that PE and the element of A which is stored three sites away in an Easterly direction, with cyclic boundary conditions imposed in the East-West direction. Similarly, there are shifts North, South, and East, with either cyclic (SHNC, SHSC, SHEC) or planar (SHNP, SHSP, SHEP, SHWP) boundary conditions. It is

also possible to use the DAP in long vector mode, in which we may think of the numbers as being stored in a vector of length 4096. It is then possible to do shifts along this vector by means of the operations SHLC, SHRC, SHLP, SHRP, which denote shifts left or right with either cyclic or planar boundary conditions.

Operations and assignments may be made conditional upon the value of logical matrices (called masks in this context) at the processing elements. The logical mask sets the A-register mentioned earlier. Such masks can be either generated within a programme or defined using built-in logical functions available in DAP Fortran. For example, the function ALTR(N) sets the first N rows .FALSE. and the next N rows .TRUE. and so on until completion. More elaborate masks may be constructed using these standard logical operators in conjunction with both the shifts discussed above and standard logical statements. For example:

```
LOGICAL LMASK(,)
                                                    (A.3)
LMASK=ALTR(1).LEQ.ALTC(1)
```

sets up a chessboard pattern, in which each PE is alternatively .TRUE. and .FALSE., as illustrated in figure A.2. Assignments may then be made conditional upon such a mask in the following way:

```
REAL*4 A(,),B(,)

A(LMASK)=B                                          (A.4)
```

Only those elements of A at which LMASK is .TRUE. are assigned the corresponding values of B. At all other PE's, the value of A remains unchanged. Another important use of logical masks is in conjunction with MERGE statements:

```
DIMENSION A(,), B(,), C(,)
```

(A.5)

```
C=MERGE(A,B,LMASK)
```

Here, C takes the value of A at those PE's where LMASK is .TRUE., and the values of B where LMASK is .FALSE..

Lattice Gauge Theory Calculations

The parallelism of the DAP makes it ideally suited to Monte Carlo simulations of lattice gauge theory, in which essentially the same sequence of steps is repeated a large number of times. The question of how to use this parallelism in the most efficient way is an important one. The situation is very different from that with a serial computer. In two dimensional models, the question of how one should map the lattice variables onto a 64x64 array is straightforward: in this work, we have identified each site of the lattice with one PE on the DAP, so that the natural choice of lattice was 64x64. At each PE were stored the gauge field variables situated on the links emanating in the positive direction from that site. In this way, the locality of the action ensures that variables need only be moved between PE's that are near each other. In higher dimensions, the situation becomes more complex. For an account of how one maps an 8^4 lattice onto the DAP, see Bowler (1983).

In chapter four, we pointed out how the parallelism of the DAP could be used in an optimum way in the generation of gauge field configurations, both quenched and periodic. The pure gauge theory was optimally simulated by updating one in two gauge fields in a given direction. The update pattern on the DAP, then, required the use of the logical

mask defined by:

$$\text{LMASK=ALTR(1).LEQ.ALTC(1)} \qquad \text{(A.6)}$$

The pseudofermion procedure used for generating unquenched configurations, and in the calculation of annihilation terms, involved not nearest neighbour interactions, but rather next nearest neighbours. The optimum update pattern was different from that used for the gauge fields, then, since sites two lattice spacings apart could not be updated simultaneously. In the two species model, where there is no one link mass term, there are no nearest neighbour interactions. When a one link mass term was introduced the nearest neighbours in the direction of the mass term are linked, but nearest neighbours in a direction perpendicular to that of the mass term remain unconnected. The same update pattern may therefore be used in either case, the necessary mask being given by:

$$\text{LMASK=(ALTR(2).LEQ.ALTC(2)).AND.(ALTC(1))} \qquad \text{(A.7)}$$

This is shown in figure A.2.

Fig. A-2

(a)

LMASK = ALTR(1)

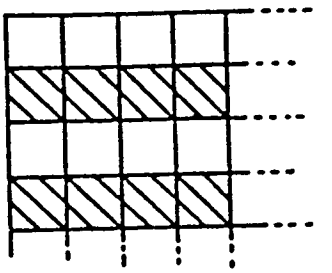

(b)

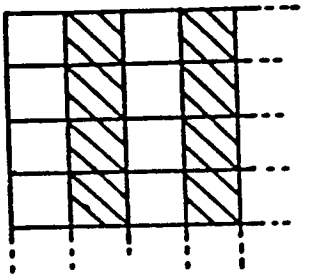

LMASK = ALTC(1)

(c)

LMASK =

ALTR(1).LEQ.ALTC(1)

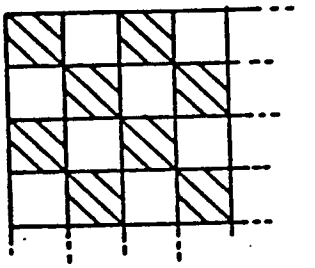

(d)

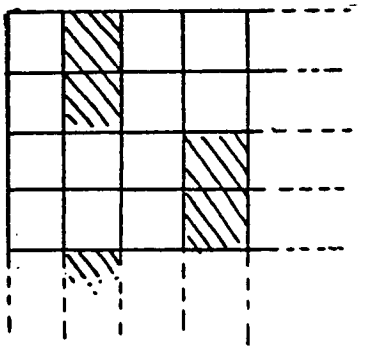

LMASK = (ALTR(2).
LEQ. ALTC(2))
.AND. ALTC(1)

Logical masks on the DAP.

REFERENCES

Adler S.L., 1969, Phys. Rev. 177 2426.

Baaquie B.E., 1982, J. Phys. G8 1621.

Bander M., 1976, Phys. Rev. D13 1566.

Banks T., Susskind L. and Kogut J.B., 1976,
Phys. Rev. D13 1043.

Banks T., Raby S., Susskind L., Kogut J.B.,
Jones D.R.T., Sharbach P.N., and Sinclair D.K., 1977,
Phys. Rev. D15 1111.

Banks T., Dothan Y., and Horn D., 1982,
Phys. Lett. 117B 413.

Barbour I., Gilchrist J., Schneider H., Schierholz G.,
Teper M., 1983, Phys.. Lett. 127B 433.

Becher P., 1981, Phys. Lett. 104B 221.

Becher P. and Joos H., 1982a, Z. Physik C15 343.

Becher P. and Joos H., 1982b,
On the geometric lattice approximation
to a realistic model of QCD, DESY preprint 82-008
(December 1982).

Bell J.S. and Jackiw R., 1969, Nuovo. Cim. 51 47.

Berg B. and Billoire A., 1982,
Phys. Lett. 114B 324; 113B 65.

Berg B., Meyer S., Montvay I., and Symanzik K., 1983,
DESY preprint 83-015.

Bhanot G., 1981, Phys. Rev. D24 461.

Bowler K.C., Pawley G.S., Wallace D.J., Marinari E.
and Rapuano F., 1983, Nucl. Phys. B220 [FS8] 137.

Bowler K.C., 1983, in proceedings of The Three Day
In-Depth Review on the Impact of Specialized Processors
in Elementary Particle Physics,
University of Padova, Italy,
March 1983.

Burkitt A.N., 1983, Nucl. Phys. B220 401.
Burkitt A.N., Kenway A., and Kenway R.D., 1983,
Phys. Lett. 128B 83.
Burkitt A.N., and Kenway R.D., 1983, Edinburgh
preprint No. 83/257 (to appear in Phys. Lett.).
Carpenter D., 1983, N. Phys. B228 365.
Carroll A., Kogut J.B., Sinclair D.K. and
Susskind L.,
1976,Phys. Rev. D13 2270 and Erratum: Phys. Rev.
D14 1729.
Casher A., Kogut J.B., and Susskind L., 1974,
Phys. Rev. D10 732.
Caswell W.E., 1973, Phys. Rev. Lett. 33 244.
Christ N.H., Friedberg R. and Lee T.D., 1982,
Nucl. Phys. B210 310.
Colemam S., 1973, Comm. Math. Phys. 31 259.
Coleman S., 1976, Ann. Phys. 101 239.
Coleman S., Jackiw R., and Susskind L., 1975,
Ann. Phys. 93 267.
Coleman S., and Weinberg S., 1973, Phys. Rev. D7 1888.
Creutz M., 1980a, Phys. Rev. Lett. 45 313.
Creutz M., 1980b, Phys. Rev. D21 2308.
Creutz M., 1983, 'Quarks, Gluons and Lattices', CUP.
DeGrand T., and Toussaint D., 1980,
Phys. Rev. D22 2478.
Drell S.D., Weinstein M., and Yankielowicz, 1976,
Phys. Rev. D14 487 and1627.
Duncan A. and Furman M., 1981,
Nucl. Phys. B190 [FS3] 767.
Elitzur S., 1975, Phys Rev D12 3978.
Fucito F., Marinari E., Parisi G. and Rebbi C.,
1981, Nucl. Phys. B180 [FS2] 369.
Gilchrist J., Schierholz G., Schneider H., Teper M.,
1984, Desy preprint 84-021
Gross D. and Wilczek F., 1973,
Phys. Rev. Lett. 30 1343.

Gross D. and Wilczek F., 1976, Phys. Rev. D8 3633.
Guerin F. and Kenway R.D., 1980,
Nucl. Phys. B176 168.
Hamber H.W., 1981, Phys. Rev. D24 951.
Hasenfratz A. and Hasenfratz P., 1980,
Phys. Lett. 93B 165.
Hasenfratz A. and Hasenfratz P., 1981,
Phys. Lett. 104B 489.
Hasenfratz A., Hasenfratz P., Kunszt Z. and Lang C.B.,
1892a, Phys. Lett. 110B 289;
1982b, Phys. Lett. 117B 81.
Hestenes M.R. and Stiefel E., 1952,
J. Res. Natt. Bur. Stand. 49 409.
Hockney R.W. and Jesshope C.R., 1981,
Parallel Computers (Adam Higler, Bristol).
Householder, 1964, 'The Theory of Matrices in
Numerical Analysis', Blaisdell Pub. Co..
Ishikawa K., Teper M., and Schierholz G., 1982,
Phys. Lett. 116B 429.
Jones D.R.T., 1974, Nucl. Phys. B75 531.
Kadanoff L.P., 1976, Ann. Phys. 100 359.
Kahler E., 1962, Rend. di Mat.(Roma) 21 425.
Kenway R. and Hamer C., 1978, Nucl. Phys. B139 85.
Karsten L.H., and Smit J., 1978, Nucl. Phys. B144 536.
Karsten L.H., and Smit J., 1979, Phys. Lett. 85B 100.
Karsten L.H., and Smit J., 1981, Nucl. Phys. B183 103.
Kawamoto N. and Smit J., 1981, Nucl. Phys. B192 10.
Kluberg-Stern H., Morel A., Napoly O. and
Peterssen B., 1983, Flavours of Lagrangian
Susskind Fermions, Saclay preprint
DPh.G.SPT/83/29(March 1983).
Kogut J., 1979, Rev. Mod. Phys. 51 659.
Kogut J., 1983, Rev. Mod. Phys. 55 775.
Kogut J. and Susskind L., 1974, Phys. Rev. D10 3468.
Kuti J., 1982, Phys. Rev. Lett. 49 183.
Lang C.B. and Nicolai H., 1982,

Nucl. Phys. B200 [FS4] 135.
Langguth W., and Montvay I., 1984,
DESY preprint 84-053.
Lautrup B., and Nauenberg M., 1980, Phys. Lett. 95B 63
Lowenstein and Swieca, 1971, Ann. Phys. 68 172.
Marinari E., Parisi G. and Rebbi C., 1981a,
Phys. Rev. Lett. 47 1795.
Marinari E., Parisi G. and Rebbi C., 1981b,
Nucl. Phys. B190 734.
Martin O., and Otto S., 1982, Nucl. Phys. B203 297.
Martinelli G., Parisi G., and Petronzio R., 1982,
Phys. Lett. 114B 251.
Matthews T. and Salam A., 1954, Nuovo Cim. 12 563;
1955, ibid 2 120.
Metropolis N., Rosenbluth A.W., Teller A.H. and
Teller E., 1953, J. Chem. Phys. 21 1087.
Michael C. and Teesdale I., 1982, Liverpool preprint.
Migdal A.A., 1975, Zh. Eksp. Teor. Fiz.
69 810, 1477.
Mitra P., 1983, Phys. Lett. 123B 77.
Mitra P. and Weisz P., 1983, Phys. Lett. 126B 355.
Napoly O., 1983, Saclay preprint SPh.T/83/77.
Neilsen H.B. and Ninomiya M., 1981,
Nucl. Phys. B185 20.
Politzer H.D., 1973, Phys. Rev. Lett. 30 1346.
Rabin J.M., 1982, Nucl. Phys. B201 315.
Ranft J., 1983, CERN preprint TH.3721-CERN.
Ranft J. and Schiller A., 1983, Phys. Lett. 122B 403
Rebbi C., 1980, Phys. Rev. D21 3350.
Reid (Ed.), 1971, 'Large Sparse Sets of Linear
Equations', Academic Press.
Scalapino D.J. and Sugar R.L., 1981,
Phys. Rev. Lett. 46 519.
Schwinger J., 1962, Phys. Rev. 125 397;
1962, ibid 128 2425.
Sharatchandra H.S., Thun H.J., and Weisz P.,

1981, Nucl. Phys. B192 205.
Stoer and Bulirsch, 1980, 'Introduction to Numerical Analysis',Springer-Verlag New York Inc..
Susskind L., 1977, Phys. Rev. D16 3031.
Symanzik K., 1982, in Mathematical Problems in Theoretical Physics, ed. R.Schroder, Lecture Notes in Physics, 153 (Springer, Berlin).
Tomboulis E., 1983, Phys. Rev. Lett. 50 791.
van den Doel, C., 1984, N. Phys. B230[FS10] 250.
Verstegen D., 1984, Edinburgh preprint 84-303.
Wegner F., 1971, J. Math. Phys. 12 2259.
Weisz P., 1982, Nucl. Phys. B212 1.
Wilson K.G., 1974, Phys. Rev. D10 2445.
Wilson K.G. and Kogut J., 1974, Phys. Rep. 12 2.
Wilson K.G., 1977, in New Phenomena in Subnuclear Physics, Ed. A.Zichichi (Plenum, New York).
Yang C.N. and Mills R.L., 1954, Phys. Rev. 96 1605.